Report by the ESA-ESO Working Group on Fundamental Cosmology

Abstract

In September 2003, the executives of ESO and ESA agreed to establish a number of working groups to explore possible synergies between these two major European astronomical institutions on key scientific issues. The first two working group reports (on Extrasolar Planets and the Herschel–ALMA Synergies) were released in 2005 and 2006, and this third report covers the area of Fundamental Cosmology.

The Working Group's mandate was to concentrate on fundamental issues in cosmology, as exemplified by the following questions: (1) What are the essential questions in fundamental cosmology? (2) Which of these questions can be tackled, perhaps exclusively, with astronomical techniques? (3) What are the appropriate methods with which these key questions can be answered? (4) Which of these methods appear promising for realization within Europe, or with strong European participation, over the next ~ 15 years? (5) Which of these methods has a broad range of applications and a high degree of versatility even outside the field of fundamental cosmology?

From the critical point of view of synergy between ESA and ESO, one major resulting recommendation concerns the provision of new generations of imaging survey, where the image quality and near-IR sensitivity that can be attained only in space are naturally matched by ground-based imaging and spectroscopy to yield massive datasets with well-understood photometric redshifts (photo-z's). Such information is essential for a range of new cosmological tests using gravitational lensing, large-scale structure, clusters of galaxies, and supernovae. All these methods can in principle deliver high accuracy, but a multiplicity of approaches is essential in order that potential systematics can be diagnosed – or the possible need for new physics revealed. Great scope in future cosmology also exists for ELT studies of the intergalactic medium and space-based studies of the CMB and gravitational waves; here the synergy is less direct, but these areas will remain of the highest mutual interest to the agencies. All these recommended facilities will produce vast datasets of general applicability, which will have a tremendous impact on broad areas of astronomy.

Background

Following an agreement to cooperate on science planning issues, the executives of the European Southern Observatory (ESO) and the European Space Agency (ESA) Science Programme and representatives of their science advisory structures have met to share information and to identify potential synergies within their future projects. The agreement arose from their joint founding membership of EIROforum (www.eiroforum.org) and a recognition that, as pan-European organisations, they serve essentially the same scientific community.

At a meeting at ESO in Garching during September 2003, it was agreed to establish a number of working groups that would be tasked to explore these synergies in important areas of mutual interest and to make recommendations to both organisations. The chair and co-chair of each group were to be chosen by the executives but thereafter, the groups would be free to select their membership and to act independently of the sponsoring organisations. During the second of these bilateral meetings, in Paris during February 2005, it was decided to commission a group to address the current state of knowledge and future prospects for progress in fundamental cosmology, especially the nature of 'dark matter' and 'dark energy'. By summer 2005, the following membership and terms of reference for the group were agreed:

Membership

John Peacock (Chair) jap@roe.ac.uk
Peter Schneider (Co-Chair) peter@astro.uni-bonn.de
George Efstathiou gpe@ast.cam.ac.uk
Jonathan R. Ellis johne@mail.cern.ch
Bruno Leibundgut bleibund@eso.org
Simon Lilly simon.lilly@phys.ethz.ch
Yannick Mellier mellier@iap.fr

Additional major contributors: Pierre Astier, Anthony Banday, Hans Böhringer, Anne Ealet, Martin Haehnelt, Günther Hasinger, Paolo Molaro, Jean-Loup Puget, Bernard Schutz, Uros Seljak, Jean-Philippe Uzan.

ST-ECF Support: Bob Fosbury, Wolfram Freudling

Thanks are also due to many colleagues who provided further useful comments on draft versions of the report at various stages.

Terms of Reference

(1) To outline the current state of knowledge of the field (this is not intended as a free-standing review but more as an introduction to set the scene);

(2) To review the observational and experimental methods used or envisaged for the characterisation and identification of the nature of Dark Matter and Dark Energy;

(3) To perform a worldwide survey of the programmes and associated instruments that are operational, planned or proposed, both on the ground and in space;

(4) For each of these, to summarise the scope and specific goals of the observation/experiment; also to point out the limitations and possible extensions;

(5) Within the context of this global effort, examine the role of ESO and ESA facilities. Analyse their expected scientific returns; identify areas of potential overlap and thus assess the extent to which the facilities complement or compete; identify open areas that merit attention by one or both organisations and suggest ways in which they could be addressed;

(6) Make an independent assessment of the scientific cases for large facilities planned or proposed.

(7) The working group membership will be established by the chair and co-chair. The views represented and the recommendations made in the final report will be the responsibility of the group alone.

Catherine Cesarsky (ESO) **Alvaro Giménez (ESA)**

September 2006

Contents

1 Executive summary

This report is written for ESA and ESO jointly, in order to summarize current understanding of the fundamental properties of the universe, and to identify the key areas in which Europe should invest in order to advance this understanding. There is an increasingly tight connection between cosmology and fundamental physics, and we have concentrated on this area. We thus exclude direct consideration of the exciting recent progress in astrophysical cosmology, such as the formation and evolution of galaxies, the processes of reionization and the first stars etc. However, many of our recommended actions will produce vast datasets of general applicability, which will also have a tremendous impact on these broader areas of astronomy.

This is an appropriate time to take stock. The past 10-15 years have seen huge advances in our cosmological understanding, to the point where there is a well-defined standard model that accounts in detail for (nearly) all cosmologically relevant observations. Very substantial observational resources have already been invested, so the next generation of experiments is likely to be expensive. Indeed, the scale of future cosmological projects will approach that of particle physics, both in financial and in human terms. We therefore need to identify the problems that are both the most fundamental, and which offer the best prospects for solution. In doing this, it is hard to look too far ahead, as our views on priorities will doubtless evolve; but planning and executing large new experiments will take time. We intend this report to cover the period up to about 2020.

The standard model consists of a universe described by Einstein's theory of general relativity, with a critical energy density dominated today by a component that is neither matter nor radiation, but a new entity termed 'dark energy', which corresponds to endowing the vacuum with energy. The remaining energy consists of collisionless 'cold dark matter' (about 22%) and ordinary 'baryonic' material (about 4%), plus trace amounts of radiation and light neutrinos. The universe is accurately homogeneous on the largest scales, but displays a spectrum of inhomogeneities whose gravitationally-driven growth is presumed to account for the formation of galaxies and large-scale structure. The simplest consistent theory for the origin of these features is that the universe underwent an early phase of 'inflation', at which time the density in dark energy was very much higher than at present. Given this background, there follows a natural set of key questions:

(1) What generated the baryon asymmetry? Why is there negligible antimatter, and what set the ratio of baryons to photons?

(2) What is the dark matter? Is it a relic massive supersymmetric particle, or something (even) more exotic?

(3) What is the dark energy? Is it Einstein's cosmological constant, or is it a dynamical phenomenon with an observable degree of evolution?

(4) Did inflation happen? Can we detect relics of an early phase of vacuum-dominated expansion?

(5) Is standard cosmology based on the correct physical principles? Are features such as dark energy artefacts of a different law of gravity, perhaps associated with extra dimensions? Could fundamental constants actually vary?

Whereas we have not attempted to rank these prime science questions in importance, we took into consideration the likelihood that substantial progress can be made with astronomical techniques. Additional information may in some cases be provided by particle-physics experiments. For example, in the case of the baryon asymmetry (1), we may hope for major progress from particle-physics experiments studying CP violation at the LHC, or at a neutrino factory in the longer term. The nature of dark matter (2) will be investigated by accelerators such as the LHC or underground dark matter experiments, while astronomical observations will constrain its possible properties; similarly, tests of the law of gravity (5) will also be conducted in the laboratory as well as on cosmological scales. Empirical studies of the properties of dark energy (3) and the physics of inflation (4) are possible only with the largest possible laboratory available, namely the universe as a whole. On the other hand, there may be some synergy with searches for the Higgs boson at the LHC; these could provide a prototype for other scalar fields, which can be of cosmological importance. Given their fundamental nature, studies of dark energy and inflation are of the utmost interest to the science community well beyond astrophysics.

Of all these cosmological issues, probably the discovery of a non-vanishing dark energy density poses the greatest challenge for physics. There is no plausible or 'natural' model for its nature, and we must adopt empirical probes of its properties. For example, undoubtedly one of the most important questions is whether the dark energy is simply the cosmological constant introduced by Einstein, or whether it has an equation of state that differs from $w = -1$, where w is the ratio of the pressure to the energy density. Several highly promising methods for studying the value of w have been identified that can be actively pursued within the next decade and which will lead to qualitatively improved insights. However, new ingredients such as w will often be almost degenerate in their effect with changes in standard parameters; numbers such as the exact value of the dark matter density must be determined accurately as part of the road to w.

Progress in answering the foregoing questions will thus require a set of high-accuracy observations, probing subtle features of cosmology that have been largely negligible in past generations of experiment. Our proposed approach is to pursue multiple independent techniques, searching for consistency between the resulting estimates of

cosmological parameters, suitably generalised to allow for the possible new ingredients that currently seem most plausible. If these estimates disagree, this could indicate some systematic limitation of a particular technique, which can be exposed by internal checks and by having more than one external check. In addition, there is also the exciting possibility of something unexpected.

The first step in these improvements will be statistical in nature: because the universe is inhomogeneous on small scales, 'cosmic variance' forces us to study ever larger volumes in order to reduce statistical errors in measuring the global properties of the universe. Thus, survey astronomy inevitably looms large in our recommendations. Remarkably, the recent progress in cosmology has been so rapid that the next generation of experiments must aspire to studying a large fraction of the visible universe – mapping a major fraction of the whole sky in a range of wavebands, out to substantial redshifts.

The key wavebands for these cosmological studies are the cosmic microwave background (CMB) around 1 mm, for the study of primordial structure at the highest redshifts possible; optical and infrared wavebands for the provision of spectroscopy and photometric redshift estimates, plus data on gravitational-lensing image distortions; the X-ray regime for the emission signatures of intergalactic gas, particularly in galaxy clusters. In principle the radio waveband can also be of importance, and the ability to survey the universe via 21-cm emission as foreseen by the Square Kilometre Array will make this a wonderfully powerful cosmological tool. However, according to current estimates, the SKA will become available close to 2020. We believe that great progress in cosmology is however possible significantly sooner than this, by exploiting the opportunities at shorter wavelengths.

The principal techniques for probing inflation and the properties of dark matter and dark energy involve the combination of the CMB with at at least one other technique: gravitational lensing; baryon acoustic oscillations; the supernova Hubble diagram; and studies of the intergalactic medium. The CMB alone is the richest source of direct information on the nature of the initial fluctuations, such as whether there exist primordial gravitational waves or entropy perturbations. But the additional datasets allow us to study the cosmological model in two further independent ways: geometrical standard rulers and the growth rate of cosmological density fluctuations. The majority of these techniques have common requirements: large-area optical and near-IR imaging with good image quality, leading to photometric redshifts. This leads to the strongest of our recommendations, which we now list:

- ESA and ESO should collaborate in executing an imaging survey across a major fraction of the sky by constructing a space-borne high-resolution wide-field optical imager and providing the essential multi-colour component from the ground, plus also a near-IR component from space. The VST KIDS project will be a pathfinder for this sort of data, but substantial increases in grasp and improve-

ments in image quality will be needed in order to match or exceed global efforts in this area.

- Near-IR photometry is essential in order to extend photometric redshifts beyond redshift unity. VISTA will be able to perform this role to some extent with regard to KIDS. However, imaging in space offers huge advantages in the near-IR via the low background, and this is the only feasible route to quasi all-sky surveys in this band that match the depth of optical surveys. We therefore recommend that ESA give the highest priority to exploring means of obtaining such near-IR data, most simply by adding a capability for near-IR photometry to the above satellite for high-resolution optical imaging.

- In parallel, ESO should give high priority to expanding its wide-field optical imaging capabilities to provide the complementary ground-based photometric data at wavelengths $\lesssim 700$ nm. The overall optical/IR dataset (essentially 2MASS with a 7 magnitude increase in depth plus an SDSS imaging survey 4 magnitudes deeper and with ~ 3 times larger area) would also be a profound resource for astronomy in general, a legacy comparable in value to the Palomar surveys some 50 years ago.

- Photometric redshift data from multi-colour imaging of this sort enable two of the principal tests of dark energy: 3D gravitational lensing, and baryon oscillations in projection in redshift shells. Photometric redshifts are also essential in order to catalogue clusters at high redshift, in conjunction with an X-ray survey mission such as eROSITA. The same is true for identifying the clusters to be detected by Planck using the Sunyaev-Zeldovich effect.

- Calibration of photometric redshifts is key to the success of this plan, thus ESO should plan to conduct large spectroscopic surveys spread sparsely over $\sim 10,000$ deg^2, involving $> 100,000$ redshifts. This will require the initiation of a large key programme with the VLT, integrated with the imaging survey. Ideally, a new facility for wide-field spectroscopy would be developed, which would improve the calibration work, and also allow the baryon oscillations to be studied directly and undiluted by projection effects.

- A powerful multi-colour imaging capability can also carry out a supernova survey extending existing samples of high-redshift SNe by an order of magnitude, although an imager of 4m class is required if this work is to be pursued from the ground. In order to exploit the supernova technique fully, an improved local sample is also required. The VST could provide this, provided that time is not required for other cosmological surveys, in particular lensing.

- Supernova surveys need to be backed up with spectroscopy to assure the classification for at least a significant subsample and to check for evolutionary effects.

The spectroscopy requires access to the largest possible telescopes, and a European Extremely Large Telescope (ELT) will be essential for the study of distant supernovae with redshifts $z > 1$.

- A European ELT will also be important in fundamental cosmology via the study of the intergalactic medium. Detailed quasar spectroscopy can limit the nature of dark matter by searching for a small-scale coherence length in the mass distribution. These studies can also measure directly the acceleration of the universe, by looking at the time dependence of the cosmological redshift.

- ELT quasar spectroscopy also offers the possibility of better constraints on any time variation of dimensionless atomic parameters such as the fine-structure constant α and the proton-to-electron mass ratio. There presently exist controversial claims of evidence for variations in α, which potentially relate to the dynamics of dark energy. It is essential to validate these claims with a wider range of targets and atomic tracers.

- In the domain of CMB research, Europe is well positioned with the imminent arrival of Planck. The next steps are (1) to deal with the effects of foreground gravitational lensing of the CMB and (2) to measure the 'B-mode' polarization signal, which is the prime indicator of primordial gravitational waves from inflation. The former effect is aided by the optical lensing experiments discussed earlier. The latter effect is potentially detectable by Planck, since simple inflation models combined with data from the WMAP CMB satellite predict a tensor-to-scalar ratio of $r \simeq 0.15$. A next-generation polarization experiment would offer the chance to probe this signature in detail, providing a direct test of the physics of inflation and thus of the fundamental physical laws at energies $\sim 10^{12}$ times higher than achievable in Earth-bound accelerators. For reasons of stability, such studies are best done from space; we thus recommend such a CMB satellite as a strong future priority for ESA.

- An alternative means of probing the earliest phases of cosmology is to look for primordial gravitational waves at much shorter wavelengths. LISA has the potential to detect this signature by direct observation of a background in some models, and even upper limits would be of extreme importance, given the vast lever arm in scales between direct studies and the information from the CMB. We thus endorse space-borne gravity-wave studies as an essential current and future priority for ESA.

2 Introduction

The current human generation has the good fortune to be the first to understand a reasonable fraction of the large-scale properties of the universe. A single human lifespan ago, we were in an utterly primitive state where the nature of galaxies was unknown, and their recessional velocities undreamed of. Today, we know empirically how the current universe emerged from a hot and dense early state, and have an accurate idea of how this process was driven dynamically by the various contributions to the energy content.

Proceeding initially on the assumption that general relativity is valid, cosmology has evolved a standard model in which all of astronomy is in principle calculable from six parameters. This success is impressive, but it is bought at the price of introducing several radical ingredients, which require a deeper explanation:

- An asymmetry between normal matter and antimatter.
- A collisionless component of 'dark matter', which has been inferred purely from its gravitational effects.
- A homogeneous negative-pressure component of 'dark energy', which has been inferred only from its tendency to accelerate the expansion of the universe.
- A set of density fluctuations with a power-law spectrum, which are acausal in the sense of having contributions with wavelengths that exceed ct at early times.

It is assumed that an understanding of these ingredients relates to the initial conditions for the expanding universe. Since about 1980, the standard assumption has been that the key feature of the initial conditions is a phase of 'inflation'. This represents a departure from the older singular 'big bang' expansion history at high energies (perhaps at the GUT scale of $\sim 10^{15}$ GeV). With this background, we can attempt a list of some of the big open questions in cosmology, which any complete theory must attempt to address:

(1) What generated the baryon asymmetry?

(2) What is the dark matter?

(3) What is the dark energy?

(4) Did inflation happen?

(5) Are there extra dimensions?

(6) Do fundamental constants vary?

There are many further features of the universe that one would wish to understand – notably the processes that connect initial conditions to complex small-scale structures: galaxies, stars, planets and life. Nevertheless, the remit of the current Working Group is restricted to what we have termed *Fundamental Cosmology*, on the assumption that the complex nonlinear aspects of small-scale structure formation involve no unknown physical ingredients. We are therefore primarily concerned with what astronomy can tell us about basic laws of physics, beyond what can be probed in the laboratory.

Not all the key questions listed above are amenable to attack by astronomy alone. For example, an important source of progress in the study of the baryon asymmetry will probably be via pure particle-physics experiments that measure aspects of CP violation. Given a mechanism for CP violation, it is relatively straightforward in principle to calculate the relic baryon asymmetry – the problem being that the standard model yields far too low a value (see e.g. Riotto & Trodden 1999). Experiments that measure CP violation and are sensitive to non-standard effects are thus automatically of cosmological interest. This applies to experiments looking at the unitarity triangle within the quark sector (BaBar, BELLE, LHCb), and to a future neutrino factory that could measure CP violation in the neutrino sector – which would be studying physics beyond the standard model by definition. Results from the LHC are expected to be relevant also to many other fundamental cosmological problems. For example, the discovery of a Higgs boson might provide some insight into the nature of dark energy or the driving force for inflation. Likewise, the discovery of supersymmetry or extra dimensions at the LHC might provide direct evidence for a dark matter candidate whose properties could be determined and compared with astrophysical and cosmological constraints. Underground direct dark matter searches may detect the constituent of the dark matter even before the LHC has a chance to look for supersymmetric signatures. Current direct detection limits for Weakly Interacting Massive Particles (WIMPs) that form the dark matter constrain a combination of the particle mass and the spin-independent WIMP-nucleon scattering cross-section. The best sensitivity is currently achieved at masses around 100 GeV, where the cross-section must be below 10^{-46} m^2. The simplest supersymmetric extensions of the standard model predict cross-sections somewhere in the four orders of magnitude below this limit, so success in direct WIMP searches is certainly plausible, if hard to guarantee. A future linear electron-positron collider would also be of cosmological relevance, since it could study in more detail the spectrum of particles accompanying such dark matter candidates. However, it is beyond our remit to consider the capabilities and relative priorities of different particle accelerators.

Within the compass of astronomy, then, one can consider the following observables and techniques, together with their associated experiments. This really focuses on a small list of observable signatures (tensor modes and the 'tilt' of the density power spectrum, plus possible non-Gaussian and isocurvature contributions in order to probe

inflation; the equation of state parameter $w(z)$ as a route to learn about dark energy):

- Cosmic Microwave Background (CMB) anisotropies
- Large-Scale Structure (LSS) from large galaxy redshift surveys
- Evolution of the mass distribution from cluster surveys
- Large Scale Structure from gravitational lensing surveys
- The Hubble diagram for Supernovae of Type Ia
- Studies of the intergalactic medium (IGM)
- Gravitational waves

Subsequent sections in this report are constructed around asking what each of these techniques can contribute to the study of fundamental cosmology. Before proceeding, we now lay out in a little more detail some of the relevant pieces of cosmological background that will be common themes in what follows.

3 The cosmological context

3.1 Overview

The expansion of the universe is one of the most fundamental observables in cosmology. On the one hand, according to the Cosmological Principle, the universe is essentially homogeneous and isotropic. In this limit, the history of the scale size describes the universe completely, and its evolution in time is the primary source of information about the history of the universe. On the other hand, the rate of expansion of the universe is controlled by the density of energy it contains, and hence is sensitive to all types of matter and their interactions. The initial discovery of the expansion of the universe was a great surprise in itself. Together with the laws of gravity, described by General Relativity, the current expansion implies that the universe evolved from a state of tremendous density and temperature, known as the Big Bang. The predictions of Big Bang theory include the abundance of the lightest chemical species generated a few minutes after the Big Bang, predominantly helium and deuterium, as well as the existence of a thermal radiation as a leftover from the early stages of cosmic evolution. Both of these predictions have been verified with an impressive accuracy.

The present acceleration of the cosmic expansion has also come as a surprise. The past history of the universe may also have featured periods of anomalous expansion, for example during an early inflationary epoch. This is thought to have left traces in the fluctuations in the microwave background radiation and to have seeded the formation of structures in the universe, whose growth has been sensitive to the subsequent expansion of the universe. *For these reasons, the detailed measurement of the history of the expansion of the universe throughout its visible epoch since the decoupling of the microwave background is one of the critical frontiers in cosmology*.

There are thought to be at least five major components in the energy density of the universe during this visible epoch, each of which has its own characteristic signature and importance. The most obvious is *conventional baryonic matter*, whose density is in principle well constrained by the concordance between the values inferred from astrophysical observations of light-element abundances and the cosmic microwave background, though there may still be discrepancies that need to be resolved. A second component is the *cosmic microwave background radiation* itself. The contributions of these components to the cosmological energy density have well-understood time evolutions, but the same cannot be said for all the other important contributions.

A third component in the energy density is the analogous *cosmic neutrino background*, whose evolution with time depends on the masses of the neutrinos. The most stringent upper limits on their masses are currently provided by cosmology, with oscillation experiments providing lower limits that are considerably smaller. *A key objective of*

future cosmological measurements will be to bring the cosmological limits into contact with the oscillation limits, and thereby determine the overall neutrino mass scale.

A fourth component in the cosmological energy density is *cold dark matter*, whose density is thought to dominate the previous three throughout the visible epoch. Measurements of the cosmic microwave background, large-scale structures, the abundance of galaxy clusters and high-redshift supernovae all contribute to the present constraints on the cold dark matter density, which is currently known with an accuracy of a few percent. *One of the key objectives of future cosmological observations will be to refine this estimate of the cold dark matter density, and thereby sharpen the confrontation with particle theories of dark matter, such as supersymmetry*. Studies have shown that, within the frameworks of specific theories, measurements of particle properties at future colliders such as the Large Hadron Collider (LHC) and International Linear Collider (ILC) may enable *ab initio* calculations of the cold dark matter density with an accuracy approaching the percent level. Future cosmological measurements should strive to meet this challenge.

The fifth, largest, most recently identified and most surprising component in the cosmological energy density is the *dark energy*. The concordance of data on the cosmic microwave background, structure formation and high-redshift supernovae points unambiguously to the current accelerated expansion of the universe, implying the existence of some distributed component of the energy density that is not associated with concentrations of matter and which exerts negative pressure. This dark energy density in the cosmic vacuum may be a constant, in which case it can be identified with the 'cosmological constant' that was first postulated by Einstein. He subsequently regarded it as his greatest mistake, but it should perhaps rather be regarded as one of his deepest insights. However, the dark energy density might not be constant; indeed, particle theories suggest that it has varied by many orders of magnitude during the history of the universe. *The big issue is whether the dark energy density has still been varying during the visible epoch, and specifically whether it is fixed today*.

In a theoretical sense, the greatest puzzle may not be that dark energy exists, since we know of no fundamental reason why it should vanish, but rather why its present value is so small. The generally accepted theory of the strong interactions, QCD, makes a contribution to the vacuum energy that is over 50 orders of magnitude larger than the observed value. The standard electroweak theory makes a contribution via the Higgs field that is a dozen orders of magnitude larger still. The energy density during inflation would have been more than 100 orders of magnitude larger than at present. Indeed, in our present state of understanding, we would not know how to exclude, with a plausible physical model, a density of vacuum energy 120 orders of magnitude larger than the present value. One way to confront this dilemma is to postulate that the vacuum energy has been relaxing towards a very small value, in which case it may be possible to observe its evolution during the visible epoch and even today.

It is probable that a full understanding of dark energy will require a quantum theory of gravity. The creation of such a theory is the most profound problem in fundamental physics today; in its absence, we can only speculate on the origin and nature of dark energy. The most prominent candidate for a quantum theory of gravity is string theory, but the guidance currently offered by string theory is difficult to interpret. It has only recently been realized that the myriads of potential string vacua are far more numerous even than had been considered previously (Susskind 2003). The overwhelming majority of the vacua in this 'string landscape' possess non-zero, constant dark energy. However, in view of the past history of theoretical ideas on this problem, it would surely be premature to conclude that no further insights remain to be gained. Under these circumstances, the most appropriate observational approach is pragmatic, seeking direct measurements of the possible evolution of the dark energy density. The only place where such an empirical approach is feasible is the largest laboratory available: our universe.

3.2 The global contents of the universe

The expansion of the universe is described by the cosmic scale factor, $R(t)$, which governs the separation of particles in a uniform model. The matter content of the universe is included in the Friedmann equation which describes the scale factor as a function of time, independent of the equation of state

$$\dot{R}^2 - \frac{8\pi G}{3}\rho R^2 = -kc^2, \tag{1}$$

where k is a constant describing the 'curvature' of the universe The density ρ is conveniently written in terms of density parameters

$$\Omega \equiv \frac{\rho}{\rho_c} = \frac{8\pi G\rho}{3H^2}, \tag{2}$$

where the 'Hubble parameter' is $H = \dot{R}/R$. Thus, a flat $k = 0$ universe requires $\sum \Omega_i = 1$ at all times, whatever the form of the contributions to the density. Empirically, it appears that the total curvature is very small (Spergel et al. 2006 suggest $|\Omega_{\rm total} - 1| \lesssim 0.02$), and it is therefore often assumed that $\Omega_{\rm total} = 1$ is exact. The curvature does however influence conclusions about other cosmological parameters, and conclusions that depend on $k = 0$ can weaken considerably if this assumption is relaxed.

If the vacuum energy is a cosmological constant, then

$$\frac{8\pi G\rho}{3} = H_0^2\left(\Omega_{\rm v} + \Omega_{\rm m}a^{-3} + \Omega_{\rm r}a^{-4}\right) \tag{3}$$

(introducing the normalized scale factor $a = R/R_0$), where here and in the following, the density parameters Ω are taken at the current epoch. The Friedmann equation then

becomes an expression for the time dependence of the Hubble parameter:

$$H^2(a) = H_0^2 \left[\Omega_{\rm v} + \Omega_{\rm m} a^{-3} + \Omega_r a^{-4} - (\Omega_{\rm total} - 1) a^{-2}\right]. \tag{4}$$

More generally, we will be interested in the vacuum equation of state

$$w \equiv P/\rho c^2 \tag{5}$$

If this is constant, adiabatic expansion of the vacuum gives

$$\frac{8\pi G \rho_{\rm v}}{3H_0^2} = \Omega_{\rm v} a^{-3(w+1)}. \tag{6}$$

If w is negative at all, this leads to models that become progressively more vacuum-dominated as time goes by. When this process is complete, the scale factor should vary as a power of time. In the limiting case of $w = -1$, i.e. a cosmological constant, the universe approaches de Sitter space, in which the scale factor attains an exponential behaviour. The case $w < -1$, sometimes known as phantom dark energy, is interesting, in particular if w is constant with time. Here the vacuum energy density will eventually diverge, which has two consequences: this singularity happens in a finite time, rather than asymptotically; as it does so, vacuum repulsion will overcome the normal electromagnetic binding force of matter, so that all objects will be torn apart in the 'big rip'.

The comoving distance-redshift relation is one of the chief diagnostics of the matter content. The general definition is

$$D(z) = \int_0^z \frac{c}{H(z')} {\rm d}z'. \tag{7}$$

Perturbing this about a fiducial $\Omega_{\rm m} = 0.25$, $w = -1$ model shows a 'sensitivity multiplier' of about 5 – i.e. a measurement of w to 10% requires an accuracy of distance measures to 2%. Also, there is a near-perfect degeneracy with $\Omega_{\rm m}$, as can be seen in Fig. 1.

The other potential way in which the matter content can be diagnosed is via the growth of structure. The equation that governs the gravitational amplification of fractional density perturbations, δ, is

$$\ddot{\delta} + 2\frac{\dot{a}}{a}\dot{\delta} = \delta\left(4\pi G \rho_{\rm m} - c_s^2 k^2/a^2\right), \tag{8}$$

where k is the comoving wavenumber (or 2π times reciprocal wavelength) of a perturbation. Pressure appears through the speed of sound, c_s, and the gravitational effects appear twice in this growth equation: explicitly via $\rho_{\rm m}$ and implicitly via the factor of

$H = \dot{a}/a$ in the damping term. This growth equation in general has two solutions, one of which is decreasing in time and thus of little interest. The other one describes the growth of density fluctuations. While the universe is matter dominated and curvature is negligible, the growing mode is just $\delta = g(a) \propto a$, but this growth tends to slow at later times:

$$g(a) \propto a\, f(\Omega); \quad f(\Omega) \simeq \tfrac{5}{2}\Omega_{\rm m}\left[\Omega_{\rm m}^{4/7} - \Omega_{\rm v} + (1+\tfrac{1}{2}\Omega_{\rm m})(1+\tfrac{1}{70}\Omega_{\rm v})\right]^{-1}, \qquad (9)$$

where the approximation for the growth suppression in low-density universes (assuming $w = -1$) is due to Carroll, Press & Turner (1992). For flat models with $\Omega_{\rm m} + \Omega_{\rm v} = 1$, this says that the growth suppression is less marked than for an open universe – approximately $\Omega_{\rm m}^{0.23}$ as against $\Omega_{\rm m}^{0.65}$ if $\Lambda = 0$. This reflects the more rapid variation of $\Omega_{\rm v}$ with redshift; if the cosmological constant is important dynamically, this only became so very recently, and the universe spent more of its history in a nearly Einstein–de Sitter state by comparison with an open universe of the same $\Omega_{\rm m}$.

However, it is important to realise that, for $w \neq -1$, these standard forms do not apply, and the second-order differential equation has to be integrated numerically to obtain the growing mode. In doing this, we see from Fig. 1 that the situation is the opposite of the distance-redshift relation: the effects of changes in w and $\Omega_{\rm m}$ now have opposite signs. Note however that the sensitivity to w displays the same 'rule of 5' as for $D(z)$: $|d\ln g/dw|$ tends not to exceed 0.2.

Models for dark energy The existence of a negative-pressure component to the universe was first strongly indicated from the mid-1980s via the lack of small-scale structure in the CMB, plus indications of a low matter density from large-scale structure (e.g. Efstathiou, Sutherland & Maddox 1990). Following the more direct results from the supernova Hubble diagram in the late 1990s (Riess et al. 1998; Perlmutter et al. 1999), it is not seriously disputed that the universe contains something close in nature to a cosmological constant.

However, there are no firm physical grounds for assuming that the dark energy is indeed a simple time-independent vacuum density. In the absence of any unique or even plausible theory, it is best to be empirical and allow the equation of state w to be different from -1 or even to vary; in this case, we should regard $-3(w+1)$ as $d\ln\rho/d\ln a$, so that

$$\frac{8\pi G\rho_{\rm v}}{3H_0^2} = \Omega_{\rm v}\exp\left(\int -3[w(a)+1]\,{\rm d}\ln a\right). \qquad (10)$$

In general, we therefore need

$$H^2(a) = H_0^2\left[\Omega_{\rm v}e^{\int -3[w(a)+1]\,{\rm d}\ln a} + \Omega_{\rm m}a^{-3} + \Omega_r a^{-4} - (\Omega_{\rm total}-1)a^{-2}\right]. \qquad (11)$$

Some complete dynamical model is needed to calculate $w(a)$. Given the lack of a unique

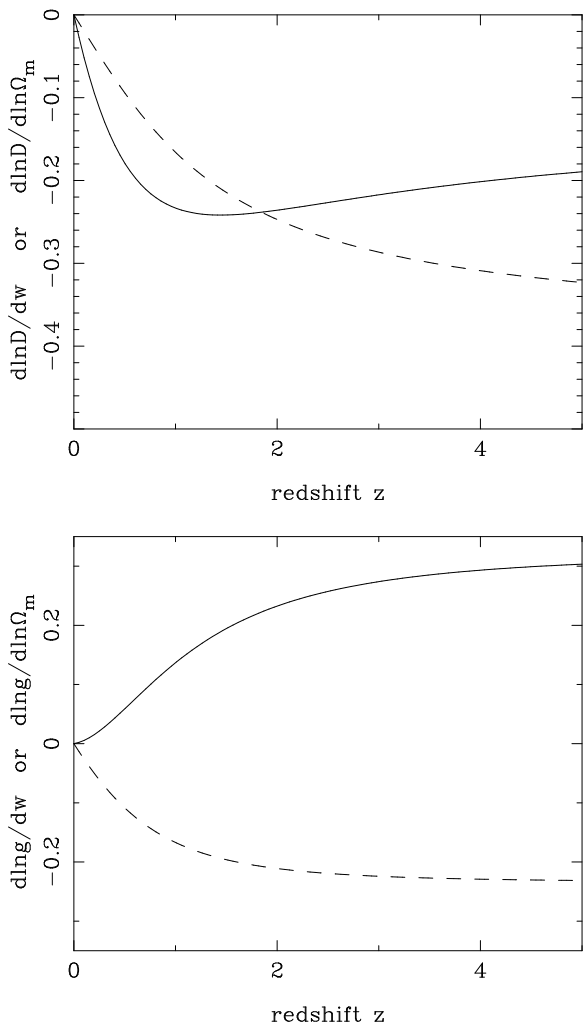

Figure 1: Perturbation of cosmological observables around a fiducial flat model with $\Omega_{\rm m} = 0.25$ and $w = -1$ for the dark energy of the distance-redshift $D(z)$ and growth factor-redshift $g(z)$ relations. The solid line shows the effect of increase in w; the dashed line the effect of an increase in $\Omega_{\rm m}$.

model, the simplest non-trivial parameterization is

$$w(a) = w_0 + w_a(1-a). \tag{12}$$

Generally here we will stick with constant w; a given experiment is mainly sensitive to w at a particular redshift of order unity, so one can treat it as constant for the purposes of comparing raw sensitivities.

The simplest physical model for dynamical vacuum energy is a scalar field, sometimes termed 'quintessence'. The Lagrangian density for a scalar field is as usual of the form of a kinetic minus a potential term:

$$\mathcal{L} = \tfrac{1}{2}\partial_\mu\phi\,\partial^\mu\phi - V(\phi). \tag{13}$$

In familiar examples of quantum fields, the potential would be a mass term:

$$V(\phi) = \tfrac{1}{2}m^2\phi^2, \tag{14}$$

where m is the mass of the field. However, it will be better to keep the potential function general at this stage. Note that we use natural units with $c = \hbar = 1$ for the remainder of this section. Gravity will be treated separately, defining the Planck mass $m_{\rm P} = (\hbar c/G)^{1/2}$, so that $G = m_{\rm P}^{-2}$ in natural units.

The Lagrangian lacks an explicit dependence on spacetime, and Noether's theorem says that in such cases there must be a conserved energy–momentum tensor. In the specific case of a scalar field, this is

$$T^{\mu\nu} = \partial^\mu\phi\partial^\nu\phi - g^{\mu\nu}\mathcal{L}. \tag{15}$$

From this, we can read off the energy density and pressure:

$$\begin{aligned} \rho &= \tfrac{1}{2}\dot\phi^2 + V(\phi) + \tfrac{1}{2}(\nabla\phi)^2 \\ p &= \tfrac{1}{2}\dot\phi^2 - V(\phi) - \tfrac{1}{6}(\nabla\phi)^2. \end{aligned} \tag{16}$$

If the field is constant both spatially and temporally, the equation of state is then $p = -\rho$, as required if the scalar field is to act as a cosmological constant; note that derivatives of the field spoil this identification.

Treating the field classically (i.e. considering the expectation value $\langle\phi\rangle$), we get from energy–momentum conservation ($T^{\mu\nu}_{;\nu} = 0$) the equation of motion

$$\ddot\phi + 3H\dot\phi - \nabla^2\phi + dV/d\phi = 0. \tag{17}$$

Solving this equation can yield any equation of state, depending on the balance between kinetic and potential terms in the solution. The extreme equations of state are: (i) vacuum-dominated, with $|V| \gg \dot\phi^2/2$, so that $p = -\rho$; (ii) kinetic-dominated, with

$|V| \ll \dot{\phi}^2/2$, so that $p = \rho$. In the first case, we know that ρ does not alter as the universe expands, so the vacuum rapidly tends to dominate over normal matter. In the second case, the equation of state is the unusual $p = \rho$, so we get the rapid behaviour $\rho \propto a^{-6}$. If a quintessence-dominated universe starts off with a large kinetic term relative to the potential, it may seem that things should always evolve in the direction of being potential-dominated. However, this ignores the detailed dynamics of the situation: for a suitable choice of potential, it is possible to have a tracker field, in which the kinetic and potential terms remain in a constant proportion, so that we can have $\rho \propto a^{-\alpha}$, where α can be anything we choose.

Putting this condition in the equation of motion shows that the potential is required to be exponential in form. More importantly, we can generalize to the case where the universe contains scalar field and ordinary matter. Suppose the latter dominates, and obeys $\rho_{\rm m} \propto a^{-\alpha}$. It is then possible to have the scalar-field density obeying the same $\rho \propto a^{-\alpha}$ law, provided

$$V(\phi) \propto \exp[-\lambda\phi/M], \tag{18}$$

where $M = m_{\rm P}/\sqrt{8\pi}$. The scalar-field density is $\rho_\phi = (\alpha/\lambda^2)\rho_{\rm total}$ (see *e.g.* Liddle & Scherrer 1999). The impressive thing about this solution is that the quintessence density stays a fixed fraction of the total, whatever the overall equation of state: it automatically scales as a^{-4} at early times, switching to a^{-3} after matter-radiation equality.

This is not quite what we need, but it shows how the effect of the overall equation of state can affect the rolling field. Because of the $3H\dot{\phi}$ term in the equation of motion, ϕ 'knows' whether or not the universe is matter dominated. This suggests that a more complicated potential than the exponential may allow the arrival of matter domination to trigger the desired Λ-like behaviour. Zlatev, Wang & Steinhardt (1999) tried to design a potential to achieve this, but a slight fine-tuning is still required, in that an energy scale $M \sim 1$ meV has to be introduced by hand, so there is still an unexplained coincidence with the energy scale of matter-radiation equality.

Modified gravity It should be emphasised that current inferences concerning dark energy rest on the assumption of the validity of the Friedmann equation, which is based on Einstein's gravitational field equations. This is the simplest possibility, but something more complex could still be permissible in general relativity: i.e. there might still be a Robertson-Walker metric, but non-standard dynamics.

The most interesting possibilities of this sort to emerge from recent work are modifications motivated by the predictions from string theory of the existence of higher dimensions. The hidden scale associated with these dimensions allows a scale dependence of the strength of gravity, which can mimic cosmic acceleration. For example, in

the DGP model (Dvali, Gabadadze & Porrati 2000), we have the relation

$$H^2(z) = H_0^2 \left(\frac{1-\Omega_{\rm m}}{2} + \sqrt{\left(\frac{1-\Omega_{\rm m}}{2}\right)^2 + \Omega_{\rm m} a^{-3}} \right)^2 \qquad (19)$$

(neglecting radiation), so that the universe tends to a de Sitter model with constant H even without an explicit vacuum energy. This particular model seems to be a less good fit than standard ΛCDM (Sawicki & Carroll 2005), but it serves to remind us that dark energy may be more complex in nature than is suggested by the standard parameterization. One way in which this can be addressed is to pursue multiple probes of dark energy within the standard framework and to search for concordance. If this fails to appear, then either the model is more complex than assumed, or there is some unidentified systematic.

An even more radical possibility under this heading is the attempt to dispense with dark matter altogether, by introducing Modified Newtonian Dynamics (MOND). This model was introduced by Milgrom in order to account for the flat rotation curves of galaxies, and for many years it remained on an ad hoc basis. However, Bekenstein (2004) has proposed a covariant generalisation in a theory whereby gravity is a mixture of tensor, vector and scalar fields (the TeVeS hypothesis). It is not yet clear whether this theory is well-defined from a field theory point of view nor whether it agrees with local constraints in the Solar System, but TeVeS certainly allows a much richer spectrum of possible tests, ranging from global cosmological models through large-scale structure and gravitational lensing. The indications are that the model still requires both dark matter and Λ in order to be consistent (Zhao et al. 2006; Skordis et al. 2006). It has also received an impressive challenge from observations of the 'bullet cluster' (Clowe et al. 2006), in which an apparently merging pair of cluster shows the X-ray emitting gas lying between the two groups of galaxies – each of which is inferred to contain dark matter on the grounds of their gravitational lensing signature. The standard interpretation is that the baryonic material is collisional, whereas the dark matter is collisionless; this object seems to dramatise that view most effectively.

3.3 The perturbed universe

It has been clear since the 1930s that galaxies are not distributed at random in the universe (Hubble 1934). For decades, our understanding of this fact was limited by the lack of a three-dimensional picture, but current studies have amassed redshifts for over 10^6 galaxies. Following the detection of structure in the CMB by NASA's COBE satellite in 1992, we are able to follow the growth of cosmological structure over a large fraction of the time between last scattering at $z \simeq 1100$ and the present. In effect, such studies pro-

vide extremely large standard rulers, which have done much to pin down the contents of the universe.

In discussing this area, it will be convenient to adopt a notation, already touched on above, in which the density (of mass, light, or any property) is expressed in terms of a dimensionless density contrast δ:

$$1 + \delta(\mathbf{x}) \equiv \rho(\mathbf{x})/\langle\rho\rangle, \tag{20}$$

where $\langle\rho\rangle$ is the global mean density. The existence of density fluctuations in the universe raises two questions: what generated them, and how do they evolve? A popular answer for the first question is inflation, in which quantum fluctuations, inflated to macroscopic scales, are able to seed density fluctuations. So far, despite some claims, this theory is not proved, although it certainly matches current data very well. The second question is answered by the growth of density perturbations through gravitational instabilities, as was discussed earlier.

The Fourier power spectrum, $P(k)$, of this fluctuation field, δ, contains a rich structure. It can be written dimensionlessly as the logarithmic contribution to the fractional density variance,

$$\Delta^2(k) \equiv \frac{k^3}{2\pi^2} P(k) \propto k^{3+n_\mathrm{s}}\, T^2(k), \tag{21}$$

where k is again the wavenumber, $T(k)$ is the matter transfer function, and n_s is the primordial scalar perturbation spectral index. This is known empirically to lie close to the 'scale-invariant' $n_\mathrm{s} = 1$, but one of the key aims in testing inflation is to measure 'tilt' in the form of $n_\mathrm{s} \neq 1$. Excitingly, the 3-year WMAP data has given the first evidence in this direction, measuring $n_\mathrm{s} \simeq 0.96$ (Spergel et al. 2006).

The transfer function is sensitive to the class of perturbation. This is normally assumed to be adiabatic, so that both nonrelativistic matter and photon density are perturbed together. The alternative is entropy or isocurvature perturbations, in which only the equation of state is altered. In the limit of very early times, these correspond to keeping the radiation uniform and perturbing the matter density only. The resulting behaviour for the transfer functions is very different for these two modes, as shown in Fig. 2. The isocurvature mode also makes rather distinct predictions for the CMB anisotropies, so that we can be confident that the initial conditions are largely adiabatic. But an isocurvature admixture at the 10% level cannot be ruled out, and this certainly relaxes many parameter constraints (e.g. Bean, Dunkley & Pierpaoli 2006).

The transfer function also depends on the density parameters, as well as on the physical properties of the dark matter. Fluctuations of wavelength smaller than the cosmological horizon have their growth affected, so that there should be a break in the spectrum at around the horizon size at the redshift of matter-radiation equality:

$$D_\mathrm{EQ}^\mathrm{H} \simeq 123\,(\Omega_\mathrm{m} h^2/0.13)^{-1}\ \mathrm{Mpc}. \tag{22}$$

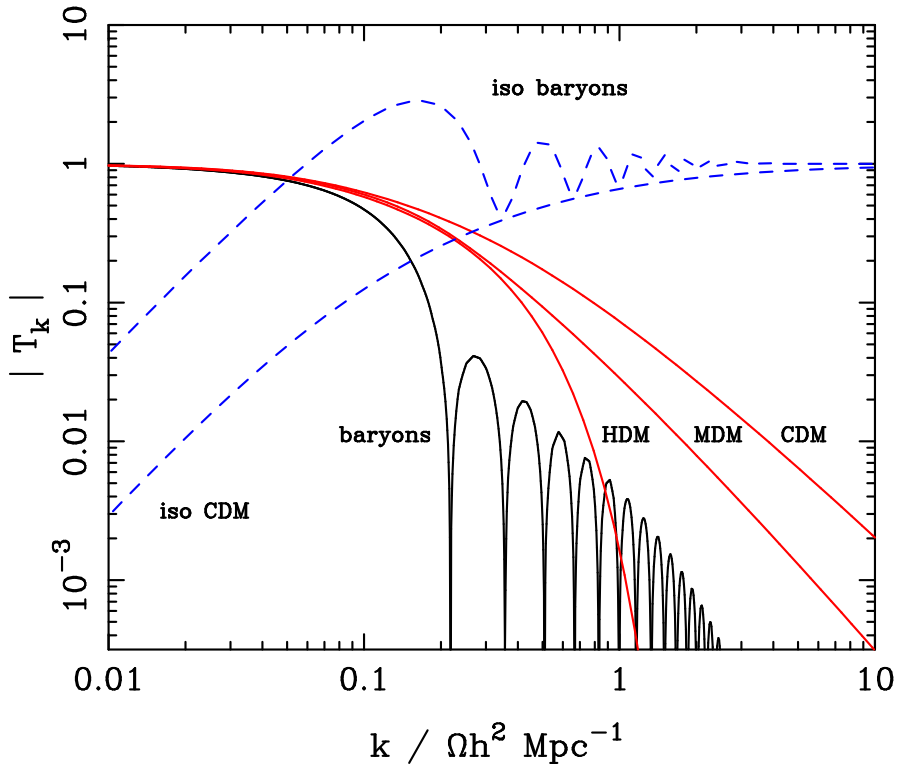

Figure 2: A plot of cosmological transfer functions for matter perturbations. Solid lines show adiabatic models, in which both matter and radiation are perturbed; dashed lines are isocurvature perturbations. A number of possible matter contents are illustrated: pure baryons; pure CDM; pure HDM. For dark-matter models, the characteristic wavenumber scales proportional to $\Omega_{\rm m}h^2$, marking the break scale corresponding to the horizon length at matter-radiation equality. The scaling for baryonic models does not obey this exactly; the plotted case corresponds to $\Omega_{\rm m} = 1$, $h = 0.5$.

In addition, small-scale perturbations will be erased by free-streaming of collisionless dark-matter particles until the point at which they become non-relativistic. This marks out the horizon size at this non-relativistic era, which depends on particle mass:

$$L_{\mathrm{free-stream}} = 112\,(m/\mathrm{eV})^{-1}\,\mathrm{Mpc}. \tag{23}$$

It is this large coherence length for the case of light neutrinos that led to such hot dark matter being rejected as the dominant constituent of the universe. We need a mass large enough that free-streaming preserves small-scale structures such as high-redshift galaxies and the Lyman-alpha forest: thus $m \gtrsim 1$ keV (unless the particle is something like the axion, which was never in thermal equilibrium). Even if the mass of the dominant dark-matter particle should turn out to be too high to affect astronomy, however, we know from neutrino-oscillation results that light neutrinos must exist with $m \gtrsim 0.05$ eV, and these can have an effect on high-precision measurements of large-scale structure. Measuring the absolute mass scale of neutrinos through such effects is important not only for particle physics, but because the neutrino effects are degenerate with changes in the vacuum equation of state, w (e.g. Goobar et al. 2006).

Finally, we should remark on the important possibility of tensor-mode perturbations, or primordial gravitational waves. These have a negligible effect on the matter distribution, and only manifest themselves via perturbations in the CMB – unless they can be detected directly via experiments sensitive to the local strain of spacetime.

3.4 Statistical methodology

The standard methodology for forecasting errors in cosmological parameters is in terms of the Fisher Matrix, which is the expected curvature matrix of the likelihood of a given model in the face of data:

$$F_{ij} = -\left\langle \frac{\partial^2 \ln L}{\partial p_i \partial p_j} \right\rangle , \tag{24}$$

where the p_i are a set of parameters characterising the model. The inverse of F_{ij} gives a pseudo-covariance matrix, such that the diagonal elements are lower limits to the true variance in a given parameter – although they are usually taken to be a reasonable estimate of the actual expected error. The Fisher matrix thus defines a multi-dimensional Gaussian ellipsoid that gives the joint confidence region for the parameters. It is straightforward to marginalize over unwanted parameters (i.e. integrating the likelihood over all values of the hidden parameters). This yields a lower-dimensional projected likelihood, which is 2D may be plotted as a confidence ellipse, as shown in several plots below (e.g. Figs 5, 12) The results of doing this can often be a little counterintuitive when experiments are combined. Here, we are inspecting the intersection of two ellipsoids in a multidimensional space, and sometimes the parameter degeneracies can work

out such that the intersection has a very compact projection onto a two-parameter plane, whereas this is not true of the individual constraints (think of two planes intersecting in a line).

Using the $w(a) = w_0 + w_a(1-a)$ model for the equation of state of dark energy, this exercise normally will show a strong correlation between w_0 and w_a. This is readily understandable: the bulk of the sensitivity comes from data at higher redshifts, so the $z = 0$ value of w is an unobserved extrapolation. It is better to assume that we are observing the value of w at some intermediate *pivot redshift*:

$$w(a) = w_{\rm pivot} + w_a(a_{\rm pivot} - a). \tag{25}$$

The pivot redshift is defined so that $w_{\rm pivot}$ and w_a are uncorrelated – in effect rotating the contours on the $w_0 - w_a$ plane. If we do not want to assume the linear model for $w(a)$, a more general approach is given by Simpson & Bridle (2006), who express the effective value of w (treated as constant) as an average over its redshift dependence, with some redshift-dependent weight. Both these weights and the simple pivot redshifts depend on the choice of some fiducial model. With reasonable justification (both from existing data, and also because it is the fiducial model that we seek to disprove), this is generally taken to be the cosmological constant case.

One question with the whole issue of measuring w and its evolution is what our target should be. In some areas of cosmology, such as the scalar spectral tilt, there are classes of simple inflationary models that make clear predictions (deviations from $n_{\rm s} = 1$ of order 1%), and a sensible first target is to test these models. With dark energy, we have much less idea what to expect. The initial detections of dark energy were made on the assumption of a cosmological constant, and this remains a common prejudice. If this is in fact the truth, how small do the errors around $w = -1$ have to be before we are convinced? Trotta (2006) gives a nice analysis of this sort of situation from a Bayesian point of view. Rather than only ever rejecting theories, he shows how it is possible to develop statistical evidence in favour of a simple model ($w = -1$ in this case). Errors on a constant w of around 0.5% would place us in this situation (unless the $w = -1$ model has been rejected before this point). This represents a 10-fold improvement on the current state of knowledge, or roughly a 100-fold expansion in data volume. This is challenging, but eminently feasible – and such advances will in any case have other astronomical motivations. Therefore, in practice the ability to confirm or disprove Λ is most likely within reach.

In the following sections we will discuss a number of astronomical methods that have the capability of yielding significant constraints on cosmological parameters via the sensitivity of their results to the growth function $g(z)$ of density perturbations and the redshift-distance relation $D(z)$. Both of these quantities contain the expansion history $a(z)$ of the universe and are thus sensitive to the function $w(z)$. Furthermore, those methods that probe the density fluctuation field can constrain the slope $n_{\rm s}$ of the primor-

dial power spectrum of density fluctuations and thus test predictions from inflationary models.

3.5 Photometric redshifts

Many of the possible projects that we describe below will require redshifts of $\sim 10^6$ to $\sim 10^9$ galaxies, most of which are faint enough to require many hours of integration on current 8m-class telescopes. Such observations may be possible with facilities we can anticipate for 2020, but are presently impossibly expensive.

Therefore, an alternative approach has been developed and tested in recent years: *photometric redshifts*. This method uses a set of photometric images in several broad-band filters and attempts to obtain an approximate redshift by isolation of the (small) effect that a given spectral feature will produce as it moves through a given bandpass. The direct approach to this problem assumes that the filter profiles are known exactly and that galaxy spectra can be expressed as a superposition of some limited set of template spectra. The results are thus potentially vulnerable to errors in the assumed filter properties and/or templates. Given a large enough calibration sample with exact spectroscopy, such errors can be removed; it is also then possible to employ 'blind' methods such as artificial neural nets, with an impressive degree of success. These methods effectively fit for the empirical redshift in multi-colour space, without needing to know about filters or spectra (see Collister & Lahav 2004).

Photometric redshift codes generate a probability distribution in redshift for each object, based on the multi-colour flux values and their estimated errors. If this probability distribution shows a single narrow peak, the corresponding redshift is a good and, most likely, correct estimate of the true redshift, and the redshift accuracy can be estimated from the width of the distribution. However, in case of very broad peaks, or multiple peaks, the interpretation and use of these redshift probabilities is less straightforward. Depending on the application, one can either discard such galaxies, take the highest peak (or the peak with the largest integrated area) as the most likely redshift, though with a potentially large error, or make use of the full redshift probability distribution.

The performance of photometric redshift estimates on a set of objects can be quantified by at least three numbers. The first is the rms deviation of the estimated redshift from the true value. Second, one characterises the deviation of the mean estimated redshift from the mean of the true redshift, say within a given photometric redshift interval. This number then yields the *bias* of the method, i.e. a systematic offset of the photometric redshifts from the true ones – this error is more of a limitation for large samples than the single-object random error. And third, there is the fraction of estimated redshifts that are grossly wrong, which are called catastrophic outliers. All these indicators

for the performance are improved if the number of photometric bands and their total λ-coverage are increased. In particular, the fraction of catastrophic outliers is substantially reduced with the inclusion of near-IR photometry, as shown in Fig. 3. The performance can also be improved by including prior information, such as assumptions regarding the evolving type- and redshift-dependent galaxy luminosity functions. In addition, the way in which the magnitudes of galaxies are measured (fixed aperture photometry vs. seeing-matched photometry) can have an important effect. See Hildebrandt et al. (2006) for a comparative study of some of these issues.

The performance of photometric redshifts depends particularly strongly on the galaxy type. Early-type galaxies are known to have very homogeneous photometric properties, due to their old stellar populations and the smallness of their intrinsic extinction. Their 4000Å break provides a clean spectral feature that yields reliable photometric redshifts, provided that the wavelength coverage is sufficiently large that this 4000Å break can be distinguished from the Lyman break, corresponding to much higher redshifts. For spiral galaxies, quite reliable redshift estimates can also be obtained. In contrast, irregular and star-forming galaxies tend to have spectra dominated by a featureless blue continuum, making redshift estimation very difficult except at the highest redshifts where UV breaks from intervening absorption can be seen.

Currently, the best performance comes from the COMBO-17 survey, which extended the method to include intermediate-width filters, for a total of 17 bands. Their brightest objects have a precision $\delta z/(1+z) \simeq 0.01$ (note the inevitable factor $1+z$, which arises when we are able to measure observed wavelengths of some feature to a given precision). For surveys with fewer bands, the fractional precision in $1+z$ is typically larger. Current photometric redshifts calibrated with deep enough spectroscopic galaxy samples have typical errors of $\Delta z/(1+z) = 0.035$ (Ilbert et al. 2006) without showing a systematic offset. The accuracy on the mean redshift is obtained via the huge number of galaxies in each bin (several tens of thousands) in this study. An rms scatter of the photometric redshifts around the true one of 3% to 5% is typical for data with several optical broad-band filters, although clearly the accuracy depends on magnitude: we expect a precision that scales with the typical magnitude error, so that the bulk of an imaging catalogue (the 5σ objects) is of little use for redshift estimation. In addition, going to fainter magnitudes, the spectroscopic redshifts also become more uncertain (and less complete), particularly affecting the 'redshift desert' between $z \simeq 1.2$ and $z \simeq 2$ where few spectroscopic signatures are located in the optical passband. Hence, the precision depends on redshift itself. We are looking to track the motion of features such as the 4000Å break though the set of bandpasses, and this procedure fails when we reach the reddest band. Thus, in order to obtain reliable photo-z's at $z \gtrsim 1$, near-IR photometry is essential.

Some applications such as weak lensing require the knowledge of the error distribution of photometric redshift to exquisite accuracy (see Sect. 7). The mean redshift

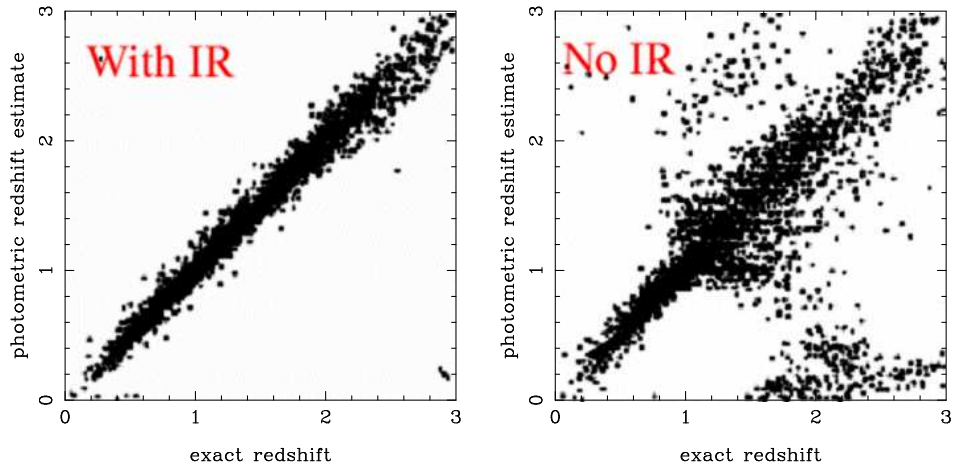

Figure 3: An illustration of how the accuracy of photometric redshift estimation is affected by the number of wavebands, based on data from R. Pelló. On the left, we show that a full optical/IR dataset (*ugrizJHK*) yields well controlled redshift estimates out to $z \simeq 3$. On the right, we see that removing the near-IR data induces catastrophic failures in the predicted redshifts at $z \gtrsim 1$.

of a given sample can be affected significantly by even a small fraction of catastrophic outliers. A key question is thus the fraction of galaxies with catastrophic or unknown photometric redshift. In principle, such objects should be identified from the redshift probability distribution obtained from the photo-z codes, but this capability is not yet routinely available. Unless we can be certain of the accuracy of each photo-z, the simple method of discarding all objects with uncertain or possibly catastrophic redshifts will not work. It is therefore much better to choose a filter set that eliminates these problems. The best filter choice depends on the redshift distribution of the underlying sample and should therefore be defined on a case by case basis.

As surveys go deeper, the typical redshift increases, so that (1) galaxies become so faint that there is no spectroscopy to calibrate the photo-z's; (2) more and more galaxies enter the redshift range $1.2 < z < 2.5$ – which cannot be sampled without the use of deep near-IR data. It is likely that the uncertainty of the redshift distribution will continue to be a dominant source of error in cosmological parameter estimation, e.g. from faint weak lensing surveys, unless we can obtain sufficiently extensive multi-colour photometry. A major step in improving the calibration of photometric redshift surveys are the VVDS and the DEEP2 spectroscopic samples on fields of the CFHT Legacy Survey fields. For much deeper surveys like those proposed with the LSST or for the JDEM/SNAP/DUNE missions, it is therefore urgent to start extremely deep visible and near infrared spectroscopic surveys that will sample galaxies at the depth of these surveys. The VIMOS instrument on the VLT has the best potential of current ESO instruments to produce spectroscopic calibration data of this sort.

4 The Cosmic Microwave Background

4.1 Current status

The anisotropies in the CMB form arguably the pre-eminent tool of modern cosmology. Almost immediately after the discovery of the background radiation, over forty years ago, cosmologists realised that the CMB could provide an entirely new way of studying the early universe. The fluctuations responsible for structures that we see today – galaxies, clusters and superclusters – must have imprinted small differences in the temperature of the CMB (so-called 'anisotropies') coming from different directions of the sky. The CMB anisotropies were first discovered in 1992 by the COBE satellite and since then the CMB sky has been mapped with great precision by many ground-based and balloon-borne experiments, culminating in the highly successful WMAP satellite.

The CMB anisotropies provide an especially powerful cosmological probe because they are imprinted at a time when the universe was only 400,000 years old. At this early stage, all of the structure in the universe is expected to be of small amplitude and to be well characterised by linear perturbation theory. The likely absence of non-linear phenomena at the time that the CMB anisotropies were generated makes them a uniquely clean probe of cosmology. We believe we understand the physical processes at that epoch and can set up and solve the corresponding equations describing anisotropies to obtain very accurate predictions that can be compared with observations.

By studying the CMB anisotropies, we are also looking back to great distances ($z \simeq 1100$). The angles subtended by structures in the CMB, together with the simple atomic physics of the recombination process that sets physical scales, provide a direct route to the geometry of the universe. This geometrical sensitivity can be used to construct an accurate inventory of the matter and energy content of the universe. In addition, the statistical properties of the CMB anisotropies provide a unique window on conditions in the ultra-early universe and, in particular, on the generation of the fluctuations.

As pointed out forcefully by Guth (1981), an early period of inflation, corresponding to near exponential expansion, offers solutions to many fundamental problems in cosmology. Inflation can explain why our universe is so nearly spatially flat without recourse to fine-tuning, since after many e-foldings of inflation spatial curvature will be negligible on the scale of the present Hubble radius. Furthermore, the fact that our entire observable universe might have arisen from a single causal patch offers an explanation of the so-called horizon problem (e.g., why is the temperature of the CMB on opposite sides of the sky so accurately the same if these regions were never in causal contact in the framework of standard Friedmann expansion?). But perhaps more importantly, inflation offers an explanation for the origin of fluctuations.

In the simplest models, inflation is driven by a single scalar field ϕ with a potential

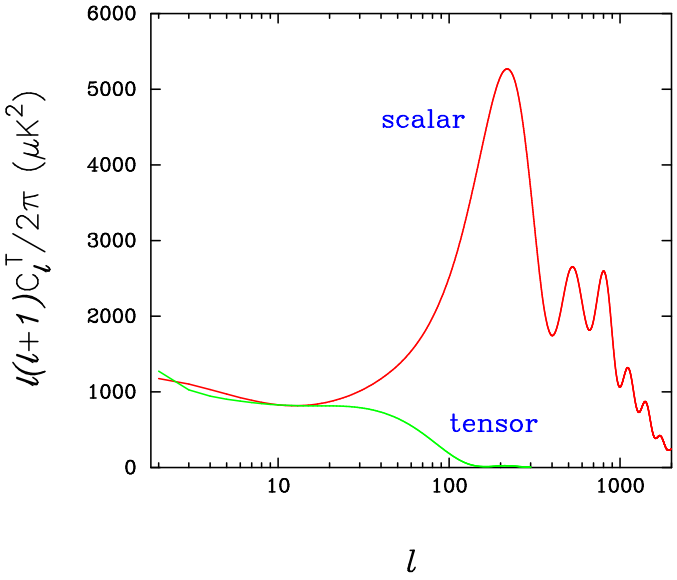

Figure 4: The contributions to the power spectrum of CMB anisotropies from scalar and tensor (gravitational wave) perturbations generated during inflation. The concordance ΛCDM model has been assumed with exactly scale-invariant initial fluctuations. The amplitudes of the tensor and scalar power spectra have been chosen arbitrarily to be equal at $\ell = 10$.

$V(\phi)$. As well as the characteristic energy density of inflation, V, inflation can be characterised by two 'slow-roll' parameters, ε and η, which are given by the first and second derivatives of V with respect to ϕ:

$$\varepsilon = \frac{m_{\rm P}^2}{16\pi}\left(\frac{V'}{V}\right)^2, \quad \eta = \frac{m_{\rm P}^2}{8\pi}\left(\frac{V''}{V}\right), \tag{26}$$

where $m_{\rm P}$ denotes the Planck mass. Generally, a successful model of inflation requires ε and η to be less than unity. In terms of these parameters, the inflationary predictions for the scalar perturbation spectral index is

$$n_{\rm s} = 1 - 6\varepsilon + 2\eta. \tag{27}$$

In simple single field models, ε and η are small during the early stages of inflation but necessarily must become of order unity for inflation to end. Thus, generically, some 'tilt' (deviation from a scale invariant spectrum, $n_{\rm s} = 1$) is expected (*e.g.* $n_{\rm s} \simeq 0.97$ for a quadratic potential $V(\phi) \propto \phi^2$). Furthermore, some deviation from a pure power law (a 'run' in the spectral index) should be seen to second order in the slow roll parameters.

In addition to scalar modes, inflation generates a spectrum of tensor perturbations (gravitational wave fluctuations), as first described by Starobinsky (1985). The char-

acteristic CMB power spectra of these two modes are shown in Fig. 4 for the concordance Λ-dominated cosmology favoured by WMAP. The relative amplitude of tensor and scalar contributions, r, is given to first order by the inflationary parameter ε alone:

$$r \equiv \frac{C_\ell^{\rm T}}{C_\ell^{\rm S}} \simeq 12\varepsilon. \tag{28}$$

Determination of the scalar spectral index $n_{\rm s}$ and the tensor-scalar ratio r thus provides important information on the slow roll parameters and hence on the shape of the inflationary potential $V(\phi)$.

The amplitude of the tensor component unambiguously fixes the energy scale of inflation,

$$V^{1/4} \simeq 3.3 \times 10^{16} r^{1/4}\ {\rm GeV}. \tag{29}$$

The detection of a tensor mode, via its signature in the polarization of the CMB, is an important target for future experiments. Such a detection would confirm that inflation really took place. It would determine the energy scale of inflation – a key discriminant between physical models of inflation – and would constrain the dynamics of the inflationary phase.

Observations of the CMB, and in particular from the WMAP satellite, have revolutionised our knowledge of cosmology. These observations favour a 'concordance' cosmology in which the universe is spatially flat and currently dominated by dark energy. However, even after three years of WMAP data, we still have only crude constraints on the dynamics of inflation. The data are consistent with an adiabatic spectrum of fluctuations generated during an inflationary phase, but the tensor mode has not yet been detected and it is not known whether there are other contributions to the fluctuations arising, for example, from cosmic strings or isocurvature perturbations (entropy perturbations, in which the photon-to-matter ratio varies). The third year WMAP data give tentative indications of a slight tilt in the scalar spectral index ($n_{\rm s} \simeq 0.96$) and at face value marginally exclude quartic potentials $V(\phi) \propto \phi^4$. Current constraints on r and $n_{\rm s}$ from WMAP and other data are summarized in Fig. 5.

4.2 Future prospects

It is expected that Planck will effectively complete the mapping of the primordial temperature pattern in the CMB. For $\ell \lesssim 2000$ the temperature power spectrum from Planck will be limited by cosmic variance. At higher multipoles, beam calibration uncertainties, unresolved point-sources and various other factors will need to be understood in order to disentangle the cosmological CMB signal. At these small angular scales, non-linear anisotropies from *e.g.* the Sunyaev–Zeldovich and Ostriker–Vishniac effects will

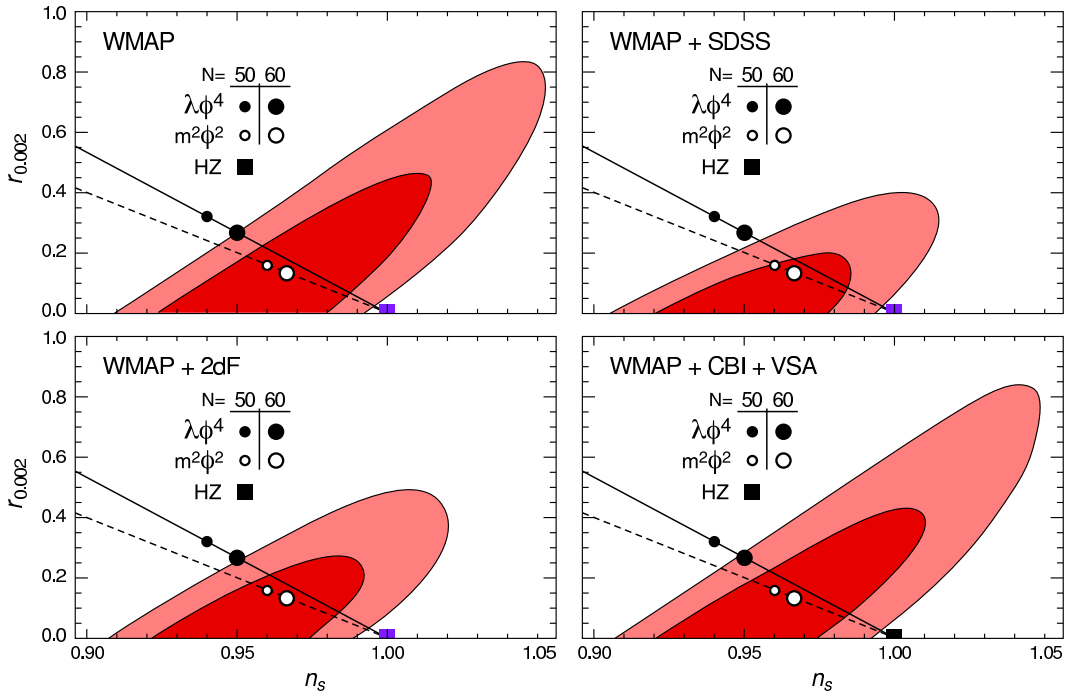

Figure 5: The marginalized 68 and 95 percentile confidence contours on the inflationary $r - n_s$ plane for WMAP3 data combined with other data sets (Spergel et al. 2006). Upper left panel shows WMAP data alone. Lower left and upper right panels show WMAP data combined with 2dFGRS and SDSS redshift survey data on galaxy clustering. Lower right panel shows WMAP combined with CMB measurements of smaller scale anisotropies. The lines show predictions for power-law potentials with $N = 60$ and $N = 50$ e-folds of inflation from the time that fluctuations on our present horizon scale were frozen until the end of inflation. Filled and open circles show the predictions for quartic and quadratic potentials respectively.

become important, as will gravitational lensing of the CMB. Planck will have polarization sensitivity over the frequency range 30–353 GHz and should provide an accurate estimate of the polarization power spectrum up to $\ell \sim 1000$.

High sensitivity polarization measurements will be an especially important goal for future CMB experiments. The polarization arises from the Thomson scattering of an anisotropic photon distribution, especially its quadrupolar anisotropy. The resulting linear polarization pattern on the sky can be decomposed into scalar E-modes and pseudo-scalar B-modes. These patterns are illustrated in Fig. 6, and are similar to the phenomenon whereby a 3D vector field can be decomposed into the gradient of a scalar potential, plus the curl of a vector potential. Here, polarization is represented by a 2×2 symmetric matrix, whose components γ_{ij} can be constructed from symmetric and antisymmetric combinations of a double derivative $\partial_i \partial_j$ acting on potentials. This decomposition was initially introduced in the context of gravitational-lens shear, which has the same mathematical properties as polarization, by Kaiser (1992) and Stebbins (1996). Scalar primordial perturbations generate only an E-mode polarization signal, while tensor perturbations generate E- and B-modes of roughly comparable amplitudes (e.g. Zaldarriaga & Seljak 1997; Kamionkowski, Kosowsky & Stebbins 1997). The detection of a primordial B-mode polarization pattern in the CMB would therefore provide unambiguous evidence for a stochastic background of gravitational waves generated during inflation. A B-mode detection would thus prove that inflation happened, and would determine the energy scale of inflation.

However, the detection of primordial B-modes from inflation poses a challenging problem for experimentalists. The *indirect* limits of $r \lesssim 0.4$ set by WMAP3 (Fig. 5) translate to an rms B-mode signal of less than 0.35μK on the sky. This is to be compared with an rms of 160μK for the temperature anisotropies and 8μK for the E-mode signal. How well will Planck do in measuring these small polarization signals? Already the Planck HFI bolometer noise figures are all below the photon noise for all CMB channels, with the exception of the polarized 353-GHz channel. The readout electronics shows white noise at the level 6 nV/Hz$^{1/2}$ from 16 mHz to 200 Hz (between the sampling period and the 1 minute spin period), comparable to or below the photon noise. Thus Planck HFI is fundamentally photon noise limited. Yet even so, the detection of B-modes will pose a formidable challenge to Planck.

This is illustrated by Fig. 7, which shows the errors on C_ℓ^B expected from Planck for a model with r arbitrarily set to 0.1. The figure suggests that for $r = 0.1$ Planck can characterise the primordial power spectrum in around four multipole bands. The B-mode polarization signal generated by weak gravitational lensing (which is, of course, independent of r) dominates the primary signal above $\ell \simeq 150$. At the very least, this lensing-induced signal should be detectable by Planck. However, even if systematic errors and polarised Galactic emission can be kept under control, Planck will at best only be able to detect tensor modes from inflation if the tensor-scalar ratio is greater

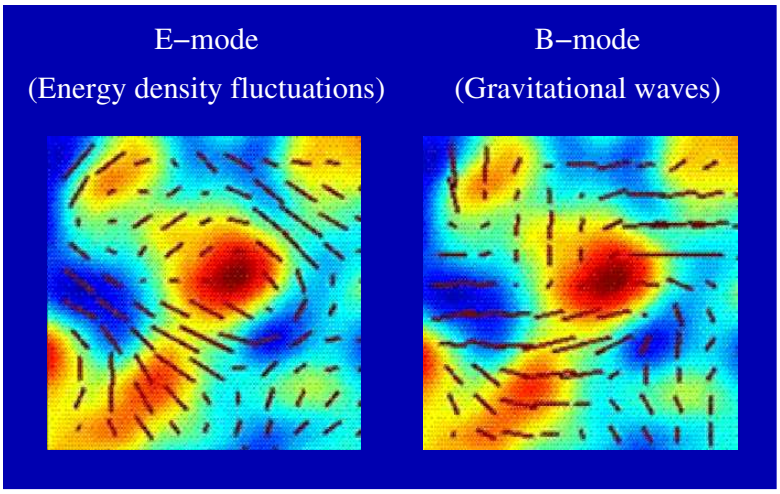

Figure 6: An illustration of the two modes of CMB polarization, and how they might be expected to correlate with total intensity. The B-mode pattern resembles the E-mode pattern but with all polars (indicated by the sticks) rotated by 45°. Scalar perturbation modes generate E-mode polarization only, whereas tensor perturbations generate both modes. The B-mode signal is thus a unique signature of the presence of primordial gravitational waves. An analogous decomposition exists for the image shear field induced in gravitational lensing. Adapted from Seljak & Zaldarriaga (1998).

than about 10 percent.

The key to achieving even higher sensitivities than Planck is to build experiments with large *arrays* of polarization sensitive detectors. This is being done for ground-based experiments (for example, Clover will use large bolometer arrays, while QUIET will use large arrays of coherent detectors) and in future balloon experiments (*e.g.* SPIDER, which plans to map about half the sky at low angular resolution using large bolometer arrays). In addition to these experiments, a number of studies are in progress in Europe and the USA for a B-mode optimised satellite designed to map the polarization pattern at high sensitivity over the whole sky.

What does theory predict for the energy scale of inflation and the amplitude of the tensor component? Many theoretical models of inflation can be grouped into one of two classes, 'chaotic' inflation in which the inflaton potential has a simple polynomial type form and 'hybrid' inflation in which the potential is relatively flat but inflation ends abruptly (as happens in string-inspired brane inflation models or because the inflationary dynamics is controlled by more than one scalar field). In chaotic inflationary models, the predicted tensor-scalar ratio is expected to be observably high, with $r \gtrsim 10^{-2}$, while in hybrid-type models the value of r could be as little as 10^{-10}, or even lower. There is therefore no guarantee that the amplitude of the tensor component will be high enough to permit detection.

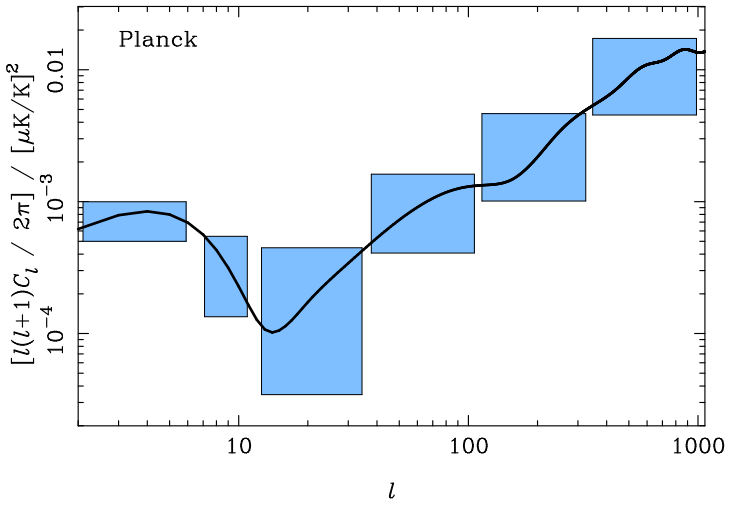

Figure 7: Forecasts for the $\pm 1\sigma$ errors on the magnetic polarization power spectrum C_ℓ^B from Planck, assuming $r = 0.1$. Above $\ell \sim 150$ the primary spectrum is swamped by weak gravitational lensing of the E-modes.

Nevertheless, CMB experiments designed to probe tensor-scalar ratios as low as $r \sim 10^{-2}$ are feasible and well motivated. Chaotic inflation models have played an important role in cosmology and, if they are correct, a tensor mode should be detectable. Inflation would then be fact, rather than conjecture. Also, all such models involve high field values in excess of the Planck scale. The physics underlying such models is therefore exotic and probes new territory beyond the realms of conventional field theory. If, on the other hand, tensor modes are not detected at this level, then this would rule out chaotic inflation and point towards an abrupt end to inflation. If this is the case, it may be more profitable to design high angular resolution experiments to search for signatures of an abrupt end to inflation (*e.g.* from cosmic strings) rather than focusing single-mindedly on searching for primordial tensor modes of even lower amplitude.

A detection of the intrinsic B-modes will require extremely good foreground removal, which will require a broad frequency coverage. The nature of the polarized foregrounds is not known in great detail, although WMAP has provided important new information on the Galactic polarized synchrotron contribution. The WMAP data suggest that the optimal frequency for measuring primordial CMB polarization at low multipoles, $\ell \lesssim 30$, is about 70 GHz, though the optimal value may be higher (perhaps 100 GHz) at higher multipoles. Realistically, to achieve a precision of $r \sim 10^{-2}$ will require sufficient sensitivity and frequency coverage to remove foregrounds using the internal data of the experiment itself, rather than relying on detailed modelling and/or extrapolation from data at different frequencies and angular resolutions. Ground-based experiments, even if they fail to detect a primordial tensor mode, will provide valuable information of the Galactic polarized synchrotron component and anomalous dust-

correlated emission below 50 GHz. Ultimately, the best control of foregrounds, particularly over large areas of the sky, would come from a B-mode optimised satellite unconstrained by atmospheric absorption and emission covering as wide a frequency range as possible (say 70 – 500 GHz for a satellite flying bolometer arrays).

In addition to the primary goal of detecting gravitational waves from inflation, a B-mode optimised satellite experiment could also tackle the following problems:

• Measuring the weak lensing effects in CMB polarization, which would result in improved constraints on neutrino properties and the physics of dark energy.

• Constrain the history of reionizaton and the astrophysical processes that ended the dark ages with a cosmic variance-limited measurement of the large-scale E-mode polarization signal.

• Explore whether anomalous features, such as multipole alignments, seen in the WMAP temperature maps are also present in polarization.

• Search for the B-mode signal of cosmic strings predicted by models of brane inflation.

• Search for non-Gaussian signatures expected in some inflation models (e.g. Bartolo et al. 2004). This is one of the main ways to distinguish different models for the generation of perturbations (single-field inflation vs multiple-field vs curvaton etc.).

Although most of this discussion has been focused on the detection of B-mode anisotropies, there is still much science to be extracted from precision measurements of temperature anisotropies on smaller angular scales than those accessible to Planck. Several large projects are underway with sub-arcminute resolution designed to detect large samples of galaxy clusters via the Sunyaev-Zeldovich (SZ) effect (for example, ACT and SPT in the USA, AMI and APEX in Europe). These surveys will be especially useful in constraining the amplitude of the primordial fluctuations and probing the evolution of fluctuations. In combination with other data, large SZ surveys will provide strong constraints on the nature of dark energy. To fully utilise the power of such surveys, the CMB SZ surveys must be supplemented by optical and infra-red imaging surveys to provide photometric redshifts for the clusters, and to provide structural parameters. Associated X-ray observations would provide valuable information on the physical properties of the hot intra-cluster gas. The high amplitude in the temperature power spectrum at $\ell \gtrsim 2000$ observed by the CBI experiment is still not understood. It is important to continue high resolution interferometric observations of the CMB over a range of frequencies to resolve this discrepancy.[1] Finally, since weak gravitational lensing generates B-modes with an effective amplitude of $r \simeq 10^{-2}$, low resolution ground

[1]Possible explanations for the CBI excess include: inaccurate subtraction of point sources; a high amplitude SZ signal; modified structure growth rates arising from a dynamic 'quintessence' field.

based experiments will be limited to a statistical detection of the primordial B-mode polarization signal and will not be able to improve on this limit no matter what their sensitivity. An all-sky B-mode satellite experiment could, in principle, achieve a tighter limit of $r \sim 10^{-3}$ by measuring the 'reionization' B-mode bump at $\ell \lesssim 10$ (see Fig. 7), but of course, this is conditional on understanding large-scale polarized foregrounds at this level. To achieve even lower values of r than this via CMB polarization will require reconstruction of the weak lensing deflection field. But to do this, a fundamentally different strategy is required – since an angular resolution of about an arcminute is required to map the weak lensing potential. Thus probing below $r \sim 10^{-2} - 10^{-3}$ will be formidably difficult, even if polarized foregrounds can be controlled at these levels. A high sensitivity, high angular resolution polarization experiment would be required covering a large part of the sky. It is premature to contemplate such an experiment until (at least) polarized foregrounds are better understood and experiments have already ruled out inflationary models with $r \gtrsim 10^{-2}$. There is, however, a strong case for measuring the weak gravitational potential by mapping restricted patches of the CMB sky at high sensitivity and angular resolution. This type of measurement would be complementary to conventional weak lensing surveys based on the distortion of galaxy images.

4.3 Conclusions on the CMB

In summary, there is a compelling case to continue studies of the CMB beyond Planck. In particular, a high priority should be given to sensitive polarization measurements of the CMB, from balloons and the ground, culminating in a B-mode optimised satellite mission. We make the following specific proposals:

• Continue to develop polarization-optimised ground-based and sub-orbital CMB experiments.

• Invest funds in developing large arrays of bolometers and coherent detectors.

• Investigate fully the scientific case and design of a low resolution ($\sim 30''$) B-mode optimised satellite. This will require: (i) identifying a suitable detector technology and associated cryogenics; (ii) optimising the frequency range to subtract polarized foregrounds to very low levels; (iii) determining a suitable scanning strategy and method of modulating the polarization pattern seen by the detectors; (iv) assessment of stray-light, polarized point sources and other potentially limiting systematic effects.

• Support specialised ground-based measurements designed to provide information on polarised foregrounds as, for example, measurements of the polarization of radio and sub-millimetre sources.

• Continue support for high-resolution experiments to measure the Sunyaev–Zeldovich clusters, using both targeted observations and surveys of 'blank' fields of sky.

• Investigate the development of high-sensitivity interferometers to measure accurately the non-linear contributions to the CMB power spectrum at multipoles $\ell \gtrsim 2000$ and to study weak lensing of the CMB.

5 Large-scale structure

5.1 Principles

The CMB contains information about the early seeds of cosmological structure formation. Its natural counterpart in the local universe is the distribution of galaxies that arises as a result of gravitational amplification of these early small density fluctuations. The pattern of present-day cosmological density inhomogeneities contains certain preferred length-scales, which permit large-scale structure to be used in a geometrical manner to diagnose the global makeup of the universe. These characteristic scales are related to the horizon lengths at certain key times – i.e. to the distance over which causal influences can propagate. There are two main length-scales of interest: the horizon at matter-radiation equality ($D_{\rm EQ}$) and the acoustic horizon at last scattering ($D_{\rm LS}$). The former governs the general break scale in the matter power spectrum and is contained in the transfer function $T(k)$, and the latter determines the *Baryon Acoustic Oscillations* (BAO) by which the power is modulated through sound waves prior to recombination:

$$\begin{aligned} D^{\rm H}_{\rm EQ} &\simeq 123\,(\Omega_{\rm m}h^2/0.13)^{-1}\ {\rm Mpc} \\ D^{\rm H}_{\rm LS} &\simeq 147\,(\Omega_{\rm m}h^2/0.13)^{-0.25}(\Omega_{\rm b}h^2/0.023)^{-0.08}\ {\rm Mpc}, \end{aligned} \tag{30}$$

Distances deduced from redshift surveys automatically include an inverse power of the Hubble parameter, being measured in units of $h^{-1}\,$Mpc. Thus the main length deduced from LSS scales as $(\Omega_{\rm m}h)^{-1}$, and so $\Omega_{\rm m}h$ is the main parameter that can be measured, plus the baryon fraction $f_{\rm b} \equiv \Omega_{\rm b}/\Omega_{\rm m}$ if the baryon oscillations are detected.

These scales can be seen projected on the sky via the CMB power spectrum. Following the superb recent 3-year WMAP results (Spergel et al. 2006), the detailed shape of the CMB power spectrum breaks many of the degeneracies implicit in the above scaling formulae. Thus, the combination of observations of cosmological perturbations at $z \simeq 1100$ and $z \simeq 0$ makes an appealingly self-consistent package within which most of the cosmological parameters can be determined very accurately.

The power spectrum The practical tool for measuring the length-scales encoded in large-scale structure is the density power spectrum. This is factorized into a product of the primordial spectrum and the transfer function, which controls the different growth rates of perturbations of different wavelength, according to the matter content of the universe. The primordial spectrum is generally taken to be a power law, $P(k) \propto k^{n_s}$, although the improving accuracy of the data is such that it is increasingly common to consider the *running* of the spectral index – i.e. a curvature of $P(k)$ in log-log space. The power spectrum is best presented in dimensionless form, as the contribution to the fractional variance in density per unit $\ln k$. In 3D, this is $\Delta^2(k) \propto k^3 P(k)$.

We can probe large-scale density fluctuations by Fourier transforming the galaxy

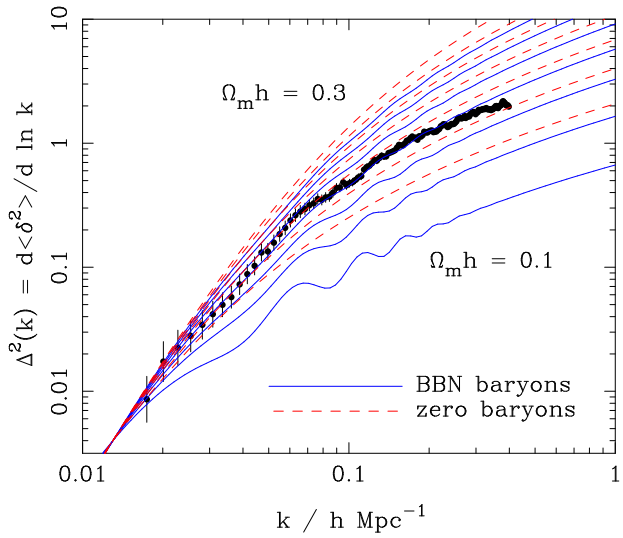

Figure 8: The 2dFGRS redshift-space dimensionless power spectrum, $\Delta^2(k)$. The solid and dashed lines show various CDM models, all assuming $n = 1$. For the case with non-negligible baryon content, a big-bang nucleosynthesis value of $\Omega_b h^2 = 0.02$ is assumed, together with $h = 0.7$. A good fit is clearly obtained for $\Omega_m h \simeq 0.2$. Note the baryon acoustic oscillations that develop as the baryon fraction is raised, and how their location depends on the overall density.

number density field. The result is limited by two forms of statistical noise: *cosmic variance*, reflecting the finite volume sampled, and *shot noise*, reflecting the small-scale nature of the galaxy distribution as a discrete point process. Both these effects can be seen in the standard expression for the fractional error in the galaxy power spectrum $P_g(k)$. For a survey of volume V and galaxy number density n, measuring power in a wavenumber range Δk, this is given by

$$\sigma_{\ln P} = \frac{2\pi}{(Vk^2\Delta k)^{1/2}} \left(\frac{1+nP_g}{nP_g} \right) \tag{31}$$

(Feldman, Kaiser & Peacock 1994). Provided nP_g is greater than of order unity, this represents largely a cosmic-variance limited measurement. Assuming that there are more targets than our capability for simultaneous spectroscopy, the volume covered in a fixed time scales as $1/n$, so that the overall power error is minimised at $nP_g = 1$ (Kaiser 1986).

Bias and other nonlinearities The use of the galaxy power spectrum in cosmology faces a number of practical obstacles compared to the ideal in which the linear power spectrum at $z = 0$ could be measured. Most fundamentally, small-scale information in the spectrum is destroyed by cosmic evolution up to the present because the modes involved have become nonlinear. The point at which $\Delta^2(k)$ reaches unity is around $0.25\,h\,\mathrm{Mpc}^{-1}$, and the power at smaller scales reflects mainly the internal structure of

dark matter haloes, rather than any relic from early times (this is the view of the 'halo model': see e.g. Cooray & Sheth 2002). Even for somewhat larger scales, the power spectrum is significantly altered in shape, and probably we can only measure the shape of the linear spectrum cleanly for $k < 0.1\,h\mathrm{Mpc}^{-1}$. In order to use the information at smaller scales to $k \simeq 0.2\,h\mathrm{Mpc}^{-1}$, an approximate nonlinear correction has to be made; alternatively, measurements have to be made at higher redshifts where non-linear evolution has had less effect on these smaller scales, a fact employed by the Lyα forest technique (see Sect. 9).

Nonlinear modification of the density power spectrum is not the only issue. One of the main results of nonlinear evolution is that the CDM fragments into a population of dark-matter haloes and subhaloes, and the latter are the hosts of galaxies. Haloes of different masses and in different environments will form stars with varying degrees of efficiency, so the galaxy distribution has a complex relation to the overall density field. This changes not only the small-scale shape of the galaxy power spectrum, but also the overall normalization even in the long-wavelength limit. Thus we have absolute and relative *biased clustering*. The scale-dependent relative bias means there is a danger of deducing a systematically incorrect value of $\Omega_{\mathrm{m}}h$ from the shape of the galaxy spectrum. This was one of the main topics addressed in the final 2dFGRS power spectrum paper (Cole et al. 2005), where it was concluded that an empirical correction could be made so that the shape of the power spectrum was unaffected within the random measuring errors. For $k < 0.15\,h\mathrm{Mpc}^{-1}$, the correction is at most 10% in power, so it is not a large effect – but this aspect will need more detailed treatment in future surveys of greater size and precision.

The absolute level of bias is a separate problem, and a frustrating one: a direct measurement of the normalization of the power spectrum (conventionally given via σ_8, which is the fractional linear density rms when smoothed with a sphere of radius $8h^{-1}\,\mathrm{Mpc}$) would allow us to measure the amount of perturbation growth since last scattering, which is sensitive to the properties of the dark energy. Within the framework of galaxy redshift surveys, two methods have been used to try to overcome this barrier. Higher-order clustering can distinguish between a two-point amplitude that is high because σ_8 is high and one where σ_8 is low but the degree of bias is high. In essence the distinguishing factor is the filamentary character of the galaxy distribution that arises with increased dynamical evolution. This can be diagnosed by a three-point statistic such as the bispectrum; in this way, Verde et al. (2002) were able to show that 2dFGRS galaxies were approximately unbiased. An alternative route is by exploiting the fact that 3D clustering measurements are made in redshift space, where the radial coordinate is affected by peculiar velocities associated with structure growth. This introduces a characteristic anisotropy in the clustering pattern, which depends on the combination $\beta \equiv \Omega_{\mathrm{m}}^{0.6}/b$, where b is the linear bias parameter. This has been measured via detection of the anisotropy signal, but so far only at a level of precision of around 15% (Peacock et al. 2001). To be useful for dark energy studies, this accuracy will need to be very

Table 1: Local galaxy redshift surveys. The numbers in brackets represent the size of samples not yet analyzed.

Survey	Depth	N_z	Ref
2dFGRS	$b_J < 19.45$	221,414	Cole et al. (2005)
SDSS	$r < 17.77$	205,443 (674,749)	Tegmark et al. (2004)
6dFGS	$K < 14$	83,014 (167,133)	Jones et al. (2005)

substantially improved, to better than 1% (a measurement of σ_8 to this precision would yield w to 5%, as shown earlier). A novel method to determine the bias factor directly consists in measuring the cross-correlation between galaxies and the shear from weak gravitational lensing, as will be discussed in Sect. 7

5.2 Current status

Local clustering The current state of the art in studying LSS in the local universe (defined arbitrarily as corresponding to $z < 0.2$) is given by the 2dFGRS, SDSS and 6dFGS surveys. Their properties are summarized in Table 1, and they collectively establish the 3D positions of around 1,000,000 galaxies.

As discussed earlier, measurements of the galaxy power spectrum principally yield an estimate of $\Omega_m h$ (in a manner that is degenerate with the assumed spectral index n_s) and the baryon fraction. These constraints have the greatest value in combination with CMB data, and the most accurate parameter estimates in the 3-year WMAP study of Spergel et al. (2006) come in combination with the 2dFGRS data. Earlier CMB datasets lacked the power to break degeneracies such as that between Ω_m and h very strongly, but the latest WMAP data allow this do be done, so that the individual parameters and thus the key horizon lengths can be estimated. Datasets at lower redshifts probe the parameters in a different way, which also depends on the assumed value of w: either directly from $D(z)$ as in SNe, or via the horizon scales as in LSS. Consistency is only obtained for a range of values of w, and the full CMB+LSS+SNe combination already yields impressive accuracy:

$$w = -0.926^{+0.051}_{-0.075} \tag{32}$$

(assuming w to be constant and a spatially flat model); this number is the marginalized limit from the full multi-dimensional parameter constraints, as in Fig. 9, and is derived

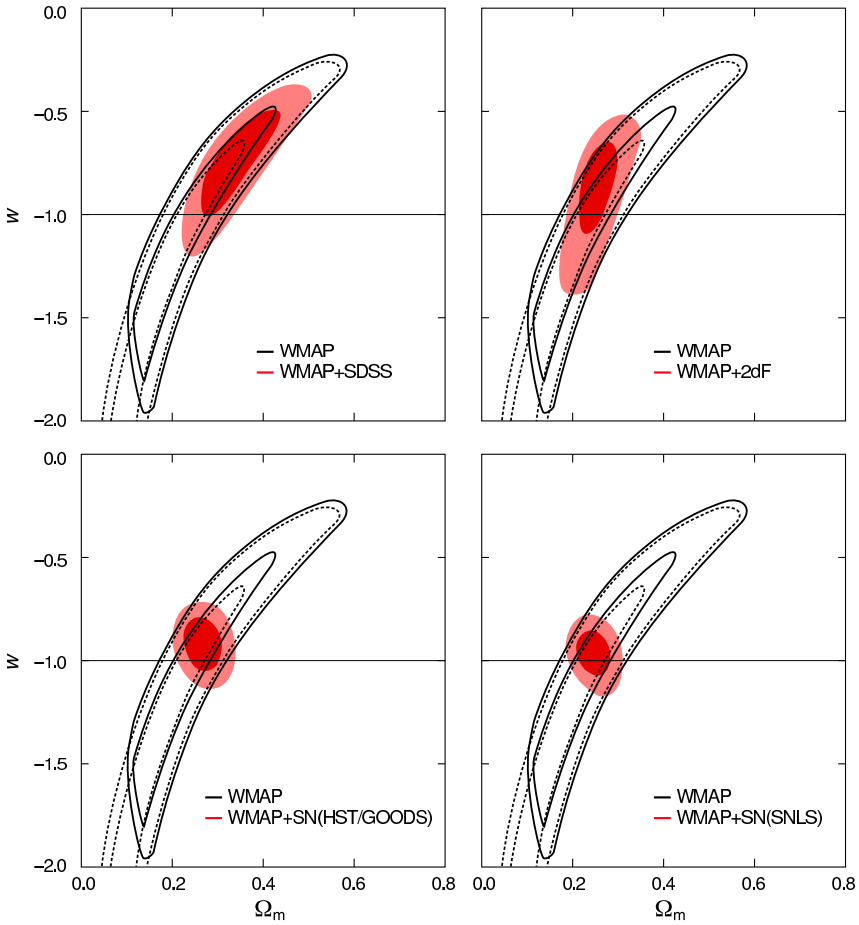

Figure 9: Confidence contours on the plane of w vs $\Omega_{\rm m}$ from WMAP year-3 results, allowing for dark-energy perturbations with c as the speed of sound (Spergel et al. 2006). It is assumed that w does not evolve, and also that the universe is spatially flat, although this latter assumption is not so critical.

assuming the SNe datasets to be independent. Any future experiment must aim for a substantial improvement on this baseline figure.

High-redshift clustering Current activity in redshift surveys is summarized in Table 2; it tends to concentrate at higher redshifts, under two distinct headings. Over the intermediate range $0.2 \lesssim z \lesssim 0.7$, Luminous Red Galaxies have been selected from the SDSS over areas of several thousand square degrees. At the other extreme, we have deeper pencil-beam surveys covering a handful of square degrees, but extending to $z \simeq 3$ or beyond.

Table 2: High-redshift galaxy surveys. We include samples based on photometric redshifts as well as full spectroscopy (denoted by '(p)'.)

Survey	Depth	N_z	Ref
COMBO-17	$R < 24$	25,000(p)	Bell et al. (2004)
VVDS	$I_{\rm AB} < 24$	11,564	Le Fèvre et al. (2004)
DEEP2	$R_{\rm AB} < 24.1$	30,000	Coil et al. (2006)
CFHTLS-VVDS	$I_{\rm AB} < 24$	550,000	Ilbert et al. (2006)
COSMOS	$I_{\rm AB} < 25.5$	300,000(p)	Scoville et al. (2006)
SDSS LRG		46,748	Eisenstein et al. (2005)
SDSS LRG		600,000(p)	Padmanabhan et al. (2006)

5.3 Future LSS experiments

It seems likely that future LSS experiments in fundamental cosmology will focus on the BAO signature. This is because it is a sharp feature in the power spectrum, and thus defines a length-scale that is relatively immune to the slow tilting of the spectrum introduced by nonlinearities, scale-dependent bias etc. Furthermore, the BAO signature has a direct and clean relation to the corresponding oscillations in the CMB power spectrum (Fig. 10).

Assuming that the survey of interest can be made to operate somewhere near the optimal number density with $nP_{\rm g} = 1$, the following rule of thumb gives the accuracy with which $D(z)$ can be measured by picking out the acoustic scale:

$$\%\ \text{error in}\ D(z) = (V/5h^{-3}\,\text{Gpc})^{-1/2}\ (k_{\rm max}/0.2h\,\text{Mpc}^{-1})^{-1/2}. \qquad (33)$$

From the earlier discussion of nonlinearities, one would not want to push much beyond $k = 0.2h\,\text{Mpc}^{-1}$. It is sometimes claimed that the high-k limit in BAO analyses should be increased at high redshift because the density field is less evolved at this point. The problem with this argument is that, precisely because of this evolution, the galaxies that are found at these distances are rarer and more strongly biased. Fig. 11 contrasts the mass and galaxy power spectra at various epochs. To some extent, this is encouraging for $z = 3$: the nonlinear mass spectrum clearly shows a third peak at $k \simeq 0.2h\,\text{Mpc}^{-1}$, which is not really apparent at either $z = 0$ or $z = 1$. On the other hand, the shapes of the galaxy and mass power spectra start to diverge at smaller k at $z = 3$ than at $z = 1$, reflecting the larger degree of bias for galaxies at that redshift – and indeed the galaxy spectrum shows no more evidence for a third peak at $z = 3$ than it does at $z = 1$. This indicates that one should be extremely cautious about expecting to use galaxy data beyond the second BAO peak at any redshift.

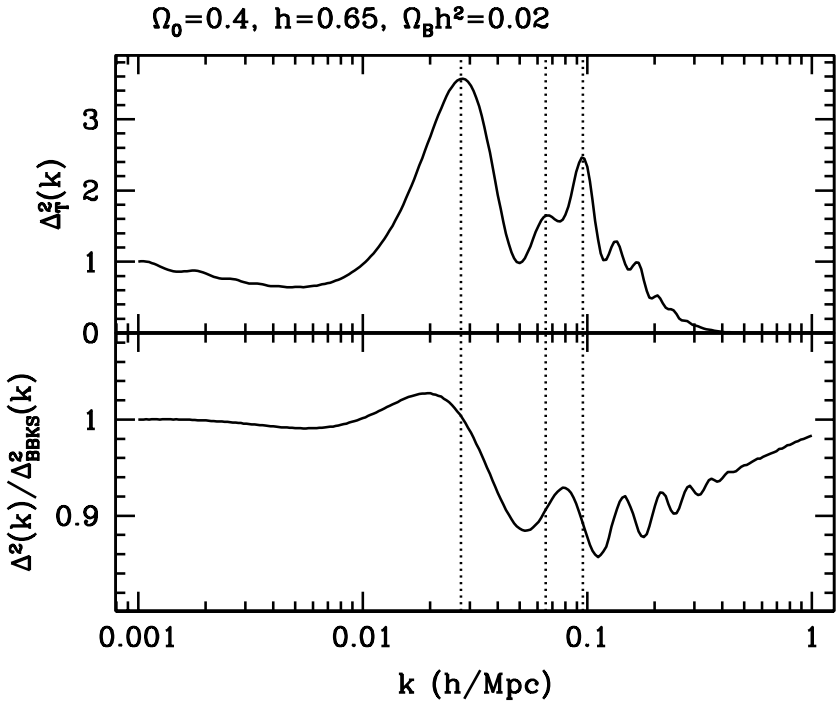

Figure 10: Acoustic oscillations in the radiation-baryon fluid imprint a pattern of harmonics in the Fourier spectrum of both CMB and density fluctuations (e.g. Meiksin, White & Peacock 1999). In the latter case for which the ratio of the power spectrum to that of a model with zero baryon content is plotted in the lower panel, the effect is much smaller, because the dominant dark matter has no intrinsic oscillations. Nevertheless, features corresponding to the same physical effect can be picked out at low and high redshift, opening the way to a relatively clean geometrical tool in cosmology.

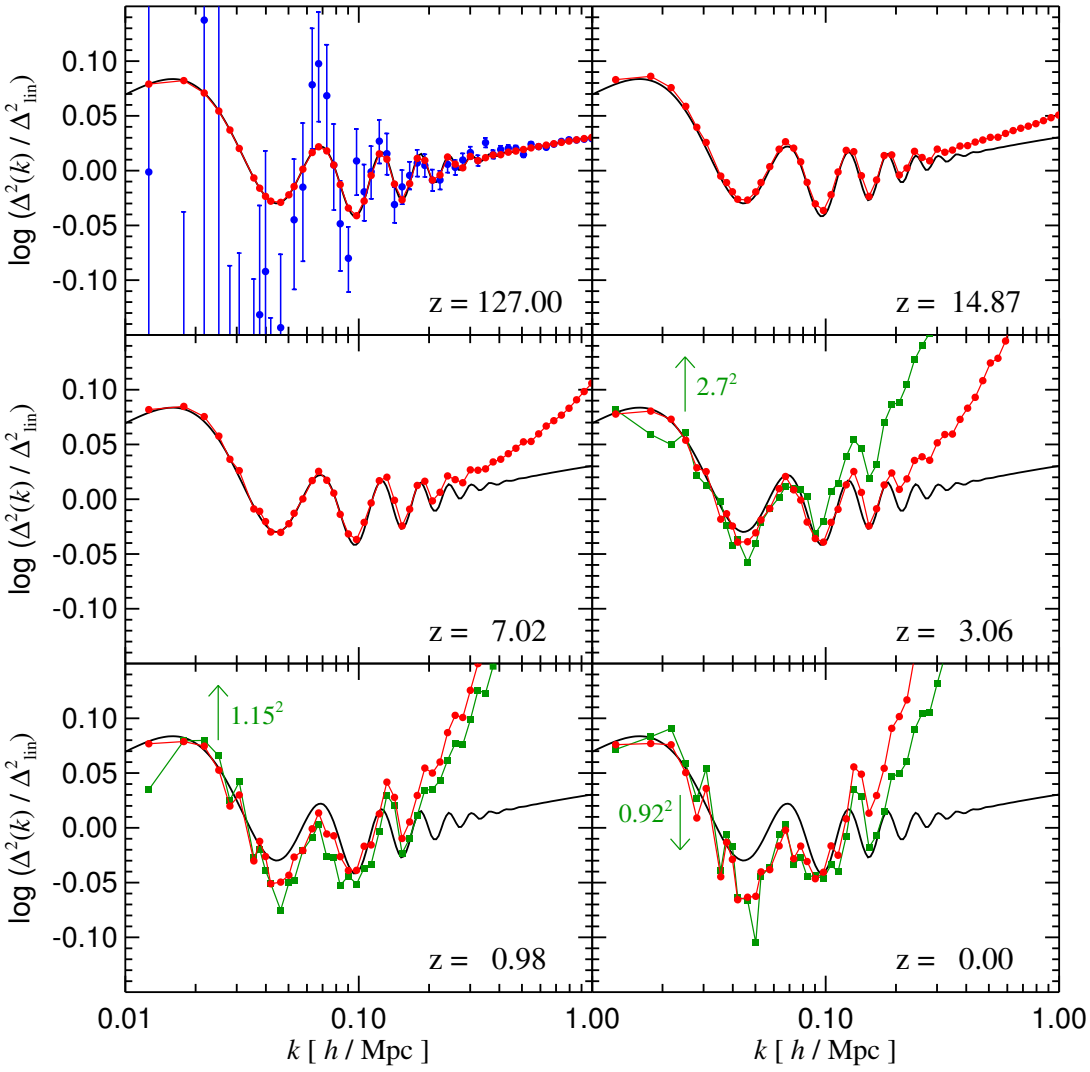

Figure 11: The power spectrum from the Millennium Simulation (Springel et al. 2005). The plot shows the linear power spectrum ratioed to a smooth model (black), the non-linear mass power spectrum (red), and the galaxies (green), scaled to allow for bias.

This discussion suggests that the minimum interesting volume for a BAO survey is $5\,h^{-3}\,\mathrm{Gpc}^3$ (1% error in distance, thus 5% in w). How many galaxies are implied by such a survey? We need to choose a typical power level to set the $nP_\mathrm{g} = 1$ sampling. At the wavenumber of the main acoustic feature ($k = 0.065\,h\,\mathrm{Mpc}^{-1}$), the observed galaxy power spectrum for a variety of high-redshift tracers displays rather little evolution, and a canonical value of $P_\mathrm{g} \simeq 2500(\,h^{-1}\,\mathrm{Mpc})^3$ is a reasonable choice, suggesting a number density of $n = 4 \times 10^{-4}\,h^3\,\mathrm{Mpc}^{-3}$. Over a broad redshift band such as can be selected by photometric means (e.g. the DEEP2 $0.7 < z < 1.3$), the corresponding surface densities are of order 1000 deg^{-2}. A minimal BAO survey thus requires around 2,000,000 galaxies, and pushing the errors on w towards 1% is clearly demanding in terms of direct spectroscopy. The alternative is to carry out BAO studies using photo-z's, but this has two related drawbacks. The large radial smearing associated even with good photo-z's, i.e, $\delta z/(1+z) = 0.03$, means that the signal level is greatly reduced. To compensate for this, a photo-z sample needs to be roughly ten times larger than one with full spectroscopy (e.g. Blake & Bridle 2005). Also, more of the signal now comes from angular variations in galaxy density, placing more stringent requirements on photometric uniformity.

Ground-based BAO studies The most powerful existing facility for BAO work is AAOmega: the upgraded 2dF on the Anglo-Australian 4m telescope. This delivers 400 spectra over a 2-degree diameter field. AAOmega will carry out the 'wigglez' project: a survey of 600,000 emission-line galaxies at $z \simeq 1$, selected using a mixture of SDSS and GALEX data. When complete (in approximately 2010), this will probably measure w (if constant) to around 10% accuracy, so is more in the nature of a proof of concept rather than being competitive with current constraints. In the longer term, it is proposed to construct WFMOS, which would offer 2000–4000 fibres over a 1.5-degree field on the Japanese Subaru 8m. For details of the project and the science, see WFMOS study (2005) in the reference list. This facility would be capable of carrying out BAO surveys of several million galaxies, pushing down the limits on constant w and yielding in parallel constraints on evolution. However, construction is not yet approved, and operation would not begin until at least 2012. In the meantime, a pilot project at the 500,000-redshift level will probably proceed using FMOS, which offers 400 near-IR fibres over the existing 0.5-degree SuprimeCam field.

A number of other projects exist that have the potential to contribute to this area, although these are generally at a less advanced stage of planning. HETDEX intends to us the 10m Hobby-Eberly Telescope to obtain spectra of around 10^6 galaxies at $1.8 < z < 3.7$ using their Lyman-alpha emission, and this would be a powerful and competitive BAO probe. Although not yet funded for construction, the claim is that the instrument could be ready within 3 years, and that the experiment would take a further 2.5 years. Other possibilities include planned twin Korean 6.5m telescopes, to be sited at San Pedro Martír, Mexico. One of these telescopes is planned to have a multi-fibre 1.5-degree field, and the intention is to begin operation around 2012. It is not yet clear if

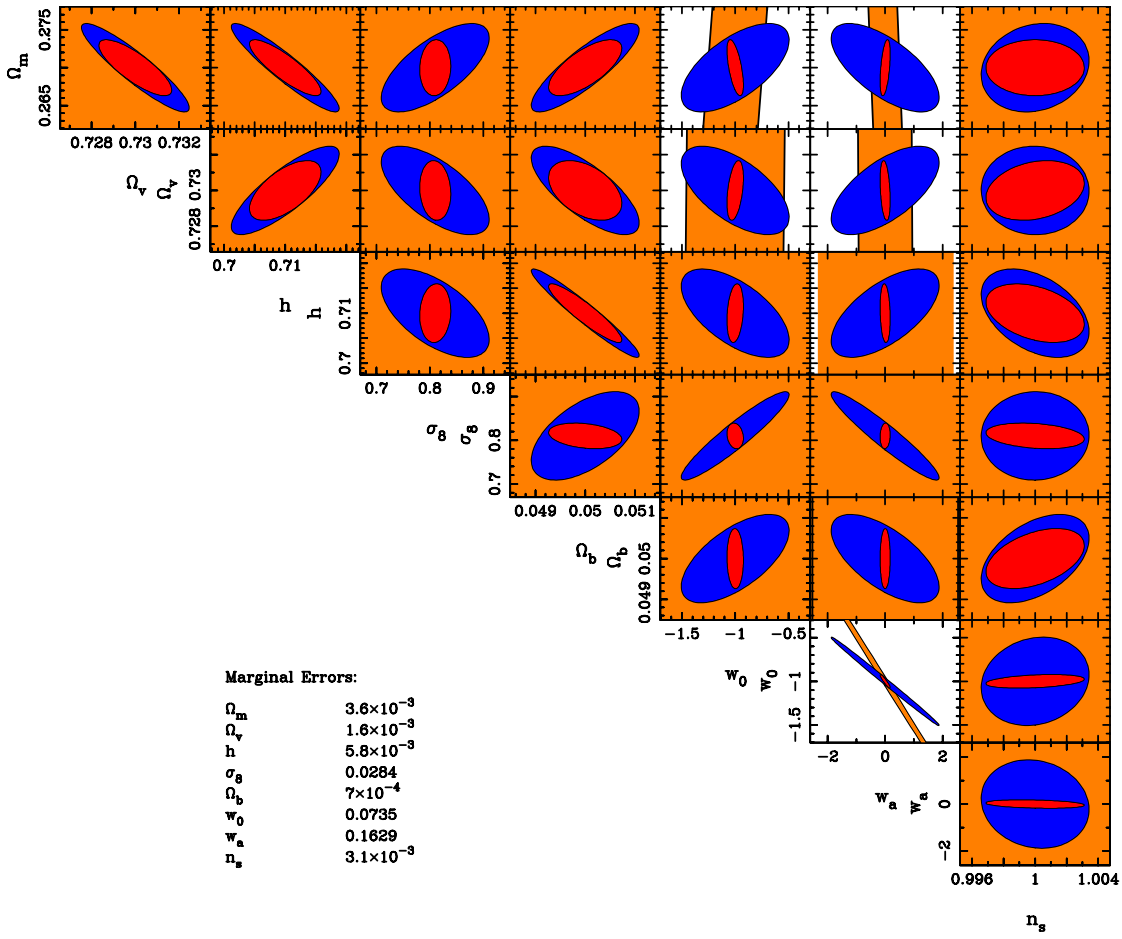

Figure 12: Fisher matrix confidence contours for the main cosmological parameters, assuming a single $z = 1$ BAO experiment of 2×10^6 galaxies and CMB data. This shows the expected one-parameter 1-σ contours on a Gaussian approximation to the likelihood distribution (i.e. $\Delta \ln L = 1$). The blue ellipse shows the expected result from Planck alone; orange is BAO alone; red is the combined constraint. Plot courtesy of T. Kitching.

there are plans to focus on BAO, but this could well be a competitive facility. Finally, one might mention Hectospec, which offers spectroscopy over a 1-degree field on the 6.5m MMT. This presently offers only 300 fibres, but would be a powerful facility if upgraded. Given the rapid growth in the number of telescopes worldwide in the 6m–8m class, we predict with some confidence that one of these will produce a spectroscopic facility of impressive grasp within the next 5–10 years. So far, there is no European proposal under this heading.

A number of projects will also attempt to measure BAO signals using photo-z's. The ESO/VST KIDS project (1400 deg^2 imaging) will probably be the first to achieve this, although the area as originally proposed is sufficiently small that the measurement of w will only be possible at the 15% level. This survey will profit from the parallel near-IR surveys UKIDSS and VIKING, the latter using the new VISTA telescope. The USA's Dark Energy Survey aims to cover 5000 deg^2 using a new camera on the CTIO 4m (see www.darkenergysurvey.org), and will do a little better, with projected error on w of 10%, but for this survey no near-IR data are yet planned, with potentially significant consequences for photometric redshift estimates. However, this photometric technique will only come into its own with imagers of larger grasp, that are able to survey most of the sky to deep limits in multiple wavebands. The Japanese HyperSuprimeCam, recently approved for construction on Subaru, has this capability, although the telescope will not be dedicated to surveys. In the longer term, LSST (www.lsst.org) should be able to measure w to about 2% using the photo-z BAO method, although again the lack of near-IR information may be an issue.

Space-based BAO studies As part of the NASA call for Dark Energy missions under the JDEM heading, the ADEPT mission has been proposed, which would carry out slitless spectroscopy of $\sim 10^7$ galaxies at $z \gtrsim 1$. Although there is a tendency to think of spectroscopy as being something best suited to ground-based studies, the low background in space means that there is an impressive speed advantage.

5.4 ESO's capability for LSS studies

How well are ESO facilities capable of meeting the challenge outlined above, of measuring tens of millions of redshifts over an area of many thousands of square degrees? The widest-field spectroscopic facilities at the VLT are VIMOS, with a field of view of 224 arcmin^2, and FLAMES, with a field of view of 490 arcmin^2. Based on experience with the VVDS and zCOSMOS surveys, VIMOS is able to deliver ~ 1000 redshifts per night to limits of order $I_{\rm AB} \lesssim 23$, and it is therefore clear that the maximum size of survey that is practical with this instrument is a few times 10^5 redshifts. This size of database is potentially significant from the point of view of photo-z calibration, since one of the key issues will be to verify that photo-z estimates are uniform and consistent over the whole

sky. In the presence of a photo-z error of at least $\delta z = 0.05$, a single VIMOS pointing would be able to establish that the mean redshift was unbiased at the level of a few parts in 1000 – as required if we are to measure w to order 1%. A sample of 10^5 redshifts would thus yield approximately 1000 calibration points, spread across several thousand square degrees. This is the best that can be done with existing instrumentation, and it would be an important contribution towards validation of the photo-z technique.

Beyond such calibration work, ESO presently lacks a facility that could undertake the large-scale spectroscopic studies needed for spectroscopic BAO work. VIMOS is optimized to multi-object spectroscopy at source densities of $\sim 10^4\,\mathrm{deg}^2$, about a factor of ~ 10 above the optimal source density of $nP_\mathrm{g} = 1$. This is a principal drawback of multi-slit spectrographs, compared to fibre instruments. The rather small field of view covered by current VLT instruments therefore prevents significant BAO work. This seems a pity, given that there will be many other science drivers for such massive spectroscopy (e.g. galaxy evolution, star formation history, photo-z's, clusters). We also see a need for optical imaging with a greater grasp than can be provided by the VST, in order to provide photo-z data at significantly higher rate, to be able to compete with world-wide efforts. Both these needs would be most efficiently satisfied by the provision of a wider field on one of the VLTs, which would involve the construction of a prime focus, entailing substantial modification of the telescope structure, or the refurbishment of an existing 4-m telescope, to allow a very wide-field camera of several square degree. In addition, ESO might consider seeking to become involved in one of the existing projects of this type elsewhere.

6 Clusters of galaxies

Going beyond the primordial relics of the initial conditions on the largest scales, it is also possible to test cosmological models and to assess the origin, geometry, and dynamics of our universe using galaxy clusters as nonlinear tracers of the large-scale structure. These systems mark the scale of transition between large-scale linearity and the complicated physics of galaxy formation, thus occupying a special place in the hierarchy of cosmic structures. They are the largest virialized dark matter aggregates (dark matter halos) in our universe, and have formed relatively recently. During their formation, they collect galaxies and diffuse gas from the surrounding cosmological environment. While their overall dynamics is still dominated by Dark Matter, the astrophysical processes taking place at the galactic scale have sizable effects on observable properties of the gas component trapped in their gravitational potential. Galaxy clusters are more easily described theoretically and modelled in simulations than other tracer objects of the large-scale matter distribution. In this sense, clusters represent the place where astrophysics and cosmology meet.

Cluster properties such as their number density and its redshift evolution, as well as their distribution on large scales, are very sensitive to the cosmological model, thus providing strong constraints on cosmological parameters (e.g. Vikhlinin et al. 2003; Schuecker et al. 2003a,b). Detailed XMM-Newton and Chandra studies revealed that clusters follow closely a self-similar structure of basic properties such as intracluster medium density and temperature profile (e.g. Vikhlinin et al. 2005), hence allowing more precise cluster modelling than expected from the mere inspection of high resolution X-ray images returned by Chandra and XMM. Among the success of cluster cosmology, the constraints on the density fluctuation amplitude σ_8 should be mentioned. Cluster X-ray data suggested low values of 0.7 – 0.8 (e.g. Schuecker et al. 2003a, Vikhlinin et al. 2003), which have recently been confirmed by the 3-year WMAP results (Spergel et al. 2006; see also Table 5 for estimates of σ_8 from weak lensing). This has strongly revived the interest in cosmological cluster surveys in X-rays (e.g. Haiman et al. 2005), SZ (e.g. Holder, Haiman & Mohr 2001), and the optical (e.g. Annis et al. 2005).

The galaxy cluster population provides information on the cosmological parameters in several complementary ways:

(1) The cluster mass function in the local universe mainly depends on the matter density Ω_m and the amplitude σ_8 of the density fluctuation power spectrum.

(2) The evolution of the mass function $n(M,z)$ is governed by the growth of structure in the universe and thus is sensitive to the density parameters and the equation of state of dark energy.

(3) The amplitude and shape of the power spectrum $P_{\rm cl}(k)$ of the cluster distribution, and its growth with time, depends on the underlying matter power spectrum, so that the cluster distribution can be used to determine cosmological parameters. In particular, wiggles due to the BAO at the time of recombination are imprinted on the large-scale distribution of clusters and thus can be employed in a similar way to the study of BAO features in the galaxy distribution, as described in Sect. 5.1.

The constraints provided by the different cosmological tests with clusters are complementary; parameter degeneracies in any of the tests can be broken by combining them. The simultaneous constraint of $\Omega_{\rm m}$ and σ_8 by combining methods 1 and 3 above is one such example (Schuecker et al. 2003a). In addition, the combination of several tests provides important consistency checks as explained below.

In addition to the above applications, galaxy clusters have been used as cosmological standard candles to probe absolute distances, analogous to the cosmological tests with supernovae type Ia:

- The assumption that the cluster baryon fraction is constant with time, combined with observations of this quantity, provides constraints on cosmological parameters (e.g. Allen et al. 2004).
- In a very similar way, combined X-ray and SZ-measurements provide a means for absolute distance measurements and constraints on the geometry of the universe (e.g. Molnar et al. 2004).

6.1 Cosmological galaxy cluster surveys

Large, well-defined and statistically complete samples of galaxy clusters (which are dynamically well evolved and for which masses are approximately known) are obvious prerequisites for such studies. Substantial progress in the field requires samples of tens to hundreds of thousands of clusters. Surveys in several wavelength regions are currently used or planned to achieve this goal:

Galaxy clusters are detected in X-ray surveys by the radiation of the hot intracluster medium ($T \simeq 3\,$keV) which provides a good tracer of the gravitational potential of the cluster and a measure of its mass. In the radio and microwave sky below 1.4 mm, galaxy clusters appear as shadows on the CMB sky due to the Sunyaev–Zeldovich effect, the Comptonization of CMB photons by the same intracluster plasma that also gives rise to the X-ray radiation. In the optical, galaxy concentrations with high velocity dispersions ($\sigma_{\rm v} \simeq 500 - 1500\,{\rm km\,s^{-1}}$) mark the appearance of galaxy clusters. While the optical

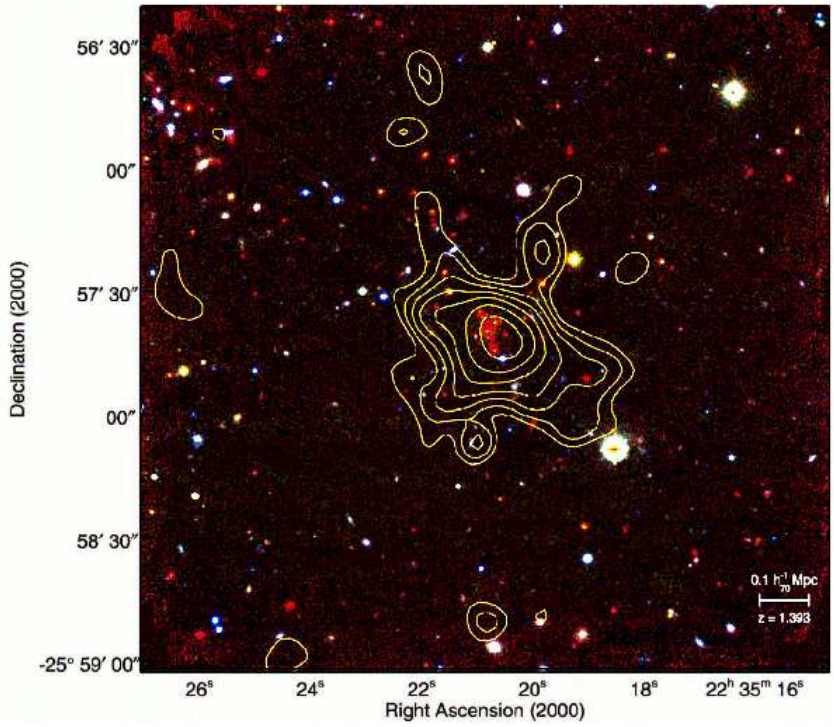

Figure 13: A newly discovered massive evolved X-ray luminous galaxy cluster at $z = 1.39$ (Mullis et al. 2005) discovered in a serendipitous XMM-Newton archive cluster survey. This shows that X-ray luminous clusters exist at high redshifts. We need the redshift leverage out to these redshifts for cluster evolution studies as a means to probe the properties of dark energy.

characterisation of galaxy clusters is affected by confusion of the cluster galaxy distribution with the fore- and background (projection effects), multi-colour imaging and highly multiplexed spectroscopy can be employed to construct effective cluster samples. Finally, clusters of galaxies can also be detected due to their gravitational lensing effect.

Apart from providing clean and complete cluster detections, these surveys also need to provide an estimate of the cluster masses. X-ray observations are presently still the most efficient means of providing cluster samples with these qualities, since the X-ray luminosity is tightly correlated to the gravitational mass (Reiprich & Böhringer 2002), and because the X-ray emission is highly peaked, thus minimizing projection effects. Furthermore, one might expect that bright X-ray emission is only observed when the cluster is well evolved, showing a very deep gravitational potential well. As a specific illustration of these advantages, Fig. 13 shows a recent detection of a cluster at $z = 1.39$ using XMM. Based on simulations, Kravtsov, Vikhlinin & Nagai (2006) claim that the total mass of such clusters can be estimated using data on the amount and temperature of baryons alone, with an impressively small uncertainty in mass of only

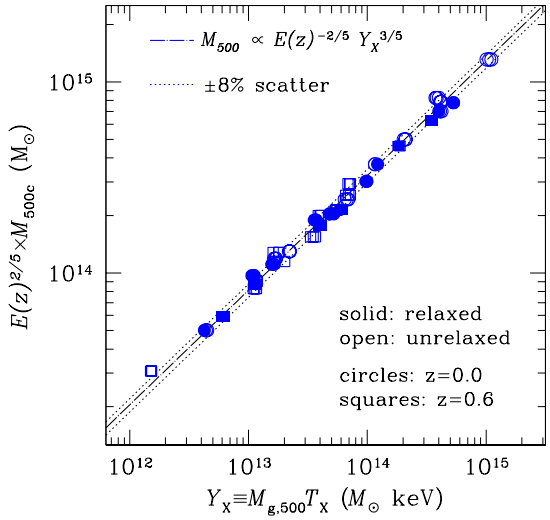

Figure 14: A plot of total cluster mass versus a proxy based on the total baryon mass and temperature, both of which can be inferred from X-ray observations (Kravtsov, Vikhlinin & Nagai 2006). This plot is based on simulated X-ray data, and shows that total cluster masses can be estimated to an rms precision of only 8%. Including the factor $E(z) \equiv [\Omega_{\rm m}(1+z)^3 + \Omega_{\rm v}]^{1/2}$ allows a single redshift-independent relation to be used.

8% (see Fig. 14).

Thus most cosmological studies involving galaxy clusters are based on X-ray surveys. In optical cluster surveys, great progress has been made in cluster detection and characterisation from the large galaxy redshift surveys such as the SDSS (e.g. Popesso et al. 2005). The detection of clusters in blind SZ surveys is a prospect for the near future, and several very promising projects are on their way, including the APEX telescope. Similarly, gravitational lensing surveys offer interesting possibilities for cluster detection. Many clusters have already been found from weak lensing surveys (Wittman et al. 2006; Schirmer et al. 2006). However, these lensing-selected 'mass peaks' will not provide an entirely clean sample of galaxy clusters (Hennawi & Spergel 2005), and they are more logically discussed in Sect. 7 below (see also Fig. 15).

Galaxy clusters are also widely used to study cosmic evolution of the visible matter: the formation and evolution of galaxies as a function of their environment, the feedback and chemical yields of supernovae, the thermal evolution of the intergalactic medium and its enrichment by heavy elements. In this way cosmological galaxy cluster studies also provide a route towards a better understanding and use of galaxies and the intergalactic medium as cosmological probes.

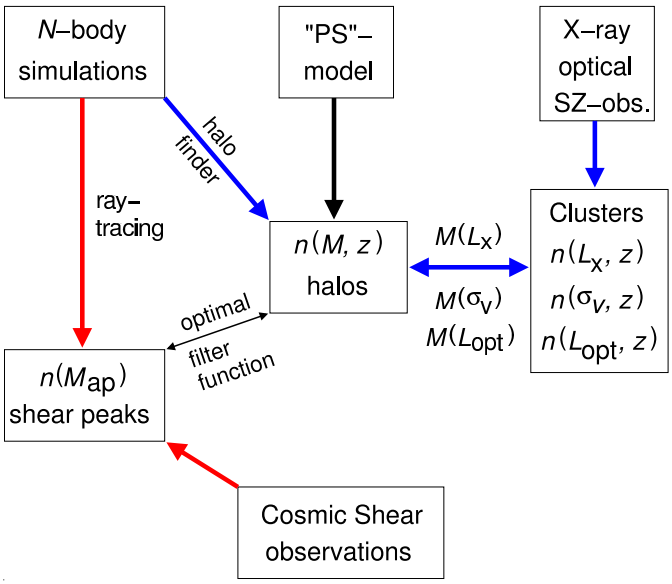

Figure 15: The principle of using the cluster abundance as a cosmological tool. The expected abundance of dark matter haloes $n(M,z)$ is obtained as a function of cosmological parameters either from a model or fitting function, or determined directly from cosmological simulations. In order to relate them to observed cluster samples, obtained from X-ray, optical or SZ-surveys, the redshift of the latter need to be determined. Furthermore, an observable quantity (like X-ray or optical luminosity, X-ray temperature, or velocity dispersion) needs to be related to the halo mass of the cluster. The mass-observable relation is the critical aspect of this method. Also illustrated is the use of mass peaks in weak lensing studies. Here, the number density $n(M_{\rm ap})$ of such peaks can be predicted directly from N-body simulations through ray-tracing. Note that weak lensing mass peaks do not provide exact cluster samples, owing to projection effects; but this does not weaken their sensitivity to cosmology. By relating the weak lensing properties to cluster masses, the latter can be calibrated.

6.2 Systematic uncertainties

The largest current limitation in using galaxy cluster data to constrain cosmological parameters is the uncertainty in the mass estimates that are derived from observed properties, such as X-ray or optical luminosities and temperatures. Cosmologists can predict the abundance and spatial distribution of dark matter haloes as a function of their mass, whereas the prediction of observable properties is substantially more difficult, due to the involved physical processes (see Fig. 15). It is therefore essential that the mass calibration of cluster samples can be performed with a minimum of bias.

Cluster masses are usually determined from their X-ray properties by mapping the surface brightness and temperature profiles, and assuming hydrostatic equilibrium of

the intracluster gas. The accuracy of the mass estimates depends on the S/N of the X-ray data, the spatial resolution with which the temperature can be measured, and the spatial extent out to which the X-ray gas can be studied. The temperature profile will be measurable only for the brightest and largest clusters; for the bulk of clusters, only an average temperature will be measurable. In this case one has to rely on scaling relations between temperature and X-ray luminosity with mass.

For the envisioned precision cosmological tests, the accuracy of the mass calibration bias has to improve from currently worse than 10% (for a representative selection of cluster morphologies) down to about one percent. In addition, the scatter in the relation has to be well quantified. This can be achieved with three different approaches:

- Detailed observations with XMM-Newton and Chandra in conjunction with comparisons to numerical simulations are currently improving our understanding of cluster structure and reducing the bias uncertainty to less than 10%. Complementary measurements of cluster structure properties with the Sunyaev–Zeldovich effect, gravitational lensing and comprehensive spectroscopic observations will help to improve on this.

- The rapidly improving precision of numerical N-body + hydrodynamical simulations is expected to allow reasonably accurate predictions of several cluster observables in addition to cluster masses within a few years. Thus the comparison between observations and theory will involve simultaneously many parameters such as X-ray luminosity, shapes etc., further reducing the uncertainty in the model testing.

- Last and not least, the consistency checks between several cosmological tests with galaxy clusters described above will provide a calibration check of the mass-observable relations. One of the most direct ways to see how this works is to consider how the amplitude of $P_{\rm cl}(k)$ depends on the cluster mass limit, since this mass-dependent bias is what naturally emerges from theory. In this way, we can use clustering to achieve an independent determination of the true cluster masses in a given subsample. In a recent breakthrough, it has been shown that the information in deep surveys is rich enough to solve for the unknown mass-observable parameters with only modest degradation of constraints on the nature of dark energy (e.g. Majumdar & Mohr 2003, 2004; Lima & Hu 2004). Hence, self-calibration of a large, clean cluster sample over large, contiguous regions of the sky can be expected to overcome the cluster mass uncertainties.

However, it is difficult to predict the accuracy to which these relations and their redshift dependence can be calibrated. Whereas theoretical models suggest that a very accurate calibration can be achieved (see Fig. 14), we have also learned that clusters are

more complex than previously thought. The lack of massive cooling flows is currently attributed to heating of the intracluster gas by a recurrently active galactic nucleus in their centre. This implies that the central regions of clusters are more difficult to model, although the global cluster characterisation is probably less affected.

A further point that merits more detailed study is the handling of non-relaxed clusters, and cluster mergers. Whereas for those clusters that have a well-resolved brightness (and temperature) profile, signatures of merging can be readily detected (and those cluster can then be excluded from further statistical consideration), for the more typical cluster in large future surveys the data will be insufficient for such an identification. Thus, proper theoretical modelling of such merging and unrelaxed clusters will be required.

Whereas we have confined our discussion on systematics to X-ray clusters, many of the foregoing remarks apply in a similar way also to optical and SZ-cluster samples. However, since the X-ray band seems to be most appropriate to use clusters as a cosmological probe, we have not considered systematics of cluster surveys obtained by different means.

6.3 Prospects with a 100k cluster survey

The prospects of a large cosmological cluster survey are best illustrated by taking the example of the well-studied eROSITA project, which has a projected launch date on the Russian Spectrum-Röntgen-Gamma-Mission in 2010. The eROSITA mission will perform the first imaging all-sky survey in the medium energy X-ray range up to 10 keV with an unprecedented spectral and angular resolution. The flux limit of the survey in the 0.5 to 2 keV band will be about 5×10^{-14} erg s^{-1} cm^{-2} over most of the sky and about ten times deeper near the poles of the survey scan pattern. The wider energy band and the better angular resolution will make the survey about 30 times more sensitive than the ROSAT All-Sky Survey. At this depth the X-ray sky is dominated by clusters and AGN, which can be separated with an angular resolution of 20 arcsec. The number-flux relationship is well known to the expected depth, and predicts that the proposed survey will identify around 100,000 clusters (see Table 4). The cluster population will essentially cover the redshift range $z = 0 - 1.5$ and will reveal all evolved galaxy clusters with masses above $3.5 \times 10^{14}\ h^{-1} M_{\odot}$ up to redshifts of 2. Above this mass threshold the tight correlations between X-ray observables and mass allow direct interpretation of the data. This sample size is necessary for the following reasons:

- to characterise the cluster mass function and power spectrum accurately in at least ten redshift bins, to follow the growth of structure with time,

- to study in detail the biasing of the cluster power spectrum as a function of the cluster mass, in order to obtain a better understanding of the cluster mass calibration. The biasing describes the ratio of the amplitude of the fluctuations in the cluster number density versus the fluctuations in the mass density. This parameter can be determined theoretically as a function of mass and the comparison with observations will serve as an important calibration check.

- A sample of 50,000 to 100,000 clusters is necessary to reveal the baryonic oscillations in the cluster distribution power spectrum (Angulo et al. 2005).

Multi-band optical (and near-IR) surveys will be needed to obtain photometric redshifts for the clusters. The issues here are discussed in Sect. 3.5. However, the required redshift accuracies ($\Delta z/(1+z) \simeq 0.02$) to $z < 1.5$ for $> 100,000$ clusters are less demanding than for the applications in galaxy surveys (Sect. 5) and weak lensing (Sect. 7), for two reasons. First, the cluster redshift estimates are obtained from several of its member galaxies, so that random errors in the galaxy redshifts average out to some degree. Second, the cluster population tends to be dominated by early-type galaxies, for which more reliable photometric redshifts can be obtained than for other galaxy types. Nevertheless, an accurate calibration of the photo-z's is required here as well in order to avoid a bias. The photometric surveys that are useful for the optical follow-up of X-ray clusters are essentially the same as can be used for weak lensing and LSS studies; those that are currently underway or planned are summarized in Table 6.

The expected constraints on dark energy parameters from a mission of the scope of eROSITA have been modelled in detail by Haiman et al. (2005), taking into account self-calibration. The cosmological sensitivity is extracted from $\mathrm{d}N/\mathrm{d}z$, the cumulative counts of clusters above a given X-ray flux, and their distribution in redshift (in $\Delta z = 0.05$ wide bins), combined with measurements of $P_{\rm cl}(k)$ in wider ($\Delta z = 0.2$) bins. Note that $\mathrm{d}N/\mathrm{d}z$ represents a unique, exponential sensitivity to dark energy through a combination of the comoving volume element, and through the growth function $g(z)$. The power spectrum contains cosmological information from the intrinsic shape of the transfer function and also from baryon acoustic oscillation features (Blake & Glazebrook 2003; Hu & Haiman 2003; Angulo et al., 2005). These wiggles will be detectable at $\simeq 3.5\sigma$ significance in 5 separate redshift bins, varying in width between $\Delta z = 0.2 - 0.5$, each containing about 20,000 clusters. Their use as standard rods account for roughly half of the $P(k)$ constraints on the dark energy (Hu & Haiman 2003). The depth of the survey also allows a measurement of the redshift evolution of the $P(k)$ normalization, which is an independent, direct assessment of fluctuation growth.

The results of the Haiman et al. analysis on the 1σ uncertainties on the dark energy density and its equation of state parameters are given in Table 3. The analysis allows for 4 additional free cosmological parameters and optionally 3 parameters describing the expected dependence of the X-ray flux $f_X(M,z)$ on the cluster mass M, and red-

Table 3: Parameter uncertainties from a 100,000–cluster sample (with an area of 20,000 deg^2 and limit flux of $f_X = 2.3 \times 10^{14}\,\mathrm{erg\,cm^{-2}\,s^{-1}}$), for the density parameter in dark energy (DE), and the two parameters w_0 and w_a parameterizing the equation of state of dark energy. The results are based on the assumption of a spatially flat universe and have been marginalized over $\Omega_\mathrm{b}h^2$, $\Omega_\mathrm{m}h^2$, σ_8, and n_s (from Haiman et al. 2005; based on Wang et al. 2004). The models with superscript (a) assume a constant w ($w_a = 0$). Models (b) correspond to using a 7-parameter cosmology–only Fisher matrix that assumes that the f_X–mass relation has been externally calibrated to 1% accuracy (i.e., it effectively assumes the self-calibration parameters are known to 1% precision).

Self-Calibrated Experiment(s)	$\sigma(w_0)$	$\sigma(w_a)$	σ(DE)
X-ray	0.093	0.490	0.0067
X-ray+Planck	0.054	0.170	0.0052
X-ray+Planck[a]	0.016	—	0.0045
Ideal Experiment[b]			
X-ray	0.021	0.120	0.0030
X-ray+Planck	0.013	0.066	0.0027
X-ray+Planck[a]	0.0087	—	0.0019

shift z. Leaving the latter 3 parameters free allows for the calibration of the mass-X-ray luminosity relation self- consistently within the survey data, making use of the complementarity of the cluster cosmological tests (self-calibration). The upper part of the table refers to these results, while for the lower set of results an external calibration of this relation to 1% was assumed. Due to the complementarity of the Planck CMB observations, a combination of the eROSITA and Planck data yields a further reduction in the allowed parameter space, as illustrated in the Table. The parameter degeneracies arising from cluster constraints are also highly complementary to those from Type Ia SNe (Wang & Steinhardt 1998; Holder, Haiman & Mohr 2001; Levine, Schulz & White 2002).

The modelling by Haiman et al. (2005) makes use of only the part of the cluster data that can be included in an overall cosmological test and it mostly relies on the application of self-calibration. This limitation could be overcome if a powerful X-ray observatory of the type envisaged for XEUS were available to complement the survey projects. Some of main applications of such a facility within the context of this report are the detailed characterisation of high redshift galaxy cluster properties to assist the cosmological X-ray, optical, and SZ cluster surveys and to confirm the nature of massive black hole mergers detected with LISA. Therefore a comprehensive use of the future observational data that can be envisaged from the X-ray waveband should offer a robust

Table 4: Sensitivity and yields for the cluster surveys planned with eROSITA.

Survey	All-Sky Survey	Wide Survey	Deep Survey
Solid Angle	42000	20000	200
Exposure time	1 yr	2.5 yrs	0.5 yrs
Clusters: 0.5–5 keV $S_{\rm min}$	1.6×10^{-13}	3.3×10^{-14}	8×10^{-15}
Clusters: numbers	32000	72000	6500

and competitive way to learn more about the properties of our universe and those of Dark Energy in particular.

7 Gravitational Lensing

7.1 Techniques

Gravitational lensing arises when cosmic density inhomogeneities deflect the light from distant objects, causing their images to be distorted. Galaxies subject to lensing can change their apparent magnitude, but the main observable is an image distortion, principally in the form of a shear. The coherent pattern of image distortions from lensing gives a direct probe of the location and distribution of mass concentrations in the universe. Because the lensing effect is insensitive to the dynamical state and the physical nature of the mass constituents of the mass distribution causing the gravitational field, lensing has been widely used over the past 15 years to analyse the distribution of dark matter in complex systems like clusters of galaxies. Lensing and X-ray mass estimates for clusters show an excellent degree of agreement between both techniques (e.g. Allen, Ettori & Fabian 2001), and this is a fundamental result: it verifies Einstein's factor of 2 in light deflection over cosmological scales, which is an important piece of knowledge when considering alternative theories of gravity.

As datasets have expanded, lensing has increasingly concentrated on the 'weak' regime, in which image ellipticities are altered by only a few per cent. By averaging the distortions of many background galaxies, it has been possible to map structures in the dark-matter distribution statistically, measuring correlations in the shear field – the so-called 'cosmic shear', as envisaged by the beginning of the past decade (Blandford et al. 1991; Miralda-Escudé 1991; Kaiser 1992). The first conclusive detections of cosmic shear were made in 2000. Remarkably, all teams found similar signals, with shape and amplitude in good agreement with the gravitational instability paradigm in a CDM-dominated universe. The impressive consistency of these results stimulated a rapidly growing field, involving an increasing number of teams and techniques.

Cosmological weak lensing is also among the most recent dark energy probes. The sensitivity to dark energy arises because lensing is sensitive to a ratio of distances from us to the lens and the lens to the source, and to the amplitude of the projected mass density contrast along the line of sight. The convergence $\kappa(\vec{\theta})$ governs the strength of lensing,

$$\kappa(\vec{\theta}) = \frac{4\pi G}{c^2} \frac{D_{\rm L} D_{\rm LS}}{D_{\rm S}} \Sigma(D_{\rm L}\vec{\theta}), \tag{34}$$

where Σ is the projected surface mass density of the lensing structure, $D_{\rm LS}$ is the angular-diameter distance between lens and source, $D_{\rm L}$ is the distance between the observer and the lens and $D_{\rm S}$ is the distance between the observer and the source.

The image shear, γ, is related to derivatives of κ. The two signatures of dark energy arise from its presence in the distance factors (a purely geometrical effect), and because

the effective mass of lensing structures reflects the power spectrum and growth rate of large-scale density perturbations. Both of these effects, geometry and growth, can be probed by taking two-point functions (e.g. shear power spectra, or correlation functions) of distant galaxy images as a function of redshift (e.g. Heavens 2003). Alternatively, the geometry of the universe can be isolated from weak lensing by measuring the ratio of shear behind dark matter haloes as a function of redshift (Jain & Taylor 2003; Zhang et al. 2005; hereafter the geometry-power spectrum decoupling technique). These methods are challenging, since the characteristic lens distance ratio scales out some of the w sensitivity, so that the precision multiplier $|\partial w/\partial \ln \mathrm{shear}|$ exceeds 10. Nevertheless, lensing is unique in being able to measure both signatures of a dynamical vacuum. The key to making this technique work is distance information, but the typical galaxies involved are too faint and too numerous for direct spectroscopy to be feasible. Therefore, one has to rely on photometric redshift estimates in order to perform 3D lensing analyses (see Sect. 3.5).

Lensing thus provides an attractive and physically based probe of dark energy. In contrast to the more empirical supernova method (Sect. 8), the lensing signal depends both on the geometry of the universe, via the angular distances, and on the dark matter power spectrum and its evolution with redshift. The direct connection with the gravity field generated by dark matter means that lensing is simultaneously a tool to explore modified gravity theories (Uzan & Bernardeau 2001; White & Kochanek 2001). Weak gravitational lensing experiments also provide byproducts: the mass properties of galaxy halos via the so-called galaxy-galaxy lensing (see e.g. Hoekstra et al. 2003); a sample of shear-selected clusters of galaxies (e.g. Schirmer et al. 2006); a sample of arcs and Einstein rings in clusters of galaxies or around galaxies; the direct measurement of the relations between light and mass through weak lensing-galaxy cross correlation to determine the galaxy bias parameter (e.g. Hoekstra et al. 2002b; Seljak et al. 2005a); and the relation of lensing signals from galaxies to lensing effects on the CMB, which must be understood in order to interpret a B-mode signal in the CMB polarization. These data are important probes of the hierarchical model of structure formation and the history of galaxy formation. Several of these byproducts also depend on the dark energy content of the universe and provide ways of cross-checking the constraints.

7.2 Current status

Past and ongoing surveys are still focused on the primary outcome expected from lensing: constraints on the dark matter density Ω_m and in particular on the amplitude of density fluctuations, σ_8. The inferred normalization depends on the matter density roughly as $\Omega_\mathrm{m}^{-0.6}$, so one really probes the product $\sigma_8\Omega_\mathrm{m}^{0.6}$. Table 5 summarizes the present status of cosmological weak lensing surveys (from Hetterscheidt et al. 2006). The constraints derived so far on $\sigma_8(\Omega_\mathrm{m})$ and on w are also given in that Table. All these results are

based solely on two-point statistics. Surveys with constraints on dark energy are still few and very recent (Jarvis et al. 2006; Semboloni et al. 2006a; Hoekstra et al. 2006). They mostly demonstrate the capability of the techniques but the results are not yet as impressive as supernovae or BAO. Overall, $\sigma_8(\Omega_m)$ is now derived with a 5%-10% accuracy, whilst w is derived with a 50% accuracy, assuming it to be constant. Nevertheless, lensing provides interesting constraints on w, when used jointly with CMB, BAO or SNe Ia surveys (Contaldi, Hoekstra & Lewis 2003; Schmid et al. 2006).

At the forefront of observations and data analysis, the most recent survey is the CFHTLS that now explores angular scales up to 2 degrees to a depth of $I_{AB} = 24$ (Fu et al. 2006). Several teams have also gone beyond two-point ellipticity correlations and explored territory that will be important in next generation surveys. Pen et al. (2003a) derived an upper limit on Ω_m by computing the skewness on the convergence field in the Virmos-Descart survey. They then tentatively broke the degeneracy between Ω_m and σ_8 contained in the two-point statistics. Analyses of three-point statistics from real data were also carried out by Bernardeau, Mellier & van Waerbeke (2002) and Jarvis et al. (2004) who found cosmological signatures. But the signal is noisy and its contamination by systematics is as yet poorly understood. So, despite its potential for the exploration of non-Gaussian signatures in cosmological structures (Bernardeau, van Waerbeke & Mellier 1997; Jain & Seljak 1997; Takada & Jain 2002; Kilbinger & Schneider 2005), cosmology from higher-order shear statistics can hardly be fully exploited from present surveys. Pen et al. (2003b) performed the first 3D dark matter power spectrum reconstruction using weak lensing and compared the results with the WMAP1 power spectrum. Both datasets are in remarkable agreement and show a continuous and monotonic shape that is consistent with a ΛCDM power spectrum. The power of employing redshift information on individual galaxies has been recognised and already applied to a weak lensing survey (Bacon et al. 2005). It was also used in its most simplistic way to derive constraints on w by a joint analysis of the deep and the wide CFHTLS surveys (Semboloni et al. 2006a; Hoekstra et al. 2006). A reliable and conclusive use of the redshift distribution in weak lensing surveys has been carried out by Heymans et al. (2005) using the COMBO-17 photometric redshifts. Their derived value for σ_8 is in excellent agreement with WMAP3. This demonstrates that redshift information will be a prerequisite for all new weak lensing surveys.

Overall, most weak lensing statistics that will be used in next generation surveys have thus already been tested and validated on present-day surveys. The results to date demonstrate that the field has the statistical tools needed to use lensing to study dark energy. An especially impressive development has been the rapid adoption of a standard test for systematics based on the E-mode/B-mode decomposition of the shear field. As with the CMB, this corresponds to separating the part of the shear field that can be generated by symmetric combinations of derivatives acting on a potential (the E mode) from the B-mode shear, which effectively corresponds to rotating all E-mode shear directions through 45°, and which is not caused by lensing (in leading order). Requiring

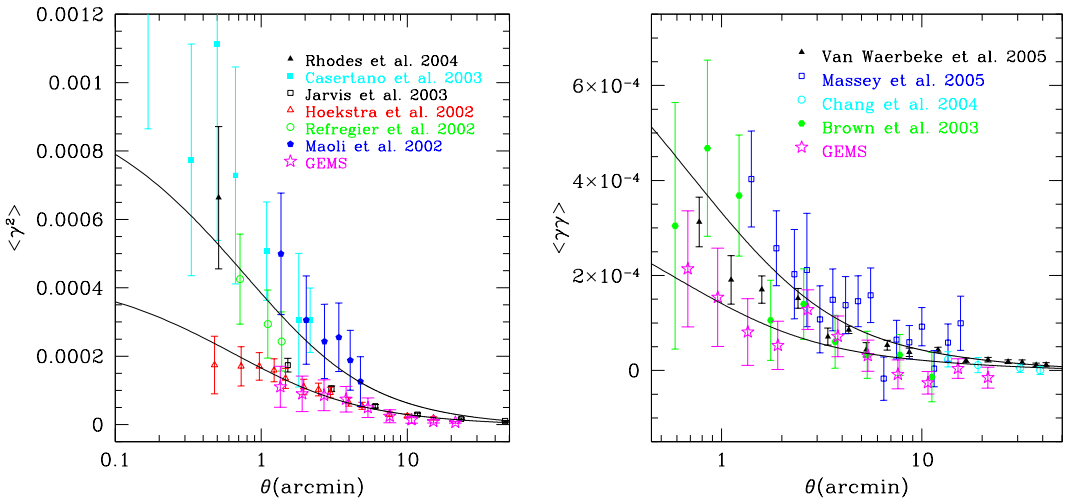

Figure 16: Left: top-hat shear variance $E[\gamma^2]_\theta$ as measured from recent space or ground based surveys. Only the E-modes are shown. The lines show theoretical ΛCDM predictions for a mean source redshift $z_m = 1$ with $\sigma_8 = 0.7$ (lower) and $\sigma_8 = 1.0$ (upper). Right: the total shear correlation function $E[\gamma\gamma]_\theta$ derived from few recent ground based or space surveys. The lines shows the same models as on the left panel. From Heymans et al. (2005).

a negligible level of B-mode contamination has been an important part of demonstrating the consistency of current results on cosmic shear. Nevertheless, as the required precision increases, the challenge will grow of assuring that results are not affected by small systematics that presently lurk beneath the random noise. We make a detailed assessment of these effects below.

7.3 Systematic uncertainties and errors

There are three major types of bias that may contaminate the lensing signal: (1) PSF correction, (2) biased selection of the galaxy sample (e.g. the redshift distribution of galaxies used for weak lensing may differ from the galaxy selection used to measure the redshift distribution of the survey) and (3) intrinsic (astrophysical) distortion signal. Most systematics that are discussed below turn out to be negligible or well under control for present day surveys. However, they may start to become severe for the short and mid-term weak lensing projects and could limit progress unless we improve present day corrections by one order of magnitude. The most critical issues are

- the interpretation of the distortion signal on angular scales below 10 arcmin where

Table 5: Summary of properties of present lensing surveys, with constraints on cosmological parameters – assuming a flat universe with $n_s = 1$.

Survey	Telescope	Sky coverage	n gal arcmin^{-2}	Mag	σ_8 ($\Omega_m = 0.3$)	w_0	Ref.
VLT-Descart	VLT	0.65 deg^2	21	$I_{AB} = 24.5$	1.05±0.05		Maoli et al. 2001
Groth Strip	HST/WFPC2	0.05 deg^2	23	I=26	$0.90^{+0.25}_{-0.30}$		Rhodes et al. 2001
MDS	HST/WFPC2	0.36 deg^2	23	I=27	0.94±0.17		Réfrégier et al. 2002
RCS	CFHT CTIO	16.4 deg^2+ 7.6 deg^2	9	R=24	$0.81^{+0.14}_{-0.19}$		Hoekstra et al. 2002a
Virmos-Descart	CFHT	8.5 deg^2	15	I_{AB}=24.5	0.98 ±0.06	-	van Waerbeke et al. 2002
RCS	CFHT CTIO	45.4 deg^2+ 7.6 deg^2	9	R=24	$0.87^{+0.09}_{-0.12}$		Hoekstra et al. 2002b
COMBO-17	2.2m	1.25 deg^2	32	R=24.0	0.72 ±0.09		Brown et al. 2003
Keck + WHT	Keck WHT	0.6 deg^2 1.0 deg^2	27.5 15	R=25.8 R=23.5	0.93 ±0.13		Bacon et al. 2003
CTIO	CTIO	75 deg^2	7.5	R=23	$0.71^{+0.06}_{-0.08}$		Jarvis et al. 2003
SUBARU	SUBARU	2.1 deg^2	32	R=25.2	$0.78^{+0.55}_{-0.25}$		Hamana et al. 2003
COMBO-17	2.2m	1.25 deg^2	R	R=24.0	0.67 ±0.10		Heymans et al. 2004
FIRST	VLA	10000 deg^2	0.01	1 mJy	1.0 ±0.2		Chang et al. 2004
GEMS	HST/ ACS	0.22 deg^2	60	I=27.1	0.68 ±0.13		Heymans et al. 2005
WHT + COMBO-17	WHT 2.2m	4.0 deg^2 + 1.25 deg^2	15 32	R_{AB}=25.8 R=24.0	 1.02 ±0.15		Massey et al. 2005
Virmos-Descart	CFHT	8.5 deg^2	12.5	I_{AB}=24.5	0.83 ±0.07	-	van Waerbeke et al. 2005
CTIO	CTIO	75 deg^2	7.5	R=23	$0.71^{+0.06}_{-0.08}$	$-0.89^{+0.16}_{-0.21}$	Jarvis et al. 2006
CFHTLS Deep+ Wide	CFHT	2.1 deg^2 + 22 deg^2	22 13	i_{AB}=25.5 i_{AB}=24.5	0.89 ±0.06 0.86 ±0.05	≤ -0.80	Semboloni et al. 2006a Hoekstra et al. 2006
GaBoDS	2.2m	15 deg^2	12.5	R=24.5	0.80 ±0.10	-	Hetterscheidt et al. 2006
ACS parallel + GEMS+GOODS	HST/STIS HST/ACS	0.018 deg^2 0.027 deg^2	63 96	R=27.0 ? V=27.0	$0.52^{+0.13}_{-0.17}$		Schrabback et al. 2006

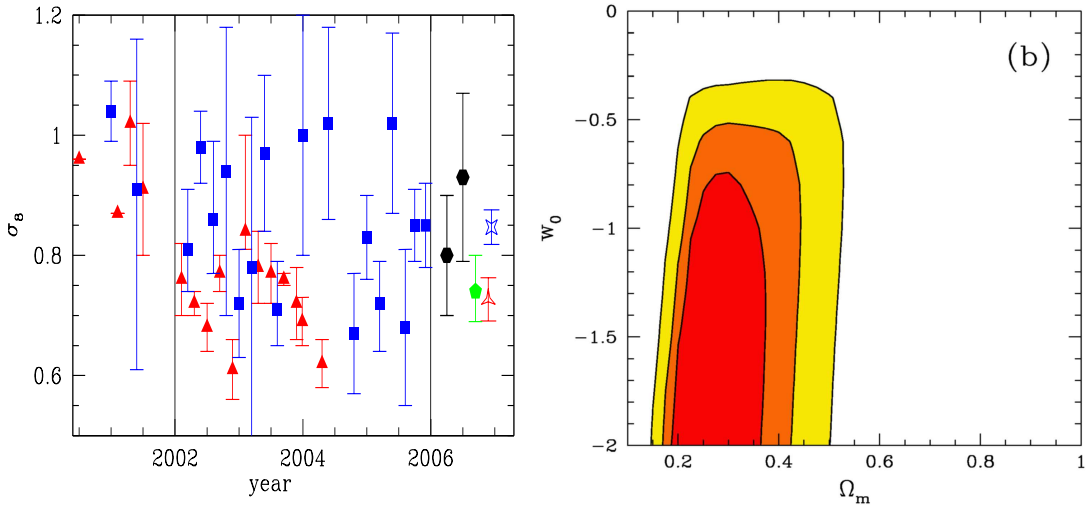

Figure 17: Left: a compilation of the most recent determination of σ_8 from the analysis of clusters of galaxies (red) and cosmological weak lensing. From Hetterscheidt et al. (2006). Right: constraints on dark energy derived from the CFHTLS Deep and Wide weak lensing survey, assuming a constant w and a flat universe. From Hoekstra et al. (2006).

non-linear evolution of the dark matter power spectrum necessitates numerical modelling for accurate predictions; furthermore, on small angular scales galaxy shapes may be intrinsically correlated;

- the measurements at very large angular scales for which the PSF corrections need to be very accurate to measure very weak gravitational distortion correlations;
- and the redshift distribution of the galaxy sample, or the redshifts of individual galaxies that will be needed in precision application of weak lensing.

For some of these issues, high-resolution numerical simulations are necessary in order to understand and calibrate systematics (nonlinear evolution, as well as the influence of the baryonic matter on the dark matter power spectrum; the validity of the Born and Limber approximations; intrinsic correlations; cosmic and sampling variance as a function of the survey design). Overall, none of these obstacles appears insuperable, but some systematics need further investigation in order to assess how they may impact on the survey designs. It is currently unclear what is the most efficient combination of sky coverage, survey geometry, and survey depth. The survey size seems, however, the primary goal. Fig.18 shows that any survey covering more than 10,000 deg^2 with a reasonable depth can recover the dark matter power spectrum with an accuracy of $\sim 1\%$ (Huterer & Takada 2005).

PSF correction The PSF correction is the most challenging and debated technical issue in weak lensing. Both the isotropic smearing and the PSF anisotropy corrections bias the amplitude of the lensing signal. The result is an additive bias produced by any error in the PSF anisotropy correction, and a multiplicative bias produced by any error in the calibration of the PSF smearing effect. So far, the multiplicative bias is the dominant source of error. The amplitude of the bias may also depend on the apparent size, the surface brightness and the intrinsic ellipticity of each galaxy (and therefore it also depends on the mean redshift of the galaxy sample). A dozen or so techniques have been proposed to handle these corrections. They provide reasonable corrections that satisfy the requirements of present-day surveys.

The status of the PSF corrections for weak lensing is discussed in great detail in Heymans et al. (2006a), who describe the thorough joint Shear TEsting Program (STEP). Most teams involved in weak lensing agreed to use blindly the same simulated data sets to assess the capability of their techniques for both space- and ground-based images. The good news is that a few techniques demonstrated that they can already measure weak lensing shear signals correctly down to 1% – but most current techniques are limited by calibration errors of order $\simeq 5\%$. Using this calibration, one can measure a shear signal up to angular scales of 2-3 degrees without showing measurable B-modes or being contaminated by systematics, but we can hardly go beyond this scale until calibration errors are decreased to less than $\simeq 2\%$. The bad news is that none of the techniques currently under evaluation surpasses others and prevails for the next generation surveys. Even the best ones still show bias residuals or turn out to be only valid in a given range of distortion amplitude. This shows that the PSF correction problems are not fully understood and under control and thus have not yet reached the goal for the next generation surveys, where the calibration error should be less than 0.1%. But the results of the STEP project (which is continuing) are very encouraging and demonstrate there is scope for improvements, as well as the will of the community to collaborate towards developing more accurate methods.

Clustering Source/lens clustering has two effects on weak lensing. First, it produces an apparent B-mode signal, plus additional E-modes that would not exist otherwise. This is a subtle effect, which arises because the angular correlation of galaxies depends on their redshift, and the angular distance between galaxies that scales the lensing amplitude also depends on the apparent angular separation between galaxy pairs. It results in a coupling between the shear two-point correlation function and the clustering terms. The amplitude is always below 2% on scales larger than one arcminute (Schneider, van Waerbeke & Mellier 2002). Though it is negligible in present-day surveys, it could however bias the E- and B-modes on small angular scales in next generation surveys. Since it only affects very small scale, even if there were no way to correct the lensing signal from this clustering effect, a safe and simple solution is to discard angular scales below one arcminute.

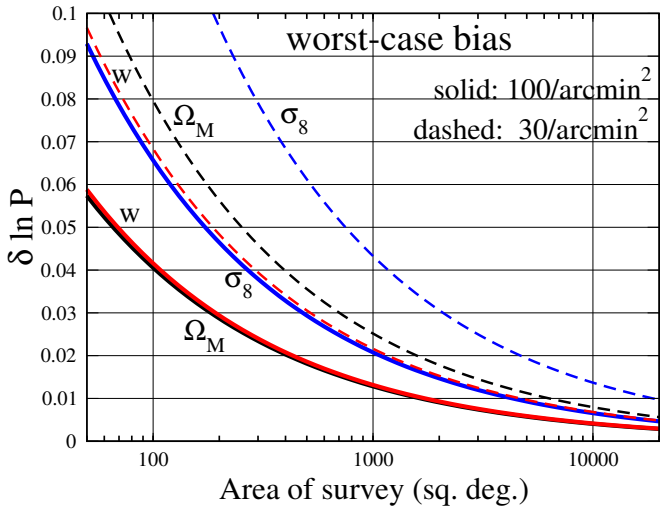

Figure 18: Required accuracy of cosmic shear power spectrum predictions. The curves show the fractional uncertainty of the predicted power spectrum that can be afforded such that the bias in the estimated cosmological parameters is not larger than the statistical uncertainties of the measured cosmic shear signal. The latter depends on the survey area, as well as on the survey depth and thus number density of source galaxies. In particular this plot demonstrates that, for large future surveys, the predictions for the lensing power spectrum need to be known with an accuracy of $\sim 1\%$ in order not to degrade the accuracy of cosmological parameter estimates (from Huterer & Takada 2005).

Second, source clustering changes the amplitude of higher-order statistics whilst keeping the second-order statistics unaffected. Bernardeau (1998) pointed out that both the skewness and the kurtosis are affected. It is likely that the three-point shear correlation functions are also affected by a similar amount. Hamana et al. (2002) showed that on scales smaller than $100'$ and for a ΛCDM model, the source/lens clustering can modify the amplitude of the skewness by 5 to 40% as compared to an uncorrelated galaxy distribution. It is worth noticing that the bias is important and is almost flat from $100'$ to $1'$. However, its amplitude can be considerably reduced by using narrow redshift distributions. The correction drops below 1% for a mean redshift of ~ 1 and by using a width of the redshift distribution below 0.15. Photometric redshifts should therefore have sufficient accuracy to permit redshift bins of this size. However, the correction is still about 10% for galaxies at redshift 0.5. The use of higher-order correlations thus definitely strengthens the need for accurate photometric redshifts.

Contamination by overlapping galaxies Very close galaxy pairs have overlapping isophotes that contaminate both the first and second surface brightness weighted mo-

ments of galaxies that are used to derive the galaxy centroid and the galaxy ellipticity. This yields incorrect shape estimates and potentially correlations in ellipticity at small angular scales. The contamination may be worst in the deepest weak lensing surveys, with a very high galaxy number density; galaxy clustering also increases the number of galaxies that may be affected. Van Waerbeke et al. (2000) found that pairs separated by less than 10 arcsec in ground-based surveys may be affected in this way. Therefore, surveys with more than 100 galaxies per arcmin^2 may be seriously contaminated by isophote overlaps.

Intrinsic alignment An intrinsic correlation of galaxy ellipticities may result from tidal interactions of close physical pairs. Compression of dark haloes or transfer of angular momentum during the interaction will modify the shapes of galaxies (e.g. Catelan, Porciani & Kamionkowski 2000). Close multiplets are then correlated, just as for the weak lensing effect. Since only close physical pairs are affected, this intrinsic signal is stronger at small angular scales. It also prevails on shallow surveys, where the fraction of true physical pairs as compared to non-physical (projected) is larger. Numerical simulations show that the intrinsic alignment is one or even two orders of magnitude below the lensing signal for a mean galaxy redshift of $\langle z \rangle \simeq 1$. However, it dominates for shallow surveys like the SDSS.

The intrinsic alignment can be corrected by a judicious weighting of galaxy pairs as function of their redshift difference. Close physical pairs can therefore be down-weighted while the relevant lensing signal between distant pairs is strengthened. Provided the redshift of each galaxy is known with only a rough accuracy ($\Delta z \simeq 0.1$) , the intrinsic alignment can be almost perfectly corrected (King & Schneider 2003; Heymans & Heavens 2003).

Intrinsic foreground-background correlation The intrinsic foreground-background correlation results from the coupling between the tidal field responsible for the intrinsic alignment of close physical pairs and the gravitational distortion this same field may produce on distant galaxies (Hirata & Seljak 2004): when the tidal field is strong, its lensing effect is also strong and both effects produce a distortion of galaxy isophotes. In contrast with pure intrinsic alignment, the coupling produces a negative lensing signal and seems to depend on the morphology of foreground galaxies (Heymans et al. 2006b). It also increases with redshift, but not in the same way as weak lensing. The intrinsic foreground-background correlation could contribute up to 10% of the lensing signal for $\langle z \rangle \simeq 1$ sources.

When not corrected, the shear-ellipticity coupling may result in an underestimate of σ_8 that could be as large as 20% for some survey parameters. However, as with intrinsic alignment, one can handle this coupling using redshift information, provided the accuracy of redshift estimates is sufficiently good (King 2005). The noise residual of this correction has however not yet been addressed.

Non-linear variance Kilbinger & Schneider (2005) and Semboloni et al. (2006b) have pointed out that non-Gaussian corrections to cosmic variance in weak lensing surveys are not negligible. On scales where the nonlinear regime dominates, below 10 arcmin, the error budget may increase by a factor 2 to 3. While non-Gaussian effects do not produce extra systematics, they significantly affect the estimated accuracies on dark energy constraints obtained from small angular scales.

Non-linear matter distribution For most weak lensing surveys that explore cosmological parameters, the non-linear evolution of the dark matter power spectrum is a serious limitation to a cosmological interpretation of the lensing signal on scales below 20 arcmin. Past and current surveys use either the Peacock–Dodds approximation (Peacock & Dodds 1996) or the halo-fit model (Smith et al. 2003). Unfortunately, these analytic equations are not sufficiently accurate for the analysis of future cosmic shear surveys with their expected small statistical errors. Furthermore, no accurate analytic predictions exist for higher-order correlation functions of the mass distribution, and thus of the corresponding shear correlations. Numerical ray-tracing simulations, employing cosmological matter distributions, are therefore essential for providing accurate predictions; without them, cosmic shear surveys must either disregard the distortion signal below ~ 20 arcmin or use more complex corrections, like the nulling tomography techniques (Huterer & White 2005), at least to derive constraints on dark energy. Such simulations will require a substantial effort by modellers and must be an integrated part of any future large lensing survey. Pure N-body simulations may not suffice to accurately predict the lensing signal on scales below $\sim 1'$; here, cooling of the baryons start to play a significant role (Jing et al. 2006).

Redshift distribution Without redshift information for the lensed sources, weak lensing cannot provide reliable information on cosmological parameters, even for present-day surveys. Tomography, i.e. the variation of the lensing signal as function of source redshift, and geometry-power spectrum decoupling techniques will be even more demanding on redshift accuracy, in particular for galaxies beyond the most distant lens planes. Furthermore, redshift information on individual galaxies is required to control systematic effects from intrinsic shape alignments, shear-shape correlations, and effects of source clustering. Therefore, full exploitation of the statistical power of future weak lensing surveys (particularly with regard to dark energy parameters) requires that the redshift properties of the galaxy samples be very accurately known, with the uncertainties of the mean and dispersion of galaxy redshifts in redshift slices limited to $\Delta z/(1+z) \sim 3 \times 10^{-3}$ (see Fig.19). Since future weak lensing surveys will analyse the shapes of $\gtrsim 10^8$ galaxies, it is impossible to obtain spectra for all galaxies; instead, photometric redshifts techniques need to be employed (see Sect. 3.5) as was already done by Heymans et al. (2005).

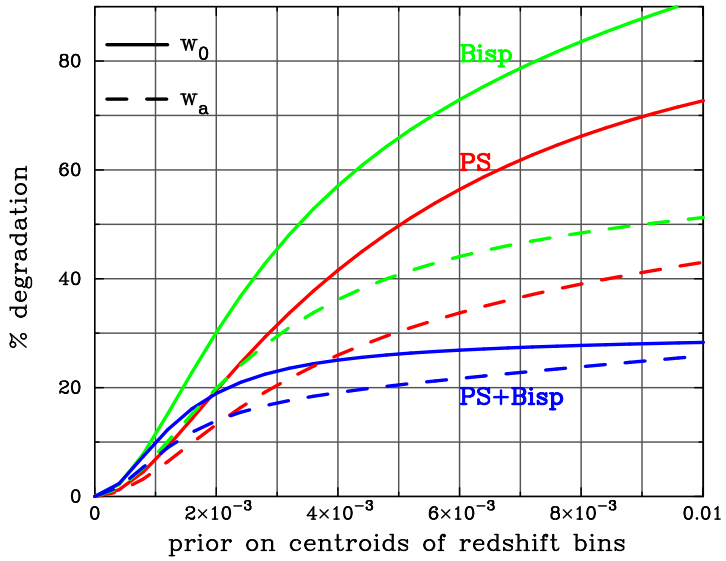

Figure 19: Effects of the accuracy of the mean redshift of source galaxies in photometric redshift bin. The curves show the degradation of the accuracies of dark energy parameters from a bias of the mean redshifts of galaxies in $\Delta z_{\rm phot} = 0.3$-broad bins. 'PS' and 'Bisp' stand for power spectrum and bispectrum, respectively. They refer to information derived from the 2-point and the 3-point shear correlation functions. The plots show that photometric redshift estimates must have a very small bias of below $\delta z \sim 3 \times 10^{-3}$ in order not to degrade the parameter accuracies by more than $\sim 50\%$ compared to the statistical uncertainties of a large-scale survey. Also noticeable is the fact that the combination of second- and third-order statistics not only increases the accuracies, but can also provide a self-calibration of photometric redshift uncertainties, seen by the saturation of the combined curve (from Huterer et al. 2006).

Table 6: Wide-field surveys that prioritize weak lensing as their top scientific goal. We distinguish three classes of project: on-going; next (funded or probably funded); future (still under discussion). VIKING complements the KIDS survey with near-infrared bands. The WL and DE acronyms in the last column stand for weak lensing and dark energy, respectively.

Survey	Telescope/ Instrument	Sky coverage	Filters	Depth	Period	Main goals
Current surveys						
Deep Lens Survey	Mayall+ Blanco	7×4 deg^2	BVRz'	R=25.	2001-2005	WL DE, Clusters High-z Univ.
CFHTLS Deep	CFHT/ Megacam	4×1 deg^2	ugriz	i_{AB}=27	2003-2008	$0.3 < z < 1.$ SNIa DE Clusters, P(k) WL ($z < 2.0$) High-z Univ.
CFHTLS Wide	CFHT/ Megacam	3×50 deg^2	ugriz	i_{AB}=24.5	2003- 2008	WL ($z < 1$), DE, P(k), Bias
SDSS-II SN Survey	APO	250 deg^2	ugriz	r'=22.	2005-2008	$0.1 < z < 0.3 <$ SNIa DE
SUPRIME-33	SUBARU/ Suprime	33 deg^2	R	R=26	2003-?	WL ($z < 1.$), DE, P(k), Bias High-z Univ.
RCS2	CFHT/ Megacam	1000 deg^2	grz	$i_{AB} \simeq$22.5	2003-?	WL ($z < 0.6$), DE, P(k), Clusters, Bias
CTIO-LS	CTIO	$12\times$ 2.5 deg^2	R	R=23	2002-2006	WL ($z < 0.6$)
COSMOS	HST/ACS	1×2 deg^2	I	I_{AB}=25.5	2003-?	WL ($z < 1$), DE, P(k), Clusters, Bias
Funded surveys						
KIDS-Wide	VST/ Omegacam	1500 deg^2	ugriz	i_{AB}=22.9	2006-2009	WL ($z < 0.6$), DE, P(k), Bias High-z Univ.
UKIDSS-Large	UKIRT/ WFCam	4000 deg^2	YJHK	K=18.4	2006-2012	Clusters $z > 7$ Univ.
UKIDSS-Deep	UKIRT WFCam	3×10 deg^2	JK	K=21	2006-2012	Clusters High-z Univ.
UKIDSS-Ultra Deep	UKIRT WFCam	0.77 deg^2	JHK	K=25	2006-2012	Gal. Formation
WIRCam Deep Survey(CFHTLS)	CFHT/ WIRCam	4×0.75 deg^2	J/H/K	K_{AB}=23.6	2005-2008	High-z Univ. Clusters, P(k)
VISTA-Wide	VISTA	5000 deg^2	JHK	K=20.5	2006-2018	
VISTA-Deep	VISTA	250 deg^2	JHK	K=21.5	2006-2018	
VISTA-VeryDeep	VISTA	25 deg^2	JHK	K=22.5	2006-2018	
PanSTARRS	MaunaKea TBD	$\sim$30000 deg^2	giz	i_{AB}=24.	2008- 2012?	WL ($z < 0.7$), DE, P(k), Bias
Planned surveys						
VIKING	VISTA/	1500 deg^2	zYJHK	i_{AB}=22.9	2007-2010	WL ($z < 0.6$), DE, P(k), Bias High-z Univ.
Dark Energy Survey	CTIO DECam	5000 deg^2	griz	i_{AB}=24.5	2009-2014	WL ($z < 0.8$), DE, P(k),
DarkCam	VISTA	$\sim$10,000 deg^2	ugriz	i_{AB}=24.	2010-2014	WL ($z < 0.7$), DE, P(k),
HyperCam	SUBARU/ Suprime	$\sim$3500 deg^2	Vis.	?	>2012?	WL ($z < 2$), DE, P(k),
SNAP/JDEM	Space	100/1000/ deg^2 5000 deg^2	Vis.+NIR	-	>2013	WL ($z < 1.5$), DE, P(k), SNIa, Bias
DUNE	Space	$\sim$20000 deg^2	ugriz+NIR?	i=25.5	$\sim$2015?	WL ($z < 1$), SNIa, DE, P(k),
LSST	Ground TBD	20000 deg^2	ugrizy	i_{AB}=26.5	>2014	WL ($z < 2.$), DE, P(k)
Dome-C	SouthPole	? deg^2	?	?	$\sim$2012?	SNIa, DE

7.4 Future prospects for weak lensing surveys

The key ingredients for next generation weak lensing surveys are

- the field-of-view, which determines the statistical accuracy of the measured shear signal; for precision measurements, many thousands of square degrees will be required;
- the depth of the survey, which determines the redshift up to which the mass distribution can be probed, but also the number density of objects;
- the number of filter bands, which determines the accuracy of the redshift information on individual galaxies;
- the accuracy of shear measurements, which is governed by the accuracy of the PSF correction made to raw data.

These parameters are internal to the survey design and to the data analysis technique. They can be set in advance to design the optimal survey as a function of intrinsic limitations and the survey goals. In addition, one needs external ingredients from numerical simulations. The most important is the non-linear evolution of the dark matter power spectrum, as well as predictions for higher-order shear signals. These precision simulations will be a challenge in their own right.

The present-day surveys have focused on rather simple but robust cosmological analyses based on two-point ellipticity correlation functions of lensed galaxies. Next generation surveys will go further, with the goal of deriving w_0 and w_a with a 1-5% and 5-10% accuracy, respectively. The goal is then to measure gravitational distortion as weak as 0.1% and to use novel techniques to derive cosmological signatures from different and independent methods, breaking the intrinsic degeneracies of the simple two-point shear correlation function. The most promising methods are the reconstruction of the three-dimensional dark matter power spectrum, lensing tomography, 3-point and higher-order statistics or the geometry-power spectrum decoupling analysis, which is much less dependent on accurate modelling of the large-scale structure.

The ongoing and next generation surveys are summarized in Table 6. The CFHTLS Cosmic Shear Survey is an example of a second generation weak lensing survey, which should eventually provide $\sigma_8(\Omega_m)$ with $\simeq 5\%$ accuracy and w with $\simeq 20-50\%$ accuracy. In addition to its depth, field of view and image quality, the CFHTLS benefits from its joint DEEP and WIDE components, plus its photometric redshifts that can be calibrated using the VVDS and the DEEP2 spectroscopic surveys. When used jointly with SNLS and WMAP3, one can reasonably expect a gain of accuracy by a factor 2 to 3 by 2008-2009.

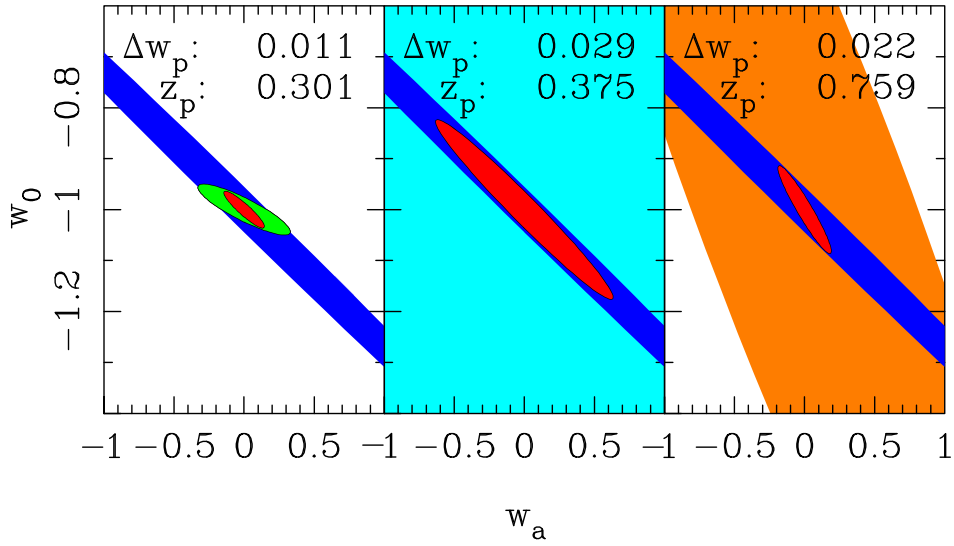

Figure 20: Comparison of Fisher-matrix uncertainties in the dark-energy parameters from weak lensing, SNe Ia and baryon oscillations (left to right). The 3D lensing survey assumes a space-borne 5-band survey covering 20,000 deg^2; the SNe experiment is as specified in the SNAP proposal; the baryon oscillation experiment assumes a survey of 2000 deg^2, yielding 2,000,000 galaxies at $z \simeq 1$. The current parameter w_0 and the evolution parameter are shown, and errors are quoted on w_p, which is w at the pivot redshift; this error is effectively the width of the confidence ellipse in the narrow direction. In all cases, the plots show projected errors from Planck alone, from the selected technique alone, and the two combined, with marginalization over hidden parameters. Adapted from Heavens, Kitching & Taylor (2006).

Beyond 2008, the ESO joint KIDS+VIKING optical/near-IR imaging survey looks promising. It will cover at least 1500 deg^2 with 4 optical and 5 near-infrared filters, about two magnitudes deeper than SDSS and one magnitude shallower than CFHTLS. If the survey could be extended by a factor 2-3 from its original goal of 1500 deg^2, KIDS+VIKING would be a unique bridge between CFHTLS and generation 3 surveys. By 2011, a joint CFHTLS+KIDS+VIKING weak lensing analysis could easily explore the equivalent of 3 to 5 redshift bins with good sampling of each bin. As compared to CFHTLS alone, one can expect a gain in accuracy by a factor 1.5 (conservative) to 3 (optimistic), depending on the genuine dependence on w with time (and the yet unknown image quality of the VST/OmegaCAM). The gain could be qualitatively much more important if the evolution of w with time could be measured. It is worth noticing that by 2011, one also expect the first results from Planck and therefore more stringent constraints from a join analysis than with WMAP.

PanSTARRS and DES are expected to be third generation weak lensing surveys. They exceed the grasp of VST by an order of magnitude, and have much more ambitious goals in terms of sky coverage and depth. Thus, unless ESO takes steps now to plan a more powerful facility, i.e. a DarkCam equivalent, European facilities will not be competitive for work on weak lensing surveys from about 2011.

From 2015 and beyond, LSST, DUNE or JDEM/SNAP are designed in order to make a major step forward in the field. We can envisage nearly all-sky imaging with resolution below $0.5''$, and this will push the measurement of w to 1% or below (see Fig. 20). The main technical challenge of these projects is the image quality. Space missions therefore seem a logical strategy, in particular with respect to long-term stability of the instrument, whereas LSST follows an alternative strategy by using short exposure times on each field. For satisfying the requirements on photometric redshift estimates, multi-colour surveys including near-IR photometry are mandatory, with the latter being only available to the necessary depth from space-based photometry.

The DUNE mission is indeed a joint ground-based and space concept where the critical shear data would be obtained from space, exploiting the image quality and stability unique to that environment. The other optical data needed for photometric redshifts as well as their spectroscopic calibrations would be gathered from the ground. This kind of joint mission provides a very attractive opportunity for synergy between the activities of ESA and ESO. This attraction would be strengthened still further if it were possible to add near-IR photometric channels to DUNE, since the background in space is greatly reduced at these wavelengths. This would greatly improve the photometric redshifts in terms of extending to $z > 1$ and improving robustness and precision at $z < 1$. It should be emphasised that the required quantity of data is well beyond the capabilities of VST and VISTA: what is required is a survey at least one magnitude deeper than KIDS+VIKING and covering a field of view ~ 10 times larger. The ideal capability would be a combination of DUNE (one optical filter for shape measurement,

two or three near-infrared bands for photometric redshifts) and a DarkCam equivalent (4 optical filters for photometric redshift), together with a campaign of deep spectroscopic surveys for photo-z calibration. The enormous data rate from such a project will be challenging, and close cooperation with high-energy particle physicists may be very useful. In addition, the time-scale of this project allows a smooth transition of expertise from the Planck community to DUNE.

8 Supernovae

8.1 Current status

Type Ia Supernovae have been among the most successful cosmological probes. As shown in Fig. 21, their peak luminosities can be calibrated empirically to yield individual relative distances accurate to about 7% (Phillips et al. 1999; Goldhaber et al. 2001; Tonry et al. 2003; Riess et al. 2004). Their use as distance indicators provides a geometric probe of the expansion of the universe, and provides the most direct evidence for a recent period of accelerated expansion, as well as the most accurate direct measurement of the Hubble constant (see Fig. 21 and Leibundgut 2001 for a review of SNe Ia as cosmological distance indicators). SNe Ia are thus an important pillar of the concordance model (cf. Fig. 9) and are currently the only method that dynamically establishes the acceleration. They remain one of the most promising tools for further study of the properties of dark energy.

Table 7 lists the major current and planned supernova survey projects. The introduction of rolling searches, i.e. observations of the same fields nearly continuously (only interrupted by the bright phases of the moon and the seasonal observability of the fields) has solved the problem of incomplete light and colour curves. The success of the CFHT Supernova Legacy Survey (and to some extent the ESSENCE project) shows that with four-colour continuous observations, exquisite light curves can be obtained for large numbers of SNe (Astier et al. 2006). From Table 7 it can be noted that the largest ground-based telescopes are used for the supernova spectroscopy. The current searches are still limited by the spectroscopic observing time, despite large time allocations at these facilities (e.g. Lidman et al. 2005; Matheson et al. 2005; Hook et al. 2005; Howell et al. 2005). These current experiments aim to determine the constant equation of state parameter w to better than 10%. This is achieved by accurately measuring distances to several hundred supernovae at $z > 0.3$ in projects of five years (or more) duration. At the same time the local sample has to be increased to provide the local expansion field and hence the comparison to the more distant objects. They provide the 'anchor' in the supernova Hubble diagram (cf. Fig. 22). These samples are increasing steadily and we can expect to have several hundred supernovae within the local Hubble flow in the next few years (cf. Table 7).

Thermonuclear supernova explosions are, however, complex events and the explosion physics as well as the radiation transport is not fully understood (e.g. Hillebrandt & Niemeyer 2000). Rather, supernova distances are based on an empirical relation that connects the light curve shape to the peak luminosity of the event (cf. Fig. 23). Several methods have been proposed and all give roughly the same results (Phillips et al. 1999; Goldhaber et al. 2001; Riess et al. 1996; Jha 2002; Guy et al. 2005).

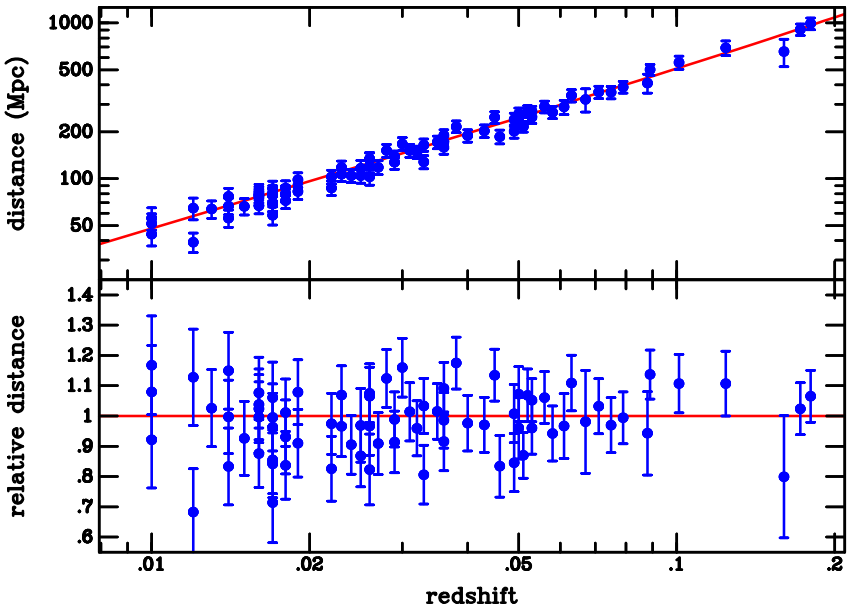

Figure 21: Hubble diagram for nearby Type Ia supernovae. The small scatter indicates the exquisite quality of these objects as relative distance indicators. With an absolute calibration, e.g. Cepheid distances, they also provide the most accurate value of the Hubble constant so far. Data from Riess et al. (2004).

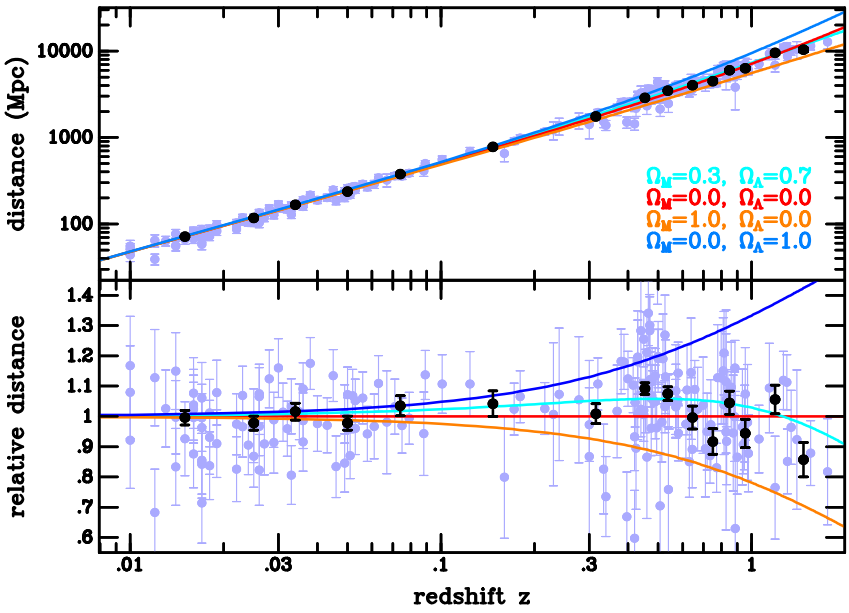

Figure 22: Type Ia supernovae Hubble diagram. The relative faintness of the distant supernovae relative to their nearby counterparts is apparent. A comparison with various cosmological models is made. Data from Riess et al. (2004).

An additional difficulty is the correction for host extinction suffered by the supernova light. This correction is mostly based on the observed colour, but there are variations in the intrinsic colours of supernovae. There are now clear indications that the standard extinction law for the solar neighbourhood is not applicable in external galaxies, where the supernovae are observed (e.g. Krisciunas et al. 2000; Elias-Rosa et al. 2006; Astier et al. 2006). A possible solution to both the above problems may be the near-infrared. Recent studies have shown that nearby Type Ia supernovae are indeed nearly standard candles in the rest-frame JHK bands (Krisciunas et al. 2004). Together with the reduced extinction at these wavelengths, the infrared is a promising route for improved supernova distances. Current projects are trying to sidestep the problem by either concentrating on supernovae in elliptical galaxies, i.e. galaxies with limited extinction, and to improve the distances to local supernovae through IR observations of Cepheid stars. This should yield a further improved value of the Hubble constant. An IR-optimised space telescope would provide a unique chance to sharpen the cosmological distances from supernovae by limiting uncertainties in extinction correction in late-type host galaxies and permitting the use of rest-frame bands for galaxies at higher redshift than present-day samples – although clearly we will not be able to probe beyond $1\,\mu$m in the rest frame.

The main systematic uncertainties at the moment are the unknown cause of the va-

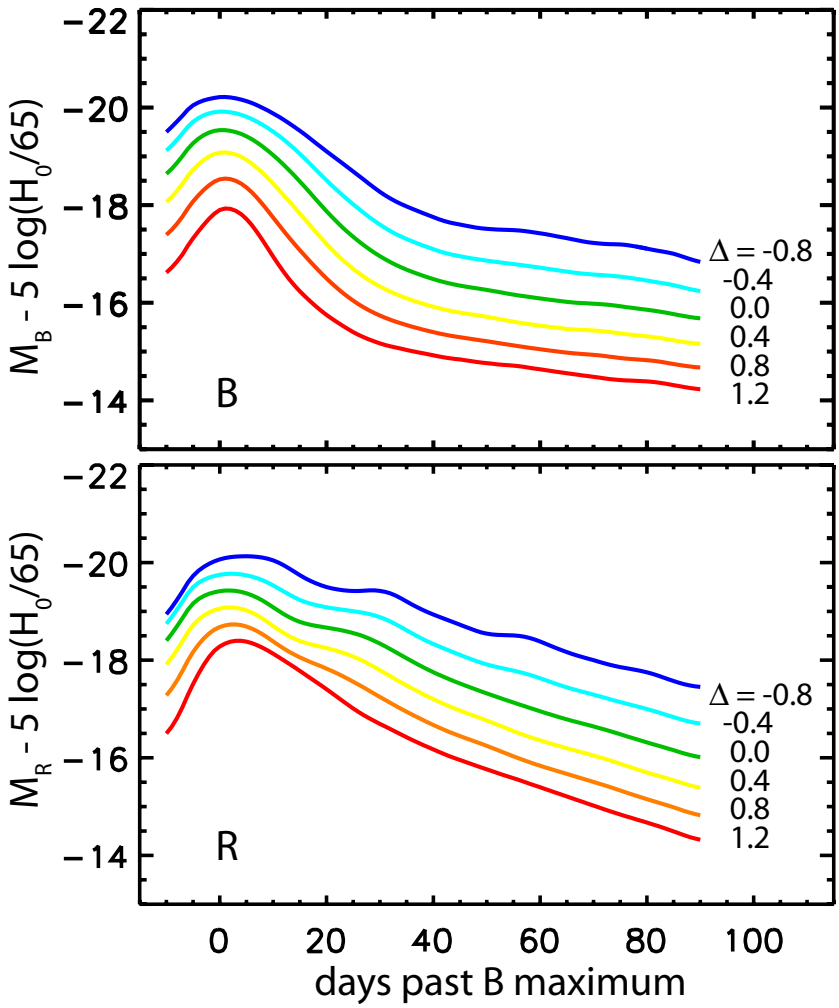

Figure 23: The basic multi-colour approach to supernova cosmology. The relation of brighter supernovae with slower light curve evolution in several filter bands is demonstrated. This correlation is used to normalize the maximum luminosity of Type Ia supernovae. Figure adapted from Jha (2002).

riety of Type Ia supernovae, possible evolution of the supernova luminosity with redshift (or age of the progenitor star), the extinction in the host galaxies (there are indications that the average extinction of the supernovae is different from the local extinction law in the solar neighbourhood), any intergalactic extinction, K-corrections and even the definition of photometric systems. Another uncertainty at the moment is the accuracy with which the normalization of the peak luminosity can be achieved. The light curve shape and colour correction remain mysterious, but ongoing intense modelling efforts may soon lead to substantial progress in our understanding (e.g. Blinnikov et al. 2006). Increasing the statistics for SNe will be useful to

– decrease the statistical error and reduce the intrinsic error,

– give information on the statistical properties and dispersion of the SN,

– and to investigate evolution effects. With the current error estimates in present day and next generation survey strategies, SN surveys will probably be limited by systematics, with 50 SNe per redshift bin (statistical error lower than $\simeq 2\%$). This is achievable in a few years with currently planned projects (see Table 7). Correlated errors across redshift bins will further bias the measured value of w_a (see below). Supernova observations at high redshifts, $z \gtrsim 1.5$, are best suited to yielding an order of magnitude improvement is the accuracy with which w_a can be measured.

Due to the degenerate dependence on cosmological parameters of the luminosity distance over limited redshift ranges, the supernova results need to be compared with independent constraints on the cosmological parameters. Constraints on the dark matter density $\Omega_{\rm m}$ from LSS are nearly orthogonal to the likelihood contours from supernovae in the $\Omega_{\rm v}$ vs. $\Omega_{\rm m}$ plane. This is true for the determination of a constant w as well as for a measurement of w_a, and an accurate determination of the matter density is crucial for meaningful limits on w.

For a time-variable equation of state parameter the redshift range has to be extended beyond $z > 1$ to provide the sufficient leverage (e.g. Linder & Huterer 2003). Currently, the sampling in redshift and the accuracy with which the most distant objects can be observed are not sufficient to constraint w_a and new surveys are being proposed. At the same time ways to sharpen the supernovae as distance indicators and to reduced the intrinsic scatter will need to be found. In addition, systematic effects will need to be controlled even more tightly than in the current projects.

Table 7: Current and planned cosmological Supernova surveys.

Survey	Telescope/ Instrument	Sky coverage	Filters	# SNe	Spectroscopy	Period	Main goals
Low-z searches; z $<$ 0.1							
LOTOSS	KAIT (70cm)	Northern Hemisphere	BVRI	$>$200	Lick/Keck	1992-	discover and follow nearby SNe
European Supernova Collaboration	2m and 4m	–	UBVRIZJHK	$\sim$20	various 4m	2002-2006	SN Ia physics, early epochs
Supernova Factory	NEAT (1.2m)	Northern Hemisphere	BVRI	300	SNIFS	2002-	establish local Hubble diagram, study systematics
Intermediate-z searches; 0.1 $<$ z $<$ 0.5							
Carnegie Supernova Project	1m,2.5m,6.5m	–	UBVRIYJH	$\sim$250	Dupont/ Magellan	2004–2009	all SN types, I Hubble diagram
SDSS II	Sloan 2.4m	250 deg^2	u'g'r'i'z'	$>$500	various 4m	2005–2008	fill in redshift gap $0.1 < z < 0.3$
High-z searches; z $>$ 0.5							
Supernova Cosmology Project	CTIO 4m	-	RI	$\sim$100	Keck/Gemini/ VLT	1990–2000	established acceleration
High-z Supernova Search Team	CTIO 4m	-	RI	$\sim$100	Keck/Gemini/ VLT	1995–2001	established acceleration
Higher-z Supernova Search	HST	GOODS Fields	RIz	17	Keck/Gemini/ VLT/Magellan	2002–2004	$z > 1$ SNe
ESSENCE	CTIO 4m	36$\times$0.36 deg^2	RI	$\sim$200	Keck/Gemini/ VLT/Magellan	2001–2007	w to 10%
SNLS (within the CFHT Legacy Survey)	CFHT	4$\times$1 deg^2	ugriz	$\sim$700	Keck/Gemini/ VLT/Magellan	2003-2008	w to 7%
Accelerating and dustfree	HST	-	griz	$\sim$20	Keck/Gemini Gemini	2005–	distant SNe in elliptical galaxies
PAENS/SHOES	HST	–	JHK	$\sim$15	???	2006–	distant SNe
PanSTARRS-4	4$\times$1.5m	$\sim$10,000 deg^2	BVrIz	thousands	????	2011?	
Dark Energy Survey	CTIO 4m	10,000 deg^2	griz	thousands	????	2010–2015	
LSST	7.5m	$>$20000 deg^2	ugriz	thousands	–	$>$2014	
JDEM/SNAP/DUNE JEDI/DESTINY	space	$>$10,000 deg^2	optical/IR	$\sim$2000	onboard	$>$2015	space missions

8.2 Systematic uncertainties

Contamination All current surveys make extensive use of the largest existing telescopes for spectroscopy. It is critical to exclude any non-Type Ia events. In particular, some Type Ib/c supernovae have light curves and colours similar to the Type Ia supernovae. The spectroscopic identification and classification has been very successful so far, but only single-epoch spectroscopy has typically been obtained. With thousands of supernovae from the future surveys, spectroscopic classification may become impractical. It will have to be demonstrated that tightly sampled light and colour curves can distinguish between the different supernova types (e.g. Sullivan et al. 2006).

Photometry Current supernova photometry is good to about 2 to 5%. The main limitations are the colour and atmospheric extinction corrections. The colour corrections from standard stars to the object in question, if applied, inherently assume a black-body spectral energy distribution. The non-thermal spectrum of Type Ia supernovae leads to small errors in the photometry. Spectroscopy can typically help (Stritzinger et al. 2002), but is not feasible for very large samples. Additional problems are the variations in mirror reflectivity, filter transmission curves and detector sensitivity, which need to be monitored closely. Light curve fitting typically alleviates the problem somewhat as the peak brightness can be determined based on several individual light curve points and hence is accurate to 2% and better, so systematic residuals may be more critical than random errors.

Malmquist bias Brightness limited samples suffer from boundary effects. Intrinsically more luminous objects can be observed to larger distances. This means that the most distant sample bins are dominated by the most luminous events. A small intrinsic scatter limits the effects of Malmquist bias. The small scatter in the normalized peak luminosity is not sufficient to eliminate the bias, but there is hope that the normalization works even for limited samples. In principle the Malmquist bias can be corrected by using the brightness distribution of galaxies that are within the redshift range where the survey is complete.

Luminosity normalization The methods with which this is achieved are quite varied. The light curve shape is the most commonly used technique, but there are other proposals including colour evolution and spectral line strengths. The successful normalization has been demonstrated and appears reliable (cf. Fig. 21). The peak luminosity is related to the amount of ^{56}Ni synthesised in the explosions (Arnett 1982, Stritzinger & Leibundgut 2005), but the physics that drives the isotope composition remains unsolved. The corrections are typically derived for local samples and then applied to the distant objects. This intrinsically assumes no evolution in the normalization, something very difficult to check (but comparing low- and high-redshift samples may test whether there is any evolution of the normalization). Alternatively, the comparison with infrared peak luminosities, which appear to be much more uniform, could test the different normal-

ization methods.

Local expansion field If the local expansion field is not uniform, but distorted through some large-scale flow, the local supernovae will not fairly represent the Hubble flow. The influence of the Virgo cluster is typically avoided by choosing objects with redshifts $z > 0.01$. There have been claims for a deviation at larger recession velocities (a 'Hubble bubble' to $z \simeq 0.027$; Zehavi et al. 1998). Even very small deviations could result in a mis-interpretation of the cosmological result. Future supernova samples will allow us to examine the local expansion field in great detail, determine the Hubble constant in velocity shells and resolve this problem. Infrared supernova observations would be particularly useful as the distance determinations are more accurate.

K-corrections K-corrections for the distant supernovae are essential and critical for an accurate determination of the rest-frame luminosity of the objects (e.g. Nugent et al. 2002). Since the spectral appearance of supernovae changes dramatically during their evolution, the K-corrections are time-dependent and small errors in phase can introduce additional scatter. Of course, the K-corrections are also correlated with the (intrinsic) supernova colour, and incorrect determination of the extinction towards the supernova can introduce additional errors. Fundamentally, the K-correction also requires precise photometric calibrations because the spectral energy distribution of the comparison stars must be known with high accuracy. Current projects are now re-measuring the SEDs of Sirius and Vega to make sure that the K-corrections do not introduce additional uncertainties.

Extinction Galactic extinction is fairly well understood and can be corrected with reasonable accuracy (most projects use the Schlegel et al. 1998 maps). Small variations in different directions could introduce an additional scatter. Much more serious, however, is the lack of knowledge of the extinction law in other galaxies. Currently, the absorption in the host galaxy is determined by the reddening of the supernova. The reddening law is known to have different dependencies on the size of the dominant dust particles. From infrared observations of supernovae it has been deduced that the reddening law in the Galaxy is not applicable to other galaxies. This remains one of the major error sources in supernova cosmology. If there is a systematic change with redshift, this would further introduce a systematic error.

Evolution Evolution is probably the most difficult systematic uncertainty to tackle. The lack of our understanding of the progenitor evolution leading to a Type Ia supernova (e.g. Livio 2000) and the missing pieces in the explosion physics make this uncertainty the most difficult to constrain. Sample evolution must be considered here as well. If supernovae can come from different progenitor channels and one of them has a longer gestation time then the samples at high redshifts will be dominated by a different population than the one observed in the local (and older) universe. Only careful observations and comparison of objects at all redshifts can lead to a better understanding. Normal-

ization of the luminosity distribution is likely to be different for each population, which may also produce a bias.

Comparison of supernova properties in individual redshift bins will become an important tool for large samples. Light curve shapes, line velocities and spectroscopy will be essential tools for these comparisons and the use of space-based telescopes (for low-resolution spectroscopy) and extremely large ground-based telescopes will be necessary. On the other hand, environment-induced evolution does not require space spectroscopy from space, and can better be addressed by splitting the samples according to host galaxy types rather than in redshift bins.

Improved progenitor and explosion models will also provide clues on possible evolutionary effects. The progress in our understanding of the progenitor evolution (e.g. Hamuy et al. 2003; Stritzinger et al. 2006), the explosion physics (Röpke et al. 2006) and the radiation transport (Blinnikov et al. 2006) have been considerable recently and a tighter connection with the observations is providing first indications of what evolutionary effects could become important (e.g. metallicity of progenitor star). The modelling effort will have to be maintained.

8.3 Future applications of supernovae to dark energy

The previous section lists many systematics that will have to be overcome in future cosmological applications of SNe. But this does not mean that the technique compares poorly with alternative methods; rather, the length of the list indicates the maturity of the field, and is the result of more than a decade of careful study. There is thus every reason to expect that supernovae are capable of measuring the properties of dark energy and its evolution. From our present understanding of structure formation, it is likely that dark energy became dominant after redshift ~ 1. The critical redshift range where the role of dark energy is increasingly important is therefore $0 \lesssim z \lesssim 2$. Extending SNe samples to redshifts $z > 1$ will therefore expand our knowledge of the critical transition between the matter-dominated and dark energy-dominated periods and will provide tighter constraints on dark-energy evolution with lookback time. This requires observations from space, as demonstrated by the successful SNe searches with HST (Strolger et al. 2004, Riess et al. 2004). The sky brightness from the ground prevents the current telescopes to reach sensitivities required for supernovae at such high redshifts. Only an extremely large ground-based telescope will be able to obtain spectroscopy of these distant supernovae in an efficient manner. Space-based telescopes will be able to obtain low-resolution spectroscopy. The real issue here are the wide-field searches, which appear to be best done from space.

In general, results are referred to a fiducial ΛCDM model with $w_0 = -1$ and $w_a = 0$. A prior on $\Omega_{\rm m}$ is applied with an error of 0.01 for the calculations below. This is already

a very small uncertainty on $\Omega_{\rm m}$. To discriminate among various theoretical models, a stringent precision at the level of 0.02 magnitudes at large z is needed. This translates in the fit to a tiny variation on the evolution of the parameter w. Covering a large redshift range is not only mandatory to discriminate between theoretical interpretations but also to control various systematic effects.

In the following, we will quantify the expected statistical errors for a large number of SNe and emphasise the level of control of systematic errors required to match the residual intrinsic limitation. It is important to stress that, even if systematics can be controlled, all next-generation surveys must in addition be backed up with a better calibrated sample of nearby SNe.

The intrinsic dispersion of supernovae Supernovae have an intrinsic dispersion of 0.12-0.15 in magnitude at maximum (e.g. Jha 2002), which constitutes the dominant error today. It can be treated as a statistical error, thus increasing statistics will reduce it to a negligible level. Indeed, if $\sigma(m) = 0.15/N^{1/2}$, using a typical sampling of 50 SNe per redshift bin would reduce the magnitude scatter to 0.02. Therefore, for large future surveys systematic errors of $>2\%$ would dominate the result.

Statistical and systematic limitation of SN surveys The uncertainty in the determination of the model parameters is dominated today by the intrinsic uncertainty in the luminosity at maximum. The current projects are designed to match the systematic uncertainty with the expected intrinsic variation in the peak luminosity of the supernovae. Increasing the statistics will not improve on the current results, if the systematics cannot be improved. As it is difficult to characterise these types of effects, we have studied what will be the impact of various types of errors on the observed brightness and estimated the control needed to let its impact decrease well below the statistical error. In doing so, we also assume that the systematic uncertainties do not introduce an intrinsic offset, but can be treated statistically. This is a somewhat naive approach, but it allows us to make an estimate on the required improvements in the experiments. Each systematic uncertainty needs to be examined individually for possible offsets as well.

The uncertainty in the luminosity distance introduced in the cosmological fit can be written for a redshift bin in the form $\sigma(m) = (0.15^2/N + \Sigma\delta m_i^2)^{1/2}$ where N is the number of SNe per redshift bin, 0.15 is the currently measured intrinsic dispersion, and the various δm_i are systematic errors that add quadratically with the statistical error. The error δm_i on the magnitude can be correlated between redshift bins.

Statistical limitation and the effect of systematics At the required statistical level, any unexpected bias in the magnitude measurement of more than $\delta m = 0.02$, which evolves with redshift, will mimic a cosmological evolution. Note that the relative error with redshift is important. An absolute error in all bins will only modify the normalization, but will not introduce a cosmological bias.

The sources of systematics are reviewed in Table 8; it is difficult today to estimate the future limitation of each. The table summarises the factors presently identified and the level needed to control the measurement at the required 2% level. The current values are estimates or upper limits from the literature. The 'needed' value is the current SNAP estimate. The statistical values indicate the level accepted per supernova if this error is corrected in a redshift bin.

Table 8: Magnitude errors estimation: 'Current' is the estimation or limit in the literature, the 'Needed' accuracy is the level of control, if we assume a large statistic (>50 SNe/bin) extracted from a future experiment (e.g. SNAP). When the error can be corrected, the requirement on one SN can be relaxed but a correction in the bin should be applied. The error on the correction is quoted as systematic. Note that cross-filter calibration and the K-correction are mixed together, although they are different sources of systematics. Gravitational lensing refers to flux amplification, which increases the variance on SN light curves.

Error source	Current	Needed	Stat	Correlated/bin
Experimental				
Data reduction	2-3%	$< 0.5\%$	–	Yes
(cross filter calibration, Kcorr)				
Malmquist Bias	4%	$< 0.5\%$	–	
Non-SN Ia Contamination	5%	$\sim$0%	–	
Astrophysical				
Galactic extinction	4%	$\sim 0.5\%$	10-20%	Yes
(Galactic extinction model)				
Host galaxy extinction	10%	$\sim 1\%$	10–20%	Yes
(reddening dust evolution)				
SN Type Ia Evolution	10%	$\sim 1\%$	10–20%	Yes ??
progenitor mass,				
metallicity (C-O)				
change of explosion				
(Amount of nickel				
synthesised)				
radiation transport				
Host galaxy properties				
Gravitational Lensing	6%	$\sim 0.5\%$	$\sim 10\%$	Yes
Absolute Calibration		1%		No
TOTAL	17%	2%		

9 The intergalactic medium

The principal means of learning about the initial conditions for cosmological structure formation has been the study of large-scale fluctuations using the CMB, galaxy clustering and gravitational lensing. But all these methods lack the ability to probe the very smallest fluctuations, those responsible for the generation of galaxies and the first stars. The best way of overcoming this limit is to use the Lyα forest measured from the absorption of light in quasar spectra. These absorptions are caused by Lyα transitions caused by neutral hydrogen along the line of sight and are thus measuring its one-dimensional (1D) distribution. Through theoretical modelling this can be related to the distribution of dark matter along the line of sight.

This is done in two steps. First, neutral hydrogen is generated through electron-proton recombination and destroyed by ionizing photons that fill the universe. This allows one to relate the neutral hydrogen density to the gas density. Second, gas and dark matter trace each other on large scales since they have the same equations of motion, while on small scales gas pressure counters gravity and prevents gas from clustering, in contrast to the dark matter. These processes are well understood and allow one to relate the information in the Lyα forest to the dark matter distribution. The process is mildly nonlinear and requires hydrodynamic simulations for proper calibration.

In this way, the Lyα forest can measure the distribution of dark matter at smaller scales and higher redshifts than other tracers, which are strongly affected by nonlinear evolution. The critical scales are around $1-40\,h\mathrm{Mpc}^{-1}$, where we have little other information on the matter power spectrum and the Lyα forest provides powerful constraints on the nature and composition of dark matter. Because of the long lever arm between the CMB measurements at the largest scales and the Lyα forest measurements at the smallest scales, the Lyα forest measurements are also particularly valuable in constraining the overall spectral shape of primordial density fluctuations. The Lyα measurements help discriminating between different flavours of inflationary models of the early universe and allows us to measure the effect of non-zero neutrino masses on the matter power spectrum.

Another example where the Lyα forest can play an important role are the dark matter models that erase structure on small scales, such as warm dark matter (WDM). These models are tightly limited since no evidence of any suppression of power is seen even on the smallest scales observed by Lyα forest.

9.1 Method and systematic uncertainties

Method The Lyα forest blueward of the Lyα emission line in QSO spectra is produced by the inhomogeneous distribution of the warm ($\sim 10^4$ K) and photoionized intergalactic medium (IGM) along the line-of-sight. The opacity fluctuations in the spectra trace the gravitational clustering of the matter distribution in the quasi-linear regime on scales larger than the Jeans length of the photoionized IGM.

The relevant physical processes can be readily modelled in hydro-dynamical simulations. The physics of a photoionized IGM that traces the dark matter distribution is, however, sufficiently simple that considerable insight can be gained from analytical modelling of the IGM opacity, based on the so-called fluctuating Gunn–Peterson approximation, which neglects the effect of peculiar velocities and thermal broadening. In this approximation and with the assumption of a power-law relation between density and temperature, the optical depth for Lyα scattering is related to the overdensity of baryons $\delta_\mathrm{b} (= \Delta\rho_\mathrm{b}/\rho_\mathrm{b})$ as

$$\begin{aligned} \tau(z) &\propto [1+\delta_\mathrm{b}(z)]^2\, T^{-0.7}(z) \;=\; \mathcal{A}(z)\,[1+\delta_\mathrm{b}(z)]^\beta\,, \qquad (35) \\ \text{with} \qquad \mathcal{A}(z) &\simeq 0.43 \left(\tfrac{1+z}{3.5}\right)^6 \left(\tfrac{\Omega_\mathrm{b} h^2}{0.02}\right)^2 \left(\tfrac{T}{6000\,\mathrm{K}}\right)^{-0.7} \\ &\times \qquad \left(\tfrac{h}{0.65}\right)^{-1} \left(\tfrac{H(z)/H_0}{3.68}\right)^{-1} \left(\tfrac{\Gamma_\mathrm{HI}}{1.5\times10^{-12}\,\mathrm{s}^{-1}}\right)^{-1}\,, \end{aligned}$$

where T is an effective average temperature, $\beta \equiv 2 - 0.7\,(\gamma - 1)$ is in the range $1.6 - 1.8$, and Γ_HI is the HI photoionization rate. For a quantitative analysis, however, full hydro-dynamical simulations are needed that properly take into account the non-linear evolution of the IGM and its thermal state.

Equation (35) shows how the observed flux $F = \exp(-\tau)$ depends on the underlying local gas density ρ_b, which in turn is simply related to the dark matter density, at least on large scales where the baryonic pressure can be neglected. Statistical properties of the flux distribution, such as the flux power spectrum, are thus closely related to the statistical properties of the underlying matter density field. Note, however, that inferring the amplitude of matter fluctuations from fluctuations of the flux level requires knowledge of the mean flux level, which has also to be determined empirically from Lyα absorption spectra.

QSO absorption spectroscopy The Lyα forest absorption in QSO spectra is superposed on the intrinsic emission spectrum of the QSO, which normally is itself a superposition of a broad continuum and numerous strong and weak emission lines. The absorption by the Lyα forest is due to the warm photoionized intergalactic medium, and the width of typical absorption features ranges from about $10 - 100\,\mathrm{km\,s^{-1}}$. Fully resolving

Table 9: Error budget for the determination of the rms fluctuation amplitude of the matter density field reproduced from Viel, Haehnelt & Springel (2004).

statistical error	4%
systematic errors	
$\tau_{\rm eff}(z=2.125)=0.17\pm0.02$	8%
$\tau_{\rm eff}(z=2.72)=0.305\pm0.030$	7%
$\gamma=1.3\pm0.3$	4%
$T_0=15,000\,{\rm K}\pm10,000\,{\rm K}$	3%
method	5%
numerical simulations	8% (?)
further systematic errors	5% (?)

these features requires high resolution spectroscopy to be performed with Echelle-type spectrographs like HIRES@KECK and UVES@VLT. At the smallest scales the information on the spatial clustering of the matter distribution is masked by the superposed metal lines and the thermal broadening in real and redshift space. The spatial scales utilised in studies of the matter power spectrum with Lyα forest data correspond to velocity scales ranging from about $50\,{\rm km\,s^{-1}}$ to about $2000\,{\rm km\,s^{-1}}$.

Systematic Uncertainties As discussed in detail by Viel, Haehnelt & Springel (2004) and McDonald et al. (2005) there is a wide range of systematic uncertainties in estimates of the matter power spectrum from the Lyα flux power spectrum. These uncertainties fall broadly into five categories:

- necessary corrections due to finite S/N, continuum normalization, associated metal absorption and damped absorption systems;
- residual uncertainty in estimates of the mean flux level;
- uncertainty of the thermal state of the IGM;
- limited ability to make accurate predictions of the flux power spectrum for a large parameter space;
- limited ability to accurately model other physical processes that potentially affect the flux power spectrum, such as galactic winds and temperature fluctuations.

Table 9 reproduces the estimates of the contribution of most of these uncertainties to the total error budget given by Viel, Haehnelt & Springel (2004). On some of these, progress has been made the estimates may be slightly pessimistic.

9.2 Major cosmological results from the IGM

Measurements of the Lyα flux power spectrum The pioneering measurements of the Lyα flux power spectrum by Croft et al. (2002) made use of a mixture of 23 high-resolution Echelle (HIRES) and 30 lower-resolution spectra (LRIS). Further measurements using high-resolution spectra were obtained by McDonald et al. (2000, 8 HIRES spectra) and Kim et al. (2004a, 2004b, 23 UVES spectra). In 2004, McDonald et al. published the flux power spectrum obtained from 3035 SDSS QSO spectra with $z > 2.2$, nearly two orders of magnitude larger than previous samples. This large data set allows one to determine the amplitude of the flux power spectrum to better than 1%. The spectra of the SDSS sample have much lower resolution and lower S/N than the high-resolution spectra. However, due to the large number and wide redshift coverage the flux power spectrum could be measured for a wider redshift range, and the statistical errors are smaller than those of the previous measurements. Note, however, that significant corrections have been applied because of the rather low S/N and resolution. There is good agreement between the different measurements of the Lyα flux power spectrum to within the quoted errors.

Measurements of the matter power spectrum On the scales probed by the Lyα forest the matter density field is mildly non-linear. This together with the fact that the relation between density and flux is non-linear makes the use of realistically simulated mock spectra mandatory for a quantitative analysis of the inferred underlying matter power spectrum. The first serious quantitative attempts were made by Croft et al. (2002) who developed an 'effective bias' method that uses mock spectra from numerical simulations to define the scale-dependent relation between linear matter and flux power spectrum:

$$P_{\rm flux}(k) = b^2(k) P^{\rm lin}_{\rm mat}(k). \tag{36}$$

The matter power spectrum is then inferred by assuming that this relation is indeed linear (i.e. that the dependence of $b(k)$ on $P_{\rm mat}(k)$ can be neglected). As mentioned above, in practice the flux power spectrum is not only sensitive to the underlying matter power spectrum but amongst other things also to the assumed mean flux level. Initially there was some controversy what values to assume for the mean flux level but recent studies have reached a consensus in this question. This is the main reason that there is now not only good agreement between the observed flux power spectra but also between the matter power spectrum inferred by different authors.

Theoretical analysis of this flux power spectrum shows that at the pivot point close to $k = 1\,h\,{\rm Mpc}^{-1}$ in comoving coordinates for standard cosmological parameters, the power spectrum amplitude is determined to about 15% and the slope to about 0.05. This is an accuracy comparable to that achieved by WMAP. More importantly, it is at a much smaller scale, so combining the two leads to a significant improvement in the constraints on primordial power spectrum shape over what can be achieved from each

Table 10: Parameter uncertainties including Lyα data.

		σ_8	n_s
Spergel et al. (2003)	WMAP1 only	0.9 ± 0.1	0.99 ± 0.04
Spergel et al. (2003)	WMAP1+Lyα	–	0.96 ± 0.02
Viel et al. (2004a)	COBE+Lyα	0.93 ± 0.1	1.01 ± 0.06
Viel et al. (2004b)	WMAP1+Lyα	0.94 ± 0.08	0.99 ± 0.03
Desjaques & Nusser (2005)	Lyα+priors	0.90 ± 0.05	–
Tytler et al. (2004)	Lyα+priors	0.90	–
McDonald et al. (2005)	Lyα+priors	0.85 ± 0.06	0.94 ± 0.05
Seljak et al. (2005b)	WMAP1+Lyα +other data	0.89 ± 0.03	0.99 ± 0.03
Viel & Haehnelt (2006)	Lyα+priors	0.91 ± 0.07	0.95 ± 0.04
Zaroubi et al. (2006)	2dF+HST+Lyα	0.92 ± 0.04	–
Viel et al. (2006a)	WMAP3+Lyα	0.80 ± 0.04	0.96 ± 0.01
Seljak et al. (2006)	WMAP3+Lyα +other data	0.85 ± 0.02	0.965 ± 0.012

data set individually.

The results for the shape of the power spectrum are consistent with the concordance ΛCDM model. A joint analysis with the first year data of WMAP gave a rather large amplitude $\sigma_8 \sim 0.9$ (Viel, Haehnelt & Springel 2004; McDonald et al. 2005). The third column of Table 10 shows the inferred fluctuation amplitude in terms of σ_8 for a range of recent studies. Not all of these results are completely independent but there is a wide range of data sets and analysis methods involved. The excellent agreement is encouraging. Note, however, that the CMB data has significant weight in the joint analysis, and with the new WMAP three year results the amplitude of a joint analysis has become somewhat lower $\sigma_8 \sim 0.8$ (Viel, Haehnelt & Lewis 2006a; see Table 10 and Fig. 24 for details).

Constraints on inflationary parameters The real strength of the Lyα forest data comes into play when it is combined with data probing matter distribution on larger scales. Due to the long lever arm provided by a joint measurements of the power spectrum from CMB and Lyα forest data it is possible to constrain the overall shape of the power spectrum and in particular the spectral index of the primordial density fluctuations n_s. The WMAP team used the results of Croft et al. (2002) to perform such an analysis and claimed evidence for a moderate tilt $n_s = 0.96 \pm 0.02$ and/or a running of the spectral index also at the 2σ level. Such an analysis has obviously very interesting

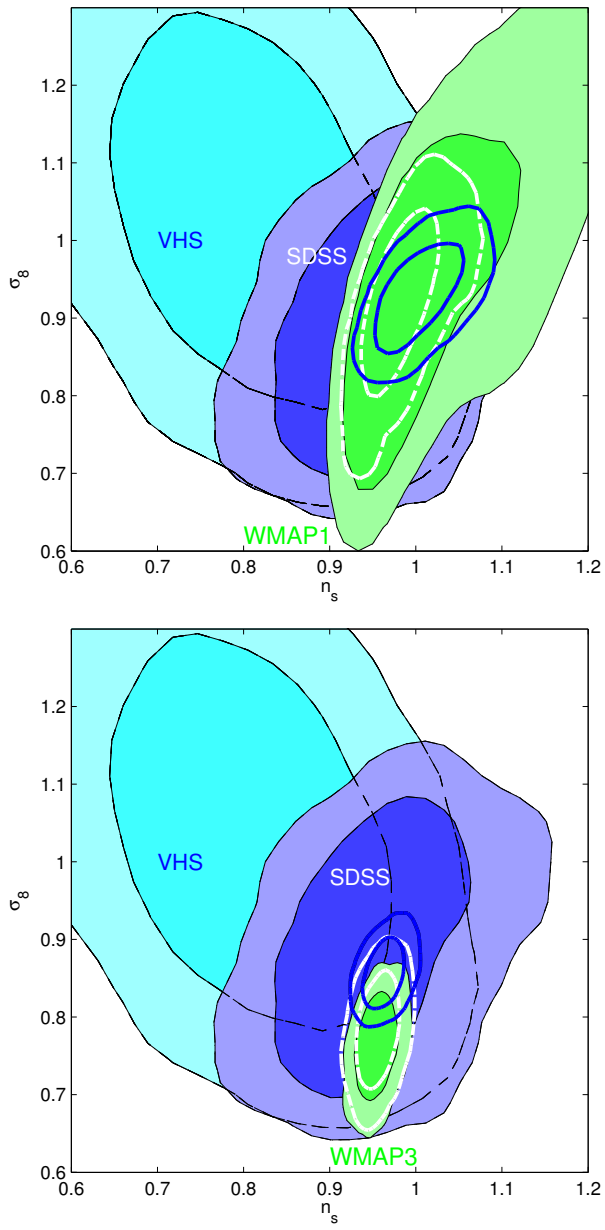

Figure 24: 1 and 2σ likelihoods for σ_8 and n_s marginalized over all other parameters. *Upper panel:* Constraints are for WMAP1 only (green), the high-resolution Lyα forest data analysed by Viel, Haehnelt & Springel (2004a; cyan) and the SDSS Lyα forest data of McDonald et al. (2005; blue). The thick dashed white contours refer to WMAP1 + VHS, while the solid blue contours are for WMAP1 + SDSS. *Lower panel:* As in the upper panel, but for the WMAP3 data set. Figure reproduced from Viel, Haehnelt & Lewis (2006a).

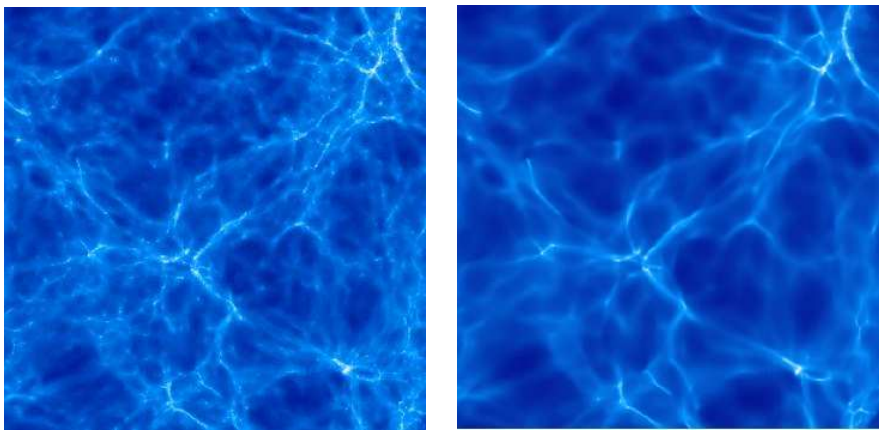

Figure 25: Numerical simulations of the matter distribution of a cold/warm (left/right) dark matter model. The reduced small scale structure due to the free-streaming of the warm dark matter ($m_{\rm WDM} = 0.5\,{\rm keV}$) is clearly seen and well probed by the Lyα forest. Simulations were run with the numerical hydrodynamical code Gadget-II on the COSMOS computer in Cambridge (box-size $30h^{-1}$ Mpc).

implications for constraining the wide range of inflationary models. Viel, Haehnelt & Springel (2004) were able to confirm the suggestion of Seljak, McDonald & Makarov (2003) that the claim of the WMAP team was due to a too low mean flux level assumed by Croft et al. As demonstrated by the fourth column in Table 10 there is consensus that a combined analysis of the WMAP first year results and the Lyα forest data is consistent with a Harrison–Zeldovich spectrum ($n_s = 1$) and no running of the spectral index. This situation has changed with the release of the three year results of WMAP. The lower Thomson optical depth has lead to a significant reduction of the fluctuation amplitude σ_8, and there is now a very significant detection of a spectral tilt (Fig. 24, Table 10).

As a further example of the power of these small-scale constraints, adding Lyα forest information reduces the errors on the running of the spectral index, one of the most important tests of inflation, by a factor of 3 relative to the case without it.

Constraints on warm dark matter As demonstrated in Fig. 25, the matter distribution is sensitive to effects of free-streaming of dark matter particles on scales probed by the Lyα forest data. Interesting constraints can be obtained for a range of putative warm dark matter particles. The lack of the signature of a cut-off in the matter power spectrum due to free-streaming constrains the mass of warm dark matter particle to be > 2 keV for early decoupled thermal relics and > 10 keV for sterile neutrinos (Viel et al. 2005, 2006b; Seljak et al. 2006). It also limits the mass of gravitinos in models for supersymmetric gauge mediation to be < 16 eV. (Viel et al. 2005; all limits are 2σ). Together with the upper limits from the X-ray background, sterile neutrinos can be ruled out as a source of (warm) dark matter.

Constraints on neutrino masses The Lyα forest data in combination with other data currently gives also the tightest upper limit on neutrino masses. In a combined analysis of the WMAP 1st year data, the SDSS galaxy power spectrum and the SDSS Lyα forest data, Seljak et al. (2005b) obtained $\sum m_\nu < 0.42$ eV (2σ) for the case of three neutrino families (see Elgaroy & Lahav 2005 for a review of astrophysical measurements of neutrino masses). Seljak et al. (2006) performed a similar analysis for the WMAP three year data and further tightened the upper limit for the sum of the neutrino masses to $\sum m_\nu < 0.17$ eV. The (moderate) discrepancy of the amplitude of the matter power spectrum inferred from the SDSS Lyα forest and the WMAP year three data mean this result merits further scrutiny.

9.3 Future Prospects

The Lyα flux power spectrum Current estimates of the Lyα flux power spectrum utilised data sets taken for different purposes. The smallest scale resolved by the high-resolution spectra is about a factor 20 smaller than can be used to infer the dark matter power spectrum. This means that many more photons have been collected than necessary for this purpose even though the additional information on smaller scales has been invaluable for an understanding of systematic uncertainties. The SDSS spectra mark the opposite regime. Substantial corrections due to insufficient resolution and S/N are required. A future spectroscopic survey with intermediate resolution of $R \sim 5000$ and sufficient S/N tailored to a determination of the Lyα flux power spectrum could reduce the statistical errors of the flux power spectrum significantly (probably by about a factor three with a moderate effort). There is also room for a more moderate improvement for samples of high- and low-resolution spectra of the kind currently studied. It does not appear worthwhile to take more high resolution spectra for this purpose but there is a significant number of spectra in observatory archives that have not yet been used. SDSS already has a data sample 3-4 times larger than previous analysis waiting to be analyzed. This could lead to a reduction of errors if increase in statistical power reduces the degeneracies between the cosmological parameters and astrophysical parameters.

Looking further into the future, a qualitative jump in the statistical power of the data will be achieved once the surface density of the quasars is sufficiently high that most of the information will come from the cross-correlation between the spectra rather than auto-correlation itself. This would significantly increase the statistical power by using 3D information instead of current 1D information. There are plans to have surveys with two orders of magnitude higher surface density of measured quasar spectra than currently available, which would be ideal for this purpose.

Matter power spectrum and systematic uncertainties The error budget of measurements of the matter power spectrum from Lyα forest data is currently limited by

the lack of knowledge of several astrophysical processes. There are a number of these that affect the spectrum of Lyα forest fluctuations, such as the UV background (responsible for maintaining the ionizing balance between ionizations and recombinations), temperature-density relation for the gas, and gas filtering length determined by time averaged gas pressure. In addition, there may be possible additional physical effects affecting the fluctuation spectrum, such as the galactic winds blowing out of the galaxy and the effects of fluctuations in UV background. The current analyses account for many of these effects by parameterizing them within a model with free parameters that are then marginalized over. In the current SDSS analysis this leads to a 5-fold increase in the error on primordial amplitude and slope of the power spectrum.

The prospects for a better understanding of some of the systematic uncertainties are good. Improved determinations of the temperature of the IGM should reduce the uncertainty due to the thermal state of the IGM. Another major uncertainty is due to the numerical modelling, where it is computationally demanding to demonstrate convergence on small and large scales simultaneously; the constant increase in computing power will obviously help here. Systematic comparisons between simulations with different methods and codes are under way that should also reduce systematic uncertainties due to the numerical simulations. Furthermore a wide redshift coverage of the data appears to be able to break the degeneracy between assumed mean flux level and amplitude of the matter power spectrum. This merits further investigation and may remove another important systematic uncertainty. Significant improvements in the measurements of the matter power spectrum can therefore be expected.

The remaining concern for the current and future prospect of Lyα forest is whether there are additional physical effects that have not yet been considered and that may affect the results at the level larger than the current or future statistical errors. To some extent the same concern can be raised for all of the tracers, which is why cross-checks between the different data sets and other types of analysis are needed to make conclusions robust. It is often argued that Lyα forest is more problematic because of many astrophysical effects that could in principle influence it, contrary to cleaner probes such as weak lensing or CMB. However, it should be remembered that not that long ago CMB was not viewed as clean at all and that only through detailed investigations of many possible effects were we able to conclude that the contaminants were subdominant relative to the signal.

Inflationary parameters Improved measurements of the matter power spectrum from Lyα forest data should reduce the errors for the spectral index n_s and its running. This should further shrink the parameter space of viable inflationary models.

Warm dark matter The main obstacle to improving the lower limits on the mass of dark matter particles are the thermal cut-off of the flux power spectrum and the increasing somewhat uncertain contribution from metal lines to the flux power spectrum

at small scales.

Neutrino masses Further improved measurements of the matter power spectrum will certainly also lead to tighter upper limits on neutrino masses. Together with the improved constraints from CMB measurements, which should break some of the degeneracies (mainly with the spectral index n_s, and the Thomson optical depth τ), it may be possible to close the gap to the lower limit for the neutrino masses from neutrino oscillations. An actual measurement of neutrino masses appears possible.

Beyond power spectra Just as with other large-scale structure data (Sections 5 and 7), there is much to be gained by going beyond the power spectrum analysis. This is particularly important for the Lyα forest, since there is a strong degeneracy between the UV background intensity (affecting the mean level of absorption) and the amplitude of the fluctuation spectrum. This degeneracy can be broken by adding non-Gaussian information, such as the bispectrum or the one-point distribution function. Within the existing data the expected improvement should be a factor of 3-4, and if this remains true even with the larger data set already available, but not yet analyzed, then one can expect an order of magnitude better determination of the amplitude of the power spectrum on megaparsec scales in the near future. This could lead to a comparable improvement in some of the cosmological parameters such as running of the spectral index and the mass of warm dark matter candidate.

A further advantage of a more general approach lies in demonstrating robustness of the conclusions. The same physical model with a small number of parameters must be able to explain not only the observed power spectrum as a function of scale and redshift, but also all the higher-order correlations, cross-correlations between the close lines of sight, cross-correlations between galaxies and Lyα forest etc. By applying these tests we should be able to test the reliability of the models, refine them and converge on the correct cosmological model.

10 Variability of fundamental constants

10.1 Background

Fundamental constants play an important role in our understanding of nature. Any variation of these constants would, for example, question the validity of the General Relativity, since it explicitly assumes laws of physics to be independent of time. Astronomical observations provide a unique way to probe any such variability. In particular, cosmological variations in the fine-structure constant α and proton-electron mass ratio $\mu = m_p/m_e$ can be probed through precise velocity measurements of metallic and molecular absorption lines from intervening gas clouds seen in spectra of distant quasars. The fine-structure constant characterises the strength of the interaction between electrons and photons and is defined as $\alpha = e^2/4\pi\varepsilon_0\hbar c$. It is a dimensionless quantity and its value is $\alpha = 1/137.03599911(46)$. The proton-electron mass ratio μ is related to the quantum chromodynamic and quantum electrodynamic scale variations (Flambaum et al. 2004).

In the 1930s, Milne and Dirac first suggested the time variation of fundamental physical constants and in particular of Newton's gravitational constant. In the subsequent decades the possible variability of fundamental physical constants has occupied quite a prominent place in theoretical physics and many modern theories predict variations of various fundamental constants. String theory predicts seven as yet undiscovered dimensions of space. In such higher-dimensional theories, the constants' values are defined in the full higher-dimensional space, and the values we observe in the four-dimensional world need not be constant. The effective values of the constants in our 4D spacetime depend on the structure and sizes of the extra dimensions. Any evolution of these sizes, either in time or space, would lead to dynamical constants in the 4D spacetime. Thus, any change in the scale of extra dimensions would be revealed by a change in the constants of our 4D spacetime.

There is a class of theoretical models in which a cosmological scalar field, which may be closely related to the cosmological acceleration, manifests itself through a time-dependent fine structure constant (see e.g. the review by Uzan 2003). Varying α is obtained by arbitrarily coupling photon to scalar fields. If the scalar fields are extremely light they could produce variations of constants only on cosmological time scales. Scalar fields provide negative pressure and may drive the cosmological acceleration (Wetterich 2003; Bento, Bertolami & Santos 2004; Fujii 2005). The functional dependence of the gauge-coupling constants on cosmological time is not known and even oscillations might be possible during the course of the cosmological evolution (Marciano 1984; Fujii 2005). In this regard, astronomical observations are the only way to test such predictions at different space-time coordinates.

In 2001, observations of spectral lines in distant quasars brought the first hints of a possible change in the fine-structure constant over time, with a variation in α of 6 parts per million (Murphy et al. 2004). More recently, also μ has been claimed to vary (Ivanchik et al. 2005; Reinhold et al. 2006). If true, such a variation would have profound implications, possibly providing a window into the extra spatial dimensions required by unified theories such as string/M-theory. However, recent results from VLT/UVES suggest no variation in α. The debate is still open and makes strong demands for a high-resolution spectrograph at a large telescope for significant progress. A precision increase in $\delta\alpha/\alpha$ of 2-to-3 orders of magnitude will resolve the present controversy and probe the variability in a presently unexplored regime.

These astronomical observations will also rival in precision the local measures that will be provided by the forthcoming satellite-borne atomic clock experiment ACES. The ACES (Atomic Clock Ensemble in Space) project, foreseen to fly on the International Space Station in 2007, will operate several cold atomic clocks in microgravity to test general relativity and search for a possible drift of the fine-structure constant. Neutral atomic clocks in microgravity have the potential to surpass ground-based clocks both in the microwave and optical domains. Rubidium clocks should enter the 10^{-17} stability range with a gain of two orders of magnitude with respect to present laboratory constraints.

10.2 Constraints on variations in the fine-structure constant

General limits The mere existence of nucleons, atoms and stars constrains $\delta\alpha/\alpha \leq 10^{-2}$ where we define $\delta\alpha/\alpha = (\alpha_z - \alpha_0)/\alpha_0$, with α_z and α_0 the values of α at an epoch z and in the laboratory, respectively. A change of 4% in α shifts the key resonance level energies in the carbon and oxygen nuclei that are needed for C and O synthesis from He nuclei. Stable matter, and therefore life and intelligent beings, would probably then not exist. Similar limits are imposed by Big Bang nucleosynthesis (BBN) at $z \simeq 10^{10}$ and the CMB power spectrum at $z \simeq 1100$.

Constraints on the present-day variation of α in laboratory experiments are based on the comparison of atomic clocks using different types of transitions in different atoms, such as ^{87}Rb and ^{133}Cs. The time-dependence of α is restricted to the level of $(\dot{\alpha}/\alpha)_{t_0} \lesssim 10^{-15}$ year^{-1}. This limit transforms into $|\delta\alpha/\alpha| < 10^{-5}$, at a cosmological time-scale of $t \sim 10$ Gyr, corresponding to $z > 1$, assuming α_z is a linear function of t. Meteoritic data on the radioactive $\beta-$decay of ^{187}Re place a bound around $\delta\alpha/\alpha \leq 10^{-7}$, but this is somewhat model dependent. An intriguing geophysical constraint comes from the Oklo uranium mine in Gabon, Africa, where a fission reaction took place about 1.8 Gyrs ago ($z \simeq 0.14$), naturally self-sustained and moderated for about 200,000 years. The isotopic abundances in the rock surrounding the mine provide

information about the nuclear rates and therefore about the value of α at that time. A key quantity is the ratio of two light isotopes of Samarium that are not fission products. This ratio is 0.9 in normal Sm but about 0.02 in Oklo samples due to the transformation of Sm after neutron capture while the reactor was active. Recent analysis of the isotopic abundances in the Oklo samples provides a hint for a variation at a very low level: $\delta\alpha/\alpha \geq 4.5 \times 10^{-8}$ (Lamoreaux & Torgerson, 2004), but this result still needs further confirmation.

Constraints from QSO spectroscopy The astronomical measurements of the fine-structure splittings of emission lines in galaxies provide a sensitivity of $\delta\alpha/\alpha \simeq 10^{-4}$ at relatively low redshift $0.4 < z < 0.8$. Early high-resolution spectroscopy of distant absorption systems lying along the lines-of-sight to background QSOs focused on the alkali-doublets (AD) such as CIV, SiII, SiIV, MgII and AlIII, since the comparison between AD separations in absorption systems with those measured in the laboratory provides a simple probe of the variation of α. The best current constraints come from the analysis of SiIV absorption systems in $R \simeq 45,000$ spectra: $\delta\alpha/\alpha = (0.15 \pm 0.43) \times 10^{-5}$ (Chand et al. 2004, 15 systems: $1.6 < z_{\rm abs} < 3$).

The many-multiplet (MM) method utilises many transitions from different multiplets and different ions associated with each QSO absorption system (Dzuba, Flambaum & Webb 1999; Webb et al. 1999). This is because the energy of each transition depends differently on changes in α. The relativistic correction to the frequency of each transition is expressed by the coefficient q (Dzuba, Flambaum & Webb 1999; Dzuba et al. 2002). The MM approach compares the line shifts of the species particularly sensitive to a change in α to those with a comparatively minor sensitivity, which are referred to as anchor-lines. Mg, Si and Al act as anchors against which the larger expected shifts in Cr, Fe, Ni and Zn transition wavelengths can be measured. The method provides an effective order-of-magnitude precision gain with respect to the AD method due to the large differences in sensitivity of light and heavy ions to a varying α.

Applied to HIRES-Keck QSO absorption spectra the MM method has yielded tentative evidence for a varying α (Webb et al. 1999), which has become stronger with successively larger samples. The most recent value $\delta\alpha/\alpha = (-0.57 \pm 0.11) \times 10^{-5}$ comes from the analysis of 143 absorption systems over the range $0.2 < z_{\rm abs} < 4.2$ (Murphy et al. 2004). The deduced variation of α at about 5σ significance, if proved correct, would have extraordinary implications. However, the result has not been confirmed by two other different groups. Chand et al. (2004) have analysed 23 Mg/Fe absorption systems in high signal-to-noise ratio (S/N) spectra from a different telescope and spectrograph, the UVES-VLT, claiming a null result over the range $0.4 < z_{\rm abs} < 2.3$ of $\delta\alpha/\alpha = (-0.06 \pm 0.06) \times 10^{-5}$.

A second group adopted a slightly different methodology. Levshakov and collaborators make use only of pairs of FeII lines observed in individual high-resolution

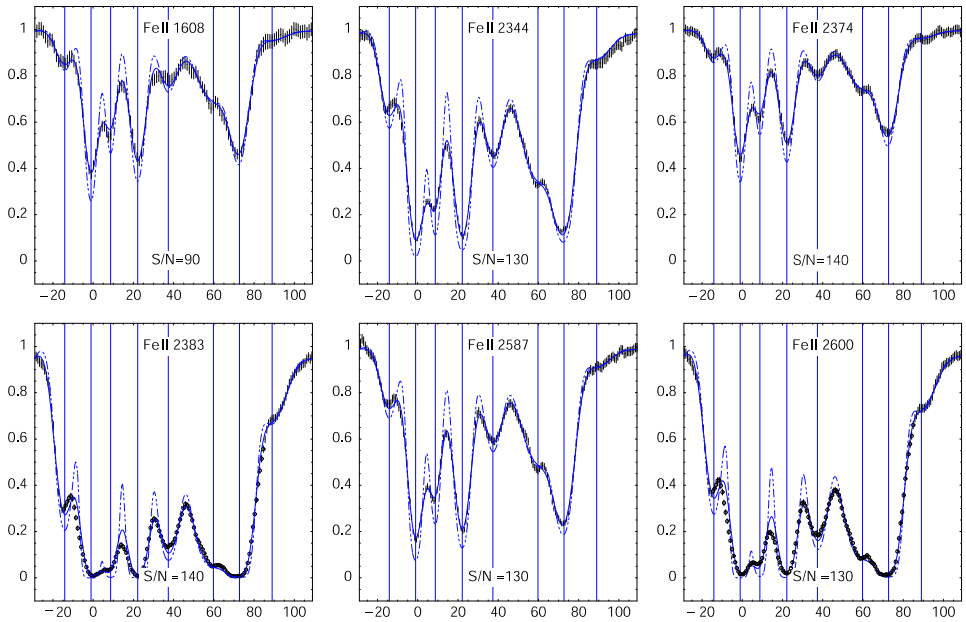

Figure 26: The FeII and MgII spectroscopic multiplets used to detect possible shifts in α (Quast, Reimers & Levshakov 2004).

exposures. This approach avoids the influence of possible spectral shifts due to ionization inhomogeneities in the absorbers or non-zero offsets between different exposures (Levshakov 2004; Levshakov et al. 2005, 2006; Quast, Reimers & Levshakov 2004). Applied to the FeII lines of the metal absorption line system at $z_{\rm abs} = 1.839$ in the spectrum of Q1101−264, and to the $z_{\rm abs} = 1.15$ system in the spectrum of HE0515−4414, this methodology provides $\delta\alpha/\alpha = (0.4 \pm 1.5_{\rm stat}) \times 10^{-6}$ and $(-0.07 \pm 0.84_{\rm stat}) \times 10^{-6}$, respectively. These values are shifted with respect to the HIRES-Keck mean at the 95% confidence level. This discrepancy between UVES-VLT and HIRES-Keck results is yet to be resolved.

Problems are likely to exist in both datasets and any significant improvement in the future will require higher precision, as we explain below. The validity of both results are still under intense scrutiny in the literature, and the final conclusion from QSO absorption lines is still far from clear.

Possible systematics: the isotopic composition in the absorbers The MM measures, which use Mg as an anchor, rely on terrestrial relative composition of the Mg isotopes. This is because the frequency shifts of $\delta\alpha/\alpha$ are of the same order of magnitude of the typical isotope shifts; thus a departure from these values can produce different results for the measures. Sub-solar ^{25,26}Mg/^{24}Mg ratios would make a variation of α even more significant. A suggestion that this may be the case comes indirectly from a

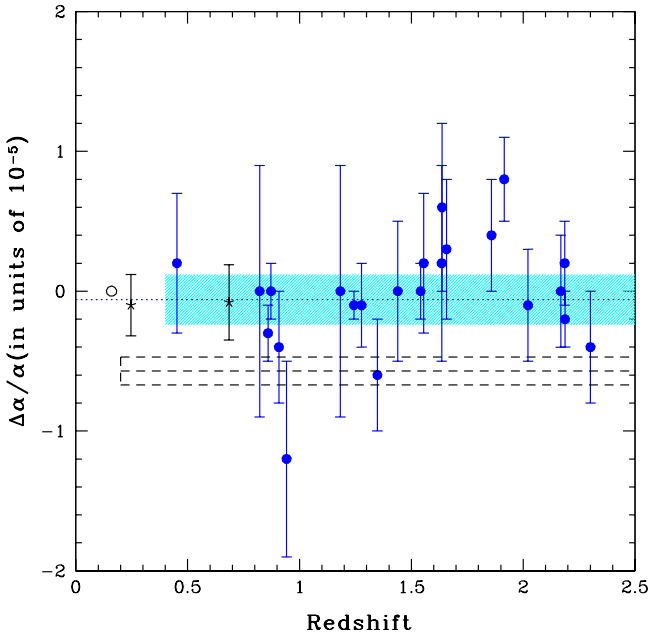

Figure 27: The VLT/UVES data of Chand et al. (2004) on variations in α, compared with the previous Murphy results which are indicated by the dashed lines.

recent upper limit in the ^{13}C abundance ($^{12}C/^{13}C > 200$, 1σ, in the system at $z = 1.15$ in the spectrum of HE0515−4414; Levshakov et al. 2006). Since both ^{25,26}Mg and ^{13}C are produced in the Hot Bottom Burning stage of AGBs, a low ^{13}C possibly implies a low ^{25,26}Mg. In the case of the Chand et al. data set the relaxation of this assumption would have implied $\delta\alpha/\alpha = (-3.6 \pm 0.6_{\rm stat}) \times 10^{-6}$. This well illustrates that the case for variability requires a better understanding of the isotopic evolution of the absorption clouds, a problem that can be addressed only with a spectrograph of very high resolution able to separate the isotopic lines.

10.3 Constraints on variations in the proton-electron mass ratio

The proton-electron mass ratio μ is another fundamental constant that can be probed by astronomical observations (Cowie and Songaila 1995). The observation of roto-vibrational transitions of H_2 in damped Lyman-α systems provides constraints on variations in the proton-to-electron mass ratio, a method first proposed by Varshalovich and Levshakov (1993).

In the context of Grand Unified Theories a possible variation in α may be related to time-variation in other gauge couplings and in particular to variations in the QCD scale.

This is because the proton mass is proportional, at first order, to this scale. Several authors have argued that the quantum chromodynamic scale should vary faster than that of the quantum electrodynamic scale producing a variation in μ even larger than expected in α, although this is rather model dependent (Flambaum et al. 2004; Dine et al. 2003). Theoretically the connections between α and μ are quite complex, but it seems that a varying α entails a varying μ.

At present the μ ratio has been measured with high accuracy:

$$\mu = 1836.15267261(85) \tag{37}$$

(Mohr and Taylor 2005). By using VLT/UVES high-resolution spectra of the quasar Q0347−3819 and unblended electronic-vibrational-rotational lines of the H_2 molecule identified at $z = 3.025$, Levshakov et al. (2002) placed a limit on cosmological variability of $\delta\mu/\mu < 5.7 \times 10^{-5}$. This measurement has been improved by Ubachs & Reinhold (2004) by using new laboratory wavelength of H_2 at the level of $\delta\mu/\mu = (-0.5 \pm 1.8) \times 10^{-5}(1\sigma)$. More recently a new measure of this system together with a new one towards Q0405−443 by Reinhold et al. (2006) and Ivanchik et al. (2005) provided $\delta\mu/\mu = (2.0 \pm 0.6) \times 10^{-5}(1\sigma)$. This would indicate a 3.5σ confidence level that μ could have decreased in the past 12 Gyr.

10.4 Outlook

A measurement of $\delta\alpha/\alpha$ or $\delta\mu/\mu$ is essentially a measurement of the wavelength for a pair or more lines. Therefore the accuracy of a variability measurement is ultimately determined by the precision with which a line position can be determined in the spectrum.

With current spectrographs with $R \equiv \lambda/\delta\lambda \simeq 4 \times 10^4$, the observed line positions can be known with an accuracy of about $\sigma_\lambda \simeq 1$ mÅ (or $\Delta v = 60\,\mathrm{m\,s^{-1}}$ at 5000 Å). Thus for $\delta\alpha/\alpha$ the accuracy is about 10^{-5} for a typical pair of lines with typical sensitivity coefficients. This value is normally further improved to reach one part per million when more transitions and/or more systems are available. Any improvement with respect to this figure is related to the possibility to measure line positions more accurately. This can be achieved with an increase in the resolving power of the spectrograph up to the point in which the narrowest lines formed in intervening physical clouds are resolved, and with an increase of the signal-to-noise ratio in the spectrum (Bohlin et al. 1983). The Bohlin formula gives a relatively simple analytical expression that has also been tested by means of Monte Carlo analysis:

$$\sigma_\lambda = \Delta\lambda_{\mathrm{pix}}(\Delta\lambda_{\mathrm{pix}}/W_{\mathrm{obs}})(1/\sqrt{N_e})(M\sqrt{M}/\sqrt{12}), \tag{38}$$

where $\Delta\lambda_{\mathrm{pix}}$ is the pixel size or the wavelength interval between pixels, W_{obs} is the observed equivalent width, N_e is the mean number of photoelectrons per pixel at the

continuum level, and M is the number of pixels covering the line profile. The metal lines that are observed in the QSO absorption systems have intrinsic widths of typically a few $\mathrm{km\,s^{-1}}$ and rarely of less than $1\,\mathrm{km\,s^{-1}}$. One can therefore expect significant improvements in the near future using higher spectral resolution. The limitation may then be in the statistics and calibration and it would be useful to have more than two QSOs with overlapping spectra to cross-calibrate the line positions.

11 Gravity-wave cosmology with LISA and its successors

11.1 LISA overview

LISA is a joint ESA-NASA space-based gravitational wave detector, currently expected to be launched in the middle of the next decade. ESA will launch a technology mission called LISA Pathfinder in 2009, but this will not make gravitational wave observations. Concept studies exist for a LISA successor, called the Big Bang Observer (BBO), which would be dedicated to observing cosmological radiation from the Big Bang.

LISA will observe gravitational radiation in the broad frequency band from about 0.1 mHz up to 1 Hz, with best sensitivity between 1 mHz and 10 mHz. Sources that radiate in this band include massive and supermassive black holes (SMBH) in the range 10^4–$10^7 M_\odot$, and compact binary systems with periods smaller than an hour or so. Unlike ground-based gravitational wave detectors such as LIGO, LISA will have great sensitivity at these low frequencies, as shown in Fig. 28. LISA will detect coalescences of binary SMBHs at redshifts of order 1 with signal-to-noise ratios exceeding 1000; this means that binary coalescences in LISA's band will be easily visible to it even at redshifts of 10 or more. Because of the redshift, LISA is sensitive at $z \sim 10$ to black holes in the shifted mass range 10^3–$10^6 M_\odot$.

LISA consists of three spacecraft in a triangular array, with separations of 5×10^6 km, in a stable configuration orbiting the Sun at 1 AU – which means that it will return three independent gravitational wave signals. It can therefore measure the polarization of the signals and its antenna pattern allows it to locate strong sources on the sky to accuracies of tens of arcminutes. Below 10 mHz the wavelength of the gravitational waves is longer than the LISA arms, and in this regime the three signals are linearly dependent on one another, which allows a linear combination that does not contain any gravitational wave signal. This provides an important check on instrumental noise and will assist in the detection of random cosmological backgrounds, as described below. As another check on LISA's operation, several known galactic binary systems must be detected in the first few weeks of operation.

11.2 Science goals for LISA

LISA will make the first observations of gravitational waves in this frequency band, so it is impossible to make definite predictions about what it will see. However, at least four kinds of observations that have cosmological implications have been discussed. These are

- Study the SMBH binary population to high redshifts.

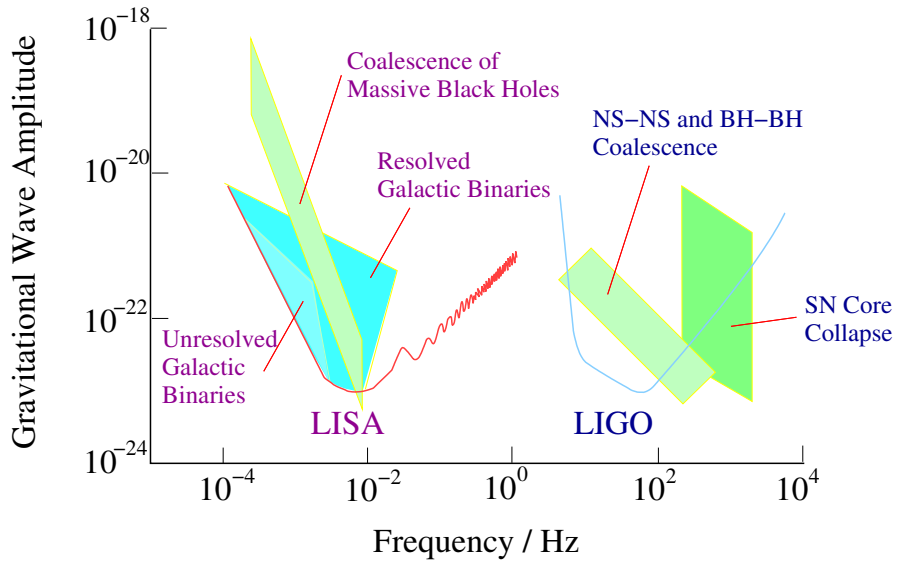

Figure 28: A comparison of the sensitivity to gravitational strain expected from LISA as compared to LIGO, together with illustrations of the expected level of astronomical signals. Although the raw strain numbers are similar, ground-based experiments cannot access the especially interesting low-frequency regime.

- Measure the Hubble expansion and the dark energy at high redshifts.
- Find or limit a cosmological gravitational wave background.
- Search for compact components of the dark matter.

SMBH binary population LISA will see all coalescences of SMBH binaries in its frequency band, no matter how far away. Black holes of masses $10^6 M_\odot$ and higher seem almost ubiquitous in galaxies. Black holes at the bottom of LISA's band (10^3–$10^4 M_\odot$) are less certain, but in some models they are even more abundant. The event rate is uncertain because it depends not only on the number of such black holes but on the processes that lead to binaries compact enough to evolve to coalescence in a Hubble time. Estimates of LISA's event rate range from one event every five years to hundreds of events per year. Recent research has tended to push up the upper bound.

Observations of such systems would tell us much about those processes that contribute most to the event-rate uncertainty. These include whether galaxies form from smaller fragments that contain smaller black holes; whether black holes in merging star systems are brought close together rapidly or slowly; whether the ubiquitous $10^6 M_\odot$ SMBHs are formed at that mass, or have grown either by gas accretion or by merging with smaller black holes; how old the oldest black holes are and whether they formed in their galaxies or helped seed the actual formation of their galaxies. The answers

to these questions clearly have a direct bearing on theories of galaxy formation, but they also have the potential to affect theories of early heavy-element nucleosynthesis, considerations of the IR background energy budget, Population III star formation and evolution, and many other early-universe issues.

Hubble expansion and dark energy LISA observations of in-spiralling SMBH binaries measure directly the cosmological distance to the source (luminosity distance). The accuracy of the distance measurement is limited in principle by the signal-to-noise ratio, but in practice random gravitational lensing introduces the major distortion. In order to use these distances to gain cosmological information, LISA's sources would have to be identified and their redshifts measured. It is by no means certain that identifications will be possible, since the merger event is not likely to emit any electromagnetic radiation. But within LISA's observational error box, galaxies hosting merging SMBHs may be identifiable because (1) they exhibit a distinctive disturbed morphology, or (2) they show evidence that earlier quasar activity has been cut off, or (3, and most interestingly) because a year or so after the merger quasar-like activity suddenly turns on when the accretion disc restores itself after the tidal disruption caused by the inspiralling holes. Much more research is needed on these questions, but it is clear that near-simultaneous observations with suitable X-ray instruments would be useful. Recent estimates suggest that LISA may see 100 or so merger events out to $z = 2$, and in this case it would be possible to determine the cosmological parameters accurately even if each of the error boxes contains a dozen or more potential host galaxies, provided the actual host is normally among the sample.

The cosmological significance of such observations would be enormous. Recent studies, taking into account the gravitational lensing limits, indicate that LISA could measure the dark-energy parameter w to accuracies around 4%. It would place strong constraints on the time-evolution of the dark energy. This is competitive with the expected accuracy of some proposed dedicated dark-energy projects, but it does depend on the as-yet undemonstrated host galaxy identifications. It is worth noting that LISA has the sensitivity to go well beyond $z = 2$ in its examination of the dark energy, albeit with decreasing accuracy.

Cosmological gravitational waves LISA can make essentially a bolometric measurement of random backgrounds: if the noise power in the background is larger than instrumental noise, LISA can identify it. This translates into a sensitivity to a cosmological background with a normalized energy density of $\Omega_{\rm gw} \sim 10^{-10}$ at 3 mHz. Note that LISA's ability to measure its own instrumental noise at low frequencies (mentioned earlier) allows it to make a gravitational wave background measurement with confidence.

The sensitivity of LISA is not good enough to see standard predictions from slow-roll inflation, which are around or below 10^{-15}. But there are many more exotic scenarios that produce stronger radiation, including interesting ones based on brane models. It

is interesting to note that radiation in the LISA band today would have had a wavelength comparable to the cosmological horizon size when the universe was passing through the electroweak phase transition. LISA therefore has the potential to study not only cosmology but to make discoveries about the electroweak interactions. The BBO mission (see below) has been suggested in order to go beyond LISA's sensitivity down to the predictions of inflation.

Dark matter components Cold dark matter is likely to consist mainly of weakly interacting uncharged particles, and dark matter searches are placing interesting constraints on the nature of these particles. But there may also be minor constituents that have such a small effect on standard cosmological indicators of dark matter — galaxy formation scenarios, gravitational lensing — that they are not predicted. These include cosmic strings, which have been eliminated as a candidate for the dominant dark matter, but which may nevertheless be a significant minor component. Other minor constituents could include black-hole systems expelled from their host star clusters during galaxy formation, or even more exotic boson stars, composed of interacting boson fields too massive to have been seen in accelerator experiments so far. All these systems have predictable gravitational waveforms, and LISA will make searches for them.

Discovering minor components of the dark matter would clearly have far-reaching implications for early-universe physics and for unified theories of the fundamental interactions. It is worth pointing out that LISA has such good sensitivity that it has a chance of discovering compact massive components even if their waveforms are not predicted beforehand. Given our ignorance of early-universe physics, and the number of surprises the universe has already given us, this may well be the area where LISA will turn out to do its most important work.

11.3 The future of gravity-wave astronomy

BBO The Big Bang Observer is a concept developed at the request of NASA to get an idea of what technology might be required to detect gravitational waves from the Big Bang if the standard inflation scenarios are correct. Two issues affect this solution: what is the appropriate frequency window, and what technology will be available on a 20-year time-scale.

There is little point making LISA itself more sensitive in an attempt to see an inflation-level background. In LISA's frequency band, astrophysically generated random backgrounds of gravitational waves are expected to lie just under LISA's instrumental noise above 1 mHz (and to exceed instrumental noise below this frequency). Studies suggest that there is an accessible "window" where a cosmological background is likely to exceed local-source backgrounds around 1 Hz. This lies just between the best

sensitivities of LISA and the current ground-based detectors, and so it would require a dedicated space mission.

Moving up in frequency from the LISA band to the 1 Hz band has a disadvantage: since the energy density per unit logarithmic frequency of gravitational waves from cosmology is expected to be relatively flat, the rms amplitude of the expected waves falls off as $f^{-3/2}$. The result is that, in order to gain an energy sensitivity of 10^6 over LISA at a frequency 10^3 times higher, BBO would have to improve on the displacement sensitivity of LISA by something like 7 orders of magnitude if it were to rely simply on a LISA-like bolometric measurement. Instead, BBO proposes two co-located LISA-like arrays of three spacecraft each, whose output can be cross-correlated to look for a residual correlated component of (cosmological) noise below the (uncorrelated) instrumental noise. Even with this, BBO has another problem: severe interference from isolated gravitational wave sources in this window. These are mainly compact neutron-star binaries (like the Hulse-Taylor pulsar system) on their way to coalescence. Their signals must be measured accurately enough to be removed before the cross-correlation is done. BBO proposes to do this with two further LISA-like arrays placed at equal spacings in the same 1 AU orbit around the Sun; these systems can triangulate the binaries and remove them wherever they occur, even at redshifts of 10 or more.

To do this still requires much more sensitivity in each array than LISA will offer. It requires lasers hundreds of times more powerful and mirrors ten times larger. It is not clear at present how realistic such advances are, even twenty years from now. But no other design has been proposed that is capable of seeing the cosmological gravitational wave background. And that goal is so fundamental that the BBO is bound to continue to be studied and to inspire near-term technology development in this field.

12 Conclusions

12.1 The next decade in cosmology

The past ten years have revolutionized our knowledge about the universe. The technical developments in observational astronomy, together with increasingly sophisticated modelling and simulations, have led to a vast deepening in understanding of the processes that have shaped the cosmos we inhabit. This understanding is best demonstrated by the great achievements of 'precision cosmology', such as the wonderful match of WMAP data and theory – surely one of the best examples of a successful theoretical prediction in all of physics. Where does the road take us from this point? Now that we have a well-established standard model for cosmology, it is likely that a good deal of interest in the field will seek to exploit the 'phenomenology' of the model by pursuing observations of the early universe. Studies of the evolution of cosmic structure, of the formation of clusters and galaxies together with their supermassive black holes, and of the history of the reionization of the universe will increasingly become the focus of astrophysical cosmology. These latter aspects have been largely neglected in this report, owing to the specific terms of reference given to the Working Group.

But even if we neglect purely astrophysical aspects, observational astronomy will continue to have huge fundamental importance. It is only through astronomy that we know that the universe consists mainly of dark energy and dark matter – although both these ingredients raise key questions for particle physicists. Inflation now counts as another effect that has become part of the standard cosmological model, not the least due to the spectacular results from WMAP. Again, the physics of inflation is a great puzzle for fundamental physics. Astrophysics, and cosmology in particular, can be regarded as the key driver for challenges and developments in fundamental physics, and the next decade will see an increasingly intense interaction and collaboration between these two communities. Each working with their own tools – accelerators and telescopes – the interpretation of their results will most likely be possible only with a joint effort.

From a European perspective, the past decade has seen the opening of the VLT, greatly increasing our capabilities for (mainly) spectroscopic studies; a vast advance in infrared astronomy through the ISO satellite and VLT instruments; the true power of the Hubble Space Telescope; as well as two high-energy cornerstone observatories, XMM-Newton and Integral. Overall, there is no doubt that the relative impact of European cosmology on the world stage is far higher than before these initiatives, and we should aim to maintain this level of achievement. Looking ahead a further decade, the second-generation VLT instruments will increase the capability of these telescopes; Planck and Herschel are now close to being launched, the former expected to yield the most precise information on cosmological parameters yet; the VST and VISTA will provide unprecedented imaging capabilities; GAIA will study the detailed mass struc-

ture of the Milky Way and bring 'near-field cosmology' to fruition. We will see ALMA in action to study very high redshift objects, and we are tremendously curious to enter the era of gravitational wave astronomy with LISA, detecting merging supermassive black holes throughout the visible universe, thus viewing the hierarchical formation of galaxies. Near the end of this period, we will see JWST taking magnificent images of unimaginable depth of the infrared sky, and taking spectra of galaxies too faint and/or too distant to be seen in even the Hubble Deep Fields. Finally, the construction of giant ground-based optical/near-IR telescopes may have begun.

This suite of new tools will give astronomers plenty to do, and is guaranteed to lead to many tremendous gains of insight. But this great perspective falls short on one aspect that we consider to be a key element for fundamental cosmology: *we need to survey a major fraction of the sky down to depths corresponding to a mean redshift of about unity*, because this is the region in our visible universe where dark energy reveals its presence. Precision measurements require us to minimize statistical errors, implying immediately a wide sky coverage, essentially independent of the method of investigation. The past decade has demonstrated the great power of surveys, e.g. with the 2dFGRS and SDSS surveys – whose results complement WMAP data to yield a substantial increase in cosmological accuracy. Imaging survey work is known to be of key interest, as is recognised in several wavebands: microwave (Planck), UV (GALEX), and X-ray (eROSITA); furthermore, GAIA will perform an all-sky astrometric survey. All-sky surveys in the optical and near-IR do exist (ESO/UKST; POSS; DENIS; 2MASS), but are restricted to shallow levels by current standards, and thus tell us about only the local universe. We believe that the coming decade will see a revival of sky surveys in these wavebands, and that these surveys will form a key ingredient in our attempts to learn about the dark side of the universe. This belief is supported by looking outside the confines of Europe.

12.2 The international perspective

The outlook for cosmology has naturally been much debated throughout the global community in the subject, and it is worth summarising the results of some other important studies. Chief among these are the USA's DoE/NASA/NSF interagency task forces on Dark Energy (Kolb et al. 2006) and CMB research (Bock et al. 2006).

Dark Energy The Dark Energy Task Force takes the standard approach of parameterising the dark energy equation of state as $w(a) = w_0 + w_a(1-a)$ and advocates a figure of merit for any given experiment that is the reciprocal area of the error ellipse in the $w_0 - w_a$ plane. This is not an unreasonable choice, but it does presume that nontrivial DE dynamics will be detected in due course, whereas the greatest immediate advance one could imagine in the field is to rule out the cosmological constant model. Until or

unless this is achieved, it arguably makes sense to optimise the error on a constant w, independent of evolution. This difference in emphasis does not matter hugely in practice. Kolb et al. define a number of stages for DE probes:

- Stage I: Current knowledge.
- Stage II: Ongoing projects.
- Stage III: Near-term, medium-cost projects, which should deliver a factor of 3 improvement in figure of merit over stage II.
- Stage IV: Long-term, high-cost projects, which should deliver a factor of 10 improvement in figure of merit over stage II. These are taken to be LSST, SKA, plus one space mission expected to emerge from the NASA/DoE JDEM process.

The Dark Energy Task Force report argues that all four principal techniques (baryon oscillations; cluster surveys; supernovae; lensing) should be pursued, since none in isolation is capable of delivering the required accuracy. We agree with this multi-pronged strategy, while noting that there are significant differences in the ideal accuracies promised by the various methods. In particular, large-scale weak lensing surveys with photometric redshifts has the best formal accuracy. However, all techniques may be subject to unanticipated systematic limits, so there is certainly a strong rationale for pursuing several independent techniques. It is also worth noting that there is scope for disagreement about timing: the DETF tend to see space-borne imaging as the ultimate long-term stage IV approach, whereas we believe that ESA's Cosmic Vision process offers the opportunity of achieving these gains on a relatively accelerated timescale.

The CMB The Bock et al. report emphasises three main points: (1) there is a huge potential science gain from detecting intrinsic large-scale 'B-mode' polarization; (2) small-scale CMB anisotropies contain important information that indirectly constrains the fundamental-physics aspects of the CMB; (3) progress in both these areas will be limited without an improved understanding of Galactic foreground emission.

The main Bock et al. recommendation under the heading of large-scale CMB polarization is a satellite mission, termed CMBPOL, which aims to detect intrinsic B modes if present at a level of about $r = 0.01$. This has a notional development period starting in 2011, with a launch in 2018. In the interim, they recommend development work on large-area polarized detector arrays for the frequency range 30 – 300 GHz, to be validated via balloon flights. Their assumption is that the preferred technology for these frequencies will continue to be bolometric.

On the small-scale CMB front, the Bock et al. outlook is dominated by two experiments currently under construction: the South Pole Telescope (SPT) and the Atacama

Cosmology Telescope (although the European APEX sub-mm dish at the Atacama site also receives some mention). These experiments have apertures between 6m and 12m, and will study the CMB with resolution of order 1 arcmin at wavelengths of a few mm or below. This allows the use of the Sunyaev–Zeldovich effect for the detection and characterisation of clusters of galaxies, over areas of sky of order 1000 deg^2. These studies of nonlinear signatures in the CMB will remove uncertainties in the power-spectrum normalization, and will also impact on dark energy – both via the use of the CMB power spectrum and via the use of SZ-detected cluster evolution. No major new experiments in this area are proposed by Bock et al.

Similarly, no specific experiment is proposed for the study of Galactic foregrounds alone. Rather, it is in the main expected that knowledge of the foregrounds will emerge through a consistent integration of the CMB data in various frequency channels. The only exception to this strategy is the acknowledged desirability of obtaining improved low-frequency maps around 10 GHz, which can constrain not only the synchrotron foreground but also the so-called anomalous foreground, which is sometimes hypothesized to arise from spinning dust grains.

12.3 Recommendations

After discussion of the issues documented in this report, the ESA-ESO Working Group arrived at the following set of recommendations. These are based on a number of considerations, given here in approximately decreasing order of relative weight:

- *What are the essential questions in fundamental cosmology?*
  Among the many issues, we identified five key questions that lie at the heart of our understanding of the fundamentals of the evolution of the universe: (1) baryogenesis; (2) the nature of dark matter; (3) the nature of dark energy; (4) the physics of inflation; and (5) tests of fundamental physics.

- *Which of these questions can be tackled, perhaps exclusively, with astronomical techniques?*
  It seems unlikely that astronomical observations can currently contribute any insight into baryogenesis. Furthermore, the nature of dark matter may well be best clarified by experiments at particle accelerators, in particular the Large Hadron Collider, or by direct dark matter searches in deep underground laboratories. This particle astrophysics approach may also tell us much about other fundamental issues, such as the law of gravity, extra dimensions etc. However, astronomical tools will also make essential contributions to these problems. They can constrain the dark matter constituents via their spatial clustering properties and/or their possible annihilation signals. Astronomy is also probably the best way to measure

any time variability of the fundamental 'constants'. Finally, the nature of dark energy and the physics of inflation can be empirically probed, according to our current knowledge, only in the largest laboratory available – the universe itself.

- *What are the appropriate methods with which these key questions can be answered?*
  Studies of the dark energy equation of state can profit from four different methods: the large-scale structure of the three-dimensional galaxy distribution, clusters of galaxies, weak lensing, and distant supernovae. An attempt was made to judge the relative strengths of these methods, though all of them will require a substantial increase of measurement accuracies compared to current results, so that unanticipated systematic limits may become a problem in future work. For this reason, and given the central importance of this key question for cosmology and fundamental physics, pursuing only a single method bears an unacceptable risk.

  The physics of inflation can be studied by three main methods: the B-mode polarization signal of the CMB; the direct detection of gravitational waves from the inflationary epoch; and a precise measurement of the density fluctuation spectrum over a very large range of length scales, to determine the slope (tilt) and possibly the curvature (running) of the power spectrum. These parameters are bounded by CMB measurements on the largest scales, and by weak lensing and Lyα forest studies on the smallest scales.

- *Which of these methods appear promising for realization within Europe, or with strong European participation, over the next* ~ 15 *years?*
  This issue is subject to considerable uncertainty, as it depends on the funding situation as much as on international developments, in particular when it comes to cooperation with partners outside Europe. Nevertheless, much work has been invested in planning for potential future projects, so in many cases there is a strong basis on which to pick the best future prospects. Certainly, there is no shortage of input, and it is a sign of the scientific vitality of European cosmology that there are unfortunately more attractive ideas than can feasibly be funded. We have paid particular attention to the findings of the ESA advisory structure, summarized in the Cosmic Vision 2015-2025 document. Given the interagency nature of this WG, we have naturally chosen to emphasise particularly timely opportunities for collaboration between these two major players in European astronomy.

- *Which of these methods has a broad range of applications and a high degree of versatility even outside the field of fundamental cosmology?*
  Given that the next major steps towards answering the key cosmological questions will in any case require substantial resources, it is desirable that the projects to be pursued should lead to datasets of general applicability. Whereas the cosmological issues are the prime science drivers of these projects, and determine their

specifications, a broad range of applications will increase the scientific value of the investments, and boost their level of support in the community.

Based on these considerations, our recommendation are as follows:

(1) *Wide-field optical and near-IR imaging survey.*
ESA and ESO have the opportunity to collaborate in executing an imaging survey across a major fraction of the sky by constructing a space-borne high-resolution wide-field optical and near-IR imager and providing the essential optical multi-colour photometry from the ground. The VST KIDS and VISTA VIKING projects will be essential pathfinders for this sort of data, but substantial increases in grasp and improvements in image quality will be needed in order to match or exceed global efforts in this area. Near-IR photometry is extremely important for obtaining reliable photometric redshifts, in particular for galaxies beyond redshift unity, but also to minimize the fraction of outliers at lower redshifts. VISTA will be able to perform this role to some extent with regard to KIDS. However, imaging in space offers huge advantages in the near-IR via the low background, and this is the only feasible route to quasi all-sky surveys in this band that match the depth of optical surveys. Therefore,

- ESA should give the highest immediate priority in its astronomy programme to a satellite that offers this high-resolution optical imaging, preferably combined with near-IR photometry, and in parallel,
- ESO should give high priority to expanding its wide-field optical imaging capabilities to provide the required multi-band photometric data.
- Furthermore, since the calibration of photo-z's is key to the success of this plan, ESO should aim to conduct large spectroscopic surveys spread sparsely over $\sim 10,000$ deg^2, involving $> 100,000$ redshifts. This will require the initiation of a large Key Programme with the VLT, integrated with the imaging survey.

This project will be an essential asset for several of the cosmological probes discussed in this report. It will provide the necessary data for weak lensing and large-scale structure studies of the dark energy component in the Universe. Furthermore, it will provide an indispensable dataset for statistical studies of dark energy using galaxy clusters, yielding the means to determine redshifts and optical luminosity of X-ray and SZ-selected clusters, as provided by, e.g., eROSITA and Planck. In addition, such a project (essentially an SDSS imaging survey 4 magnitudes deeper and with ~ 3 times larger area, plus 2MASS with a 7 magnitude increase in depth), together with highly accurate photometric redshifts for galaxies and quasars, would be a profound resource for astronomy in general, a legacy comparable in value to the Palomar surveys some 50 years ago. Among

the numerous applications of such a dataset, we mention the selection of targets for deep spectroscopic studies, either for the VLT, the JWST and finally an ELT.

(2) The existence of major future imaging surveys presents a challenge for spectroscopic follow-up. For some applications, such as weak gravitational lensing, photometric redshifts with few % precision are sufficient. But some science questions need true spectroscopy, and this presents of problem of grasp. A capability for massive multiplexed deep spectroscopy (at the level of several thousand simultaneous spectra over a field of order one degree) is required for this. Such a facility would permit surveys of $> 10^6$ redshifts needed to probe dark energy using the galaxy power spectrum as a standard ruler, and there are a number of international plans for instruments of this sort. ESO should secure access to such an instrument, either through the development of such a facility for the VLT, or as a collaborative arrangement with an external project, perhaps in conjunction with sharing some of Europe's proposed imaging data.

(3) A powerful multi-colour imaging capability can also carry out a supernova survey extending existing samples of $z = 0.5 - 1$ SNe by an order of magnitude, although an imager of 4m class is required if this work is to be pursued from the ground. In order to exploit the supernova technique fully, an improved local sample is also required. The VST could provide this, provided that time is not required for other cosmological surveys, in particular lensing.

(4) Whereas the WG sees the main science drivers for a European Extremely Large Telescope (ELT) as lying in other fields of astronomy, we recommend that the following applications in fundamental cosmology should be regarded as forming an essential part of the ELT capability:

- Supernova surveys need to be backed up with spectroscopy to assure the classification for at least a significant subsample and to check for evolutionary effects. The spectroscopy requires access to the largest possible telescopes, and an ELT will be essential for the study of distant supernovae with redshifts $z > 1$.
- A European ELT will also be important in fundamental cosmology via the study of the intergalactic medium. Detailed quasar spectroscopy can limit the nature of dark matter by searching for a small-scale coherence length in the mass distribution. These studies can also measure directly the acceleration of the universe, by looking at the time dependence of the cosmological redshift. Furthermore, by providing information of the density fluctuation power spectrum at the smallest scales, the Lyman-α forest provides the biggest lever arm on the shape of the power spectrum, and thus on its tilt and its potentially running spectral index.

- ELT quasar spectroscopy also offers the possibility of better constraints on any time variation of dimensionless atomic parameters such as the fine-structure constant α and the proton-to-electron mass ratio. There presently exist controversial claims of evidence for variations in α, which potentially relate to the dynamics of dark energy. It is essential to validate these claims with a wider range of targets and atomic tracers.

(5) In the domain of CMB research, Europe is well positioned with the imminent arrival of Planck. The next steps are (1) to deal with the effects of foreground gravitational lensing of the CMB and (2) to measure the 'B-mode' polarization signal, which is the prime indicator of primordial gravitational waves from inflation. The former effect is aided by the optical/near-IR imaging experiments discussed earlier. The latter effect is potentially detectable by Planck, since simple inflation models combined with data from the WMAP CMB satellite predict a tensor-to-scalar ratio of $r \simeq 0.15$. A next-generation polarization experiment would offer the chance to probe this signature in detail, providing a direct test of the physics of inflation and thus of the fundamental physical laws at energies $\sim 10^{12}$ times higher than achievable in Earth-bound accelerators. For reasons of stability, such studies are best done from space; we thus recommend such a CMB satellite as a strong future priority for ESA, together with the support of corresponding technological developments.

(6) An alternative means of probing the earliest phases of cosmology is to look for primordial gravitational waves at much shorter wavelengths. LISA has the potential to detect this signature by direct observation of a background in some models, and even upper limits would be of extreme importance, given the vast lever arm in scales between direct studies and the information from the CMB. We thus endorse space-borne gravity-wave studies as an essential current and future priority for ESA.

12.4 The longer-term outlook for cosmology

Beyond the time-frame considered here (up to about 2020), the power of cosmological facilities in astronomy will inevitably increase still further. One of the most exciting prospects will be the Square Kilometre Array, which will be capable of detecting redshifted neutral hydrogen throughout the visible universe. The general science programme of the SKA and its impact on all areas of extragalactic astronomy is described in Carilli & Rawlings (2004). For the present purpose, the most obvious application is that the SKA will obtain redshifts for $10^8 - 10^9$ galaxies (depending on the configuration chosen), thus pushing baryon-oscillation studies of the dark energy into new regimes. This project will operate on a longer timescale, and is a natural successor to the studies

described above. A strong European participation in the SKA is therefore essential, although of course the justification for this lies as much in the domain of astrophysics as in fundamental cosmology.

In this report, we have shown that there are many exciting opportunities for ESA and ESO to act in concert to achieve great advances in our knowledge of cosmology. Where we will stand in 2020 is impossible to predict, but some speculation is irresistible. There is a good case that the current evidence for tilt places us half-way to a proof of inflation, and the great hope must be be that primordial gravitational waves will be detected in the CMB to complete the picture. If we were also to have found by this time that the dark energy is more than a cosmological constant, then we would have two completely new windows into previously unstudied physics. Continuing this optimistic view, the simplest models for dark matter suggest that the WIMP responsible for this phenomenon will have been seen both directly in underground experiments and at the LHC by 2020. Of course, it is possible that none of these developments will come to pass – but then future cosmological research will be steered into new and equally interesting directions.

Bibliography

Allen, S.W., Ettori, S., Fabian, A.C., 2001, MNRAS, 324, 877

Allen, S.W., Schmidt, R.W., Ebeling, H., Fabian, A.C., van Speybroeck, L., 2004, MNRAS, 353, 457

Angulo, R., Baugh, C.M., Frenk, C.S., Bower, R.G., Jenkins, A., Morris, S.L., 2005, MNRAS, 362, L25

Annis, J., et al., 2005, astro-ph/0510195

Arnett, W.D., 1982, ApJ, 253, 785

Astier, P., et al., 2006, A&A, 447, 31

Bacon, D.J., Massey, R.J., Réfrégier, A.R., Ellis, R.S., 2003, MNRAS, 344, 673

Bacon, D.J., et al., 2005, MNRAS, 363, 723

Bartolo, N., Komatsu, E., Matarrese, S., Riotto, A., 2004, Physics Reports, 402, 103

Bean, R., Dunkley, J., Pierpaoli, E., 2006, astro-ph/0606685

Bekenstein, J.D., 2004, Phys. Rev. D, 70, 3509

Bell, E.F., et al., 2004, ApJ, 608, 752

Bento, M.C., Bertolami, O., Santos, N.M., 2004, Phys. Rev. D, 70, 107304

Bernardeau, F., 1998, A&A, 338, 375

Bernardeau, F., Mellier, Y., van Waerbeke, L., 2002, A&A, 389, L28

Bernardeau, F., van Waerbeke, L., Mellier, Y., 1997, A&A, 322, 1

Blake, C., Bridle, S., 2005, MNRAS, 363, 1329

Blake, C., Glazebrook, K., 2003, ApJ, 594, 665

Blandford, R.D., Saust, A.B., Brainerd, T.G., Villumsen, J.V., 1991, MNRAS, 251, 600

Blinnikov, S., et al., 2006, A&A, 543, 229
Bock, J., et al., 2006, astro-ph/0604101
Bohlin, R.C., Jenkins, E.B., Spitzer, L., Jr., York, D.G., Hill, J.K., Savage, B.D., Snow, T.P., Jr., 1983, ApJ Suppl., 51, 277
Brown, M.L., Taylor, A.N., Bacon, D.J., Gray, M.E., Dye, S., Meisenheimer, K., Wolf, C. 2003, MNRAS, 341, 100
Carilli, C.L., Rawlings, S. (eds), 2004, New Astronomy Review, 48
Catelan, P., Porciani, C., Kamionkowski, M., 2000, MNRAS, 318, L39
Carroll, S.M., Press, W.H., Turner, E.L., 1992, ARAA, 30, 499
Chand, H., Srianand, R., Petitjean, P., Aracil, B., 2004, A&A, 417, 853
Chang, T.-C., Réfrégier, A., Helfand, D.J., 2004, ApJ, 617, 794
Clowe, D., Bradac, M., Gonzalez, A.H., Markevitch, M., Randall, S.W., Jones, C., Zaritsky, D., 2006, astro-ph/0608407
Coil, A.L., Newman, J.A., Cooper, M.C., Davis, M., Faber, S.M., Koo, D.C., Willmer, C.N.A., 2006, ApJ, 644, 671
Cole, S., et al., (The 2dFGRS Team), , 2005, MNRAS, 362, 505
Collister, A.A., Lahav, O., 2004, PASP, 116, 345
Contaldi, C.R., Hoekstra, H., Lewis, A., 2003, Physical Review Letters, 90, 221303
Cooray, A., Sheth, R., 2002, Physics Reports, 372, 1
Cowie, L.L., Songaila, A., 1995, ApJ, 453, 596
Croft, R.A.C., Weinberg, D.H., Bolte, M., Burles, S., Hernquist, L., Katz, N., Kirkman, D., Tytler, D., 2002, ApJ, 581, 20
Desjacques, V., Nusser, A., 2005, MNRAS, 361, 1257
Dine, M., Nir, Y., Raz, G., Volansky, T., 2003, Phys. Rev. D, 67, 015009
Dvali, G., Gabadadze, G., Porrati, M., 2000, Physics Letters B, 485, 208
Dzuba, V.A., Flambaum, V.V., Kozlov, M.G., Marchenko, M., 2002, Phys. Rev. A, 66, 022501
Dzuba, V.A., Flambaum, V.V., Webb, J.K., 1999, Phys. Rev. A, 59, 230
Efstathiou, G., Sutherland, W., Maddox, S.J., 1990, Nature, 348, 705
Eisenstein, D.J., et al., 2005, ApJ, 633, 560
Elgaroy, O., Lahav, O., 2005, New Journal of Physics, 7, 61
Elias-Rosa, N., et al., 2006, MNRAS, 369, 1880
Feldman, H.A., Kaiser, N., Peacock, J.A., 1994, ApJ, 426, 23
Flambaum, V.V., Leinweber, D.B., Thomas, A.W., Young, R.D., 2004, Phys. Rev. D, 69, 115006
Fu et al., 2006, in preparation
Fujii, Y., 2005, Physics Letters B, 616, 141
Goldhaber, G., et al., 2001, ApJ, 558, 359
Goobar, A., Hannestad, S., Mörtsel, E., Tu, H., 2006, JCAP, 06, 019
Guth, A.H., 1981, Phys. Rev. D, 23, 347
Guy, J., et al., 2005, A&A, 443, 781
Haiman, Z., et al., 2005, astro-ph/0507013

Hamana, T., Colombi, S., Thion, A., Devriendt, J., Mellier, Y., Bernardeau, F., 2002, MNRAS, 330, 365
Hamana, T., et al., 2003, ApJ, 597, 98
Hamuy, M., et al., 2003, Nature, 424, 651
Heavens, A.F., 2003, MNRAS, 343, 1327
Heavens, A.F, Kitching, T.D., Taylor, A.N., 2006, astro-ph/0606568
Hennawi, J.F., Spergel, D.N., 2005, ApJ, 624, 59
Hetterscheidt, M., Simon, P., Schirmer, M., Hildebrandt, H., Schrabback, T., Erben, T., Schneider, P., 2006, astro-ph/0606571
Heymans, C., Brown, M., Heavens, A., Meisenheimer, K., Taylor, A., Wolf, C., 2004, MNRAS, 347, 895
Heymans, C., et al., 2005, MNRAS, 361, 160
Heymans, C., Heavens, A., 2003, MNRAS, 339, 711
Heymans, C., et al., 2006a, MNRAS, 368, 1323
Heymans, C., White, M., Heavens, A., Vale, C., Van Waerbeke, L., 2006b, MNRAS, 371, 750
Hildebrandt, H., et al. in preparation
Hillebrandt, W., Niemeyer, J.C., 2000, ARAA, 38, 191
Hirata, C.M., Seljak, U., 2004, Phys. Rev. D, 70, 063526
Hoekstra, H., et al., 2006, ApJ, 647, 116
Hoekstra, H., Franx, M., Kuijken, K., Carlberg, R.G., Yee, H.K.C., 2003, MNRAS, 340, 609
Hoekstra, H., Yee, H.K.C., Gladders, M.D., 2002a, ApJ, 577, 595
Hoekstra, H., van Waerbeke, L., Gladders, M.D., Mellier, Y., Yee, H.K.C., 2002b, ApJ, 577, 604
Holder, G., Haiman, Z., Mohr, J.J., 2001, ApJ, 560, L111
Hook, I., et al., 2005, AJ, 130, 2788
Howell, D.A., et al., 2005, AJ, 131, 2216
Hubble, E., 1934, ApJ, 79, 8
Huterer, D., Takada, M., 2005, Astroparticle Physics, 23, 369
Huterer, D., Takada, M., Bernstein, G., Jain, B., 2006, MNRAS, 366, 101
Huterer, D., White, M., 2005, Phys. Rev. D, 72, 043002
Hu, W., Haiman, Z. 2003, Phys. Rev. D, 68, 063004
Ilbert, O., et al., 2006, astro-ph/0603217
Ivanchik, A., Petitjean, P., Varshalovich, D., Aracil, B., Srianand, R., Chand, H., Ledoux, C., Boissé, P., 2005, A&A, 440, 45
Jain, B., Seljak, U., 1997, ApJ, 484, 560
Jain, B., Taylor, A., 2003, Physical Review Letters, 91, 141302
Jarvis, M., Bernstein, G.M., Fischer, P., Smith, D., Jain, B., Tyson, J.A., Wittman, D. 2003, AJ, 125, 1014
Jarvis, M., Bernstein, G., Jain, B., 2004, MNRAS, 352, 338
Jarvis, M., Jain, B., Bernstein, G., Dolney, D., 2006, ApJ, 644, 71

Jha, S., 2002, PhD Thesis, Harvard University
Jing, Y.P., Zhang, P., Lin, W.P., Gao, L., Springel, V., 2006, ApJ, 640, L119
Jones, D.H., Saunders, W., Read, M., Colless, M., 2005, Publications of the Astronomical Society of Australia, 22, 277
Kaiser, N., 1986, MNRAS, 219, 785
Kaiser, N., 1992, ApJ, 388, 272
Kamionkowski, M., Kosowsky, A., Stebbins, A., 1997, Phys. Rev. D, 55, 7368
Kilbinger, M., Schneider, P., 2005, A&A, 442, 69
Kim, T.-S., Viel, M., Haehnelt, M.G., Carswell, B., Cristiani, S., 2004a, MNRAS, 351, 1471
Kim, T.-S., Viel, M., Haehnelt, M.G., Carswell, R.F., Cristiani, S., 2004b, MNRAS, 347, 355
King, L.J., 2005, A&A, 441, 47
King, L.J., Schneider, P., 2003, A&A, 398, 23
Kohler, K., Gnedin, N.Y., 2006, astro-ph/0605032
Kolb, R., et al., 2006, DoE/NASA/NSF interagency task force on Dark Energy
Kravtsov, A.V., Vikhlinin, A., Nagai, D., 2006, astro-ph/0603205
Krisciunas, K., et al., 2000, ApJ, 539, 658
Krisciunas, K., Phillips, M.M., Suntzeff, B.N., 2004, ApJ, 602, L81
Lamoreaux, S.K., Torgerson, J.R., 2004, Phys. Rev. D, 69, 121701
Le Fèvre, O., et al., 2004, A&A, 428, 1043
Leibundgut, B., 2001, ARAA, 39, 67
Levine, E.S., Schulz, A.E., White, M., 2002, ApJ, 577, 569
Levshakov S.A., Centurión, M., Molaro, P., D'Odorico, S., 2005, A&A, 434, 827
Levshakov S.A., Centurión, M., Molaro, P., Kostina, M.V., 2006, A&A, 447, L21
Levshakov, S.A., 2004, LNPVol.648: Astrophysics, Clocks and Fundamental Constants, 648, 151
Levshakov, S.A., Dessauges-Zavadsky, M., D'Odorico, S., Molaro, P., 2002, MNRAS, 333, 373
Liddle, A.R., Scherrer, R.J., 1999, Phys. Rev. D, 59, 023509
Lidman, C., et al., 2005, A&A, 430, 843
Lima, M., Hu, W., 2004, Phys. Rev. D, 70, 043504
Linder, E.V., 2003, Phys. Rev. D, 68, 083503
Linder, E.V., Huterer, D., 2003, Phys. Rev. D, 67, 1303
Livio, M., 2000, in Type Ia Supernovae: Theory and Cosmology, eds. J. C. Niemeyer and J. W. Truran, Cambridge, Cambridge University Press, 33
Majumdar, S., Mohr, J.J., 2003, ApJ, 585, 603
Majumdar, S., Mohr, J.J., 2004, ApJ, 613, 41
Maoli, R., Van Waerbeke, L., Mellier, Y., Schneider, P., Jain, B., Bernardeau, F., Erben, T., Fort, B., 2001, A&A, 368, 766
Marciano, W.J., 1984, Physical Review Letters, 52, 489
Massey, R., Réfrégier, A., Bacon, D.J., Ellis, R., Brown, M.L., 2005, MNRAS, 359,

1277
McDonald P., Miralda-Escudé J., Rauch, M., Sargent, W.L.W., Barlow, T.A., Cen, R., Ostriker, J.P., 2000, ApJ, 543, 1
McDonald, P., et al., 2005, ApJ, 635, 761
Matheson, T., et al., 2005, AJ, 129, 2352
Meiksin, A., White, M., Peacock, J.A., 1999, MNRAS, 304, 851
Miralda-Escudé, J., 1991, ApJ, 380, 1
Mohr, P.J., Taylor, B.N., 2005, Reviews of Modern Physics, 77, 1
Molnar, S.M., Haiman, Z., Birkinshaw, M., Mushotzky, R.F., 2004, ApJ, 601, 22
Mullis, C.R., Rosati, P., Lamer, G., Böhringer, H., Schwope, A., Schuecker, P., Fassbender, R., 2005, ApJ, 623, L85
Murphy, M.T., Flambaum, V.V., Webb, J.K., et al., 2004, LNP Vol.648: Astrophysics, Clocks and Fundamental Constants, 648, 131
Nugent, P., Kim, A., Perlmutter, S., 2002, PASP, 114, 803
Peacock, J.A., Dodds, S.J., 1996, MNRAS, 280, L19
Peacock, J.A., et al. (The 2dFGRS Team), 2001, Nature, 410, 169
Pen, U.-L., Zhang, T., van Waerbeke, L., Mellier, Y., Zhang, P., Dubinski, J., 2003a, ApJ 592, 664
Pen, U.-L., Lu, T., van Waerbeke, L., Mellier, Y., 2003b, MNRAS, 346, 994
Perlmutter, S., et al. 1998, ApJ, 517, 656
Phillips, M.M., et al., 1999, AJ, 118, 1766
Popesso, P., Biviano, A., Böhringer, H., Romaniello, M., Voges, W., 2005, A&A, 433, 431
Quast, R., Reimers, D., Levshakov, S.A., 2004, A&A, 415, L7
Réfrégier, A., Rhodes, J., Groth, E.J., 2002, ApJ, 572, L131
Reinhold, E., Buning, R., Hollenstein, U., Ivanchik, A., Petitjean, P., Ubachs, W., 2006, Physical Review Letters, 96, 151101
Reiprich, T.H., Böhringer, H., 2002, ApJ, 567, 716
Rhodes, J., Réfrégier, A., Groth, E.J., 2001, ApJ, 552, L85
Riess, A.G., et al., 1998, AJ, 116, 1009
Riess, A.G., et al., 2004, ApJ, 607, 665
Riess, A.G., et al., 1996, ApJ, 473, 88
Riotto, A., Trodden, M., 1999, Annual Review of Nuclear and Particle Science, 49, 35
Röpke, F.K., et al., 2006, A&A, 453, 203
Sawicki, I., Carroll, S.M., 2005, astro-ph/0510364
Seljak, U., Zaldarriaga, M., 1998, astro-ph/9805010
Schmid, C., et al., 2006, astro-ph/0603158
Schirmer, M., Erben, T., Hetterscheidt, M., Schneider, P., 2006, astro-ph/0607022
Schlegel, D., Finkbeiner, D.B., Davis, M., 1998, ApJ, 500, 525
Schneider, P., van Waerbeke, L., Mellier, Y., 2002, A&A, 389, 729
Schrabback, T., et al., 2006, astro-ph/0606611
Schuecker, P., Böhringer, H., Collins, C.A., Guzzo, L., 2003a, A&A, 398, 867

Schuecker, P., Caldwell, R.R., Böhringer, H., Collins, C.A., Guzzo, L., Weinberg, N.N., 2003b, A&A, 402, 53
Scoville N.Z. et al., (the COSMOS Team), 2006, ApJ, submitted
Seljak, U., McDonald, P., Makarov, A., 2003, MNRAS, 342, L79
Seljak, U., et al., 2005a, Phys. Rev. D, 71, 043511
Seljak, U., et al., 2005b, Phys. Rev. D, 71, 103515
Seljak, U., Makarov, A., McDonald, P., Trac, H., 2006, astro-ph/0602430
Semboloni, E., et al., 2006a, A&A, 452, 51
Semboloni, E., van Waerbeke, L., Heymans, C., Hamana, T., Colombi, S., White, M., Mellier, Y., 2006b, astro-ph/0606648
Seo, H.-J., Eisenstein, D.J., 2003, ApJ, 598, 720
Simpson, F., Bridle, S., 2006, Phys. Rev. D, 73, 083001
Skordis C., Mota D.F., Ferreira P.G., Boehm, C., 2006, Physical Review Letters, 96, 011301
Smith, R.E., et al., 2003, MNRAS, 341, 1311
Spergel, D.N., et al., 2006, astro-ph/0603449
Spergel, D.N., et al., 2003, ApJ Suppl., 148, 175
Stebbins, R.T., 1996, astro-ph/9609149
Springel, V., et al., 2005, Nature, 435, 629
Starobinskiĭ, A.A., 1985, Sov. Astr. Lett., 11, 133
Strolger, L.-G., et al., 2004, ApJ, 613, 200
Stritzinger, M., Leibundgut, B., 2005, A&A, 431, 423
Stritzinger, M., et al., 2002, AJ, 124, 2100
Stritzinger, M., Leibundgut, B., Walch, S., Contardo, G., 2006, A&A, 450, 241
Sullivan, M., et al., 2006, AJ, 131, 960
Susskind, L., 2003, hep-th/0302219
Takada, M., Jain, B., 2002, MNRAS, 337, 875
Tegmark, M., et al., 2004, ApJ, 606, 702
Tonry, J.L., et al., 2003, ApJ, 594, 1
Trotta, R., 2006, astro-ph/0607496
Tytler, D., et al., 2004, ApJ, 617, 1
Ubachs, W., Reinhold, E., 2004, Physical Review Letters, 92, 101302
Uzan, J.-P., 2003, Reviews of Modern Physics, 75, 403
Uzan, J.-P., Bernardeau, F., 2001, Phys. Rev. D, 64, 3501
Van Waerbeke, L., et al., 2000, A&A, 358, 30
Van Waerbeke, L., Mellier, Y., Pelló, R., Pen, U.-L., McCracken, H.J., Jain, B. 2002, A&A, 393, 369
Van Waerbeke, L., Mellier, Y., Hoekstra, H., 2005, A&A, 429, 75
Varshalovich, D.A., Levshakov, S.A., 1993, Journal of Experimental and Theoretical Physics Letters, 58, 237
Verde, L., et al., 2002, MNRAS, 335, 432
Viel, M., Haehnelt, M.G., Springel, V., 2004, MNRAS, 354, 684

Viel, M., Lesgourgues, J., Haehnelt, M.G., Matarrese, S., Riotto, A., 2005, Phys. Rev. D, 71, 063534
Viel, M., Haehnelt, M.G., Lewis, A., 2006a, MNRAS, 370, L51
Viel, M., Lesgourgues, J., Haehnelt, M.G., Matarrese, S., Riotto, A., 2006b, astro-ph/0605706
Vikhlinin, A., Markevitch, M., Murray, S.S., Jones, C., Forman, W., Van Speybroeck, L., 2005, ApJ, 628, 655
Vikhlinin, A., et al., 2003, ApJ, 590, 15
Voit, G.M., 2005, Reviews of Modern Physics, 77, 207
Wang, L., Steinhardt, P.J., 1998, ApJ, 508, 483
Wang, S., Khoury, J., Haiman, Z., May, M., 2004, Phys. Rev. D, 70, 123008
Webb, J.K., Flambaum, V.V., Churchill, C.W., Drinkwater, M.J., Barrow, J.D., 1999, Physical Review Letters, 82, 884
WFMOS study, 2005, http://www.gemini.edu/files/docman/science/aspen/WFMOS_feasibility_report_public.pdf
Wetterich, C., 2003, Phys. Lett. B, 561, 10
White, M., Kochanek, C.S., 2001, ApJ, 574, 24
Wittman, D., Dell'Antonio, I.P., Hughes, J.P., Margoniner, V.E., Tyson, J.A., Cohen, J.G., Norman, D., 2006. ApJ, 643, 128
Zaldarriaga, M., Seljak, U., 1997, Phys. Rev. D, 55, 1830
Zaroubi, S., Viel, M., Nusser, A., Haehnelt, M., Kim, T.-S., 2006, MNRAS, 369, 734
Zehavi, I., Riess, A.G., Kirshner, R.P., Dekel, A., 1998, ApJ, 503, 483
Zhang, J., Hui, L., Stebbins, A., 2005, ApJ, 635, 806
Zhao, H., Bacon, D.J., Taylor, A.N., Horne, K., 2006, MNRAS, 368, 171
Zlatev, I., Wang, L., Steinhardt, P.J., 1999, Physical Review Letters, 82, 896

List of abbreviations

2dF: Two-degree Field
2dFGRS: The Two-degree Field Galaxy Redshift Survey
2MASS: Two Micron All Sky Survey
6dFGS: Six-degree Field Galaxy Survey
AAOmega: the upgraded two degree field (2dF) on the Anglo-Australian 4m telescope
ACES: Atomic Clock Ensemble in Space
ACS: Advanced Camera for Surveys
ACT: Atacama Cosmology Telescope
AD: alkali-doublets
ADEPT: Advanced Dark Energy Physics Telescope
AGB: Asymptotic Giant Branch
ALMA: Atacama Large Millimetre Array

ALPACA: Advanced Liquid-mirror Probe for Astrophysics, Cosmology and Asteroids
AMI: Arcminute Micro-Kelvin Imager
APEX: Atacama Pathfinder Experiment
APO: Apache Point Observatory
AU: Astronomical Unit
BAO: Baryon Acoustic Oscillations
BBN: Big Bang Nucleosynthesis
BBO: Big Bang Observer
BaBar: CP-violation experiment located at the Stanford Linear Accelerator Center
BELLE: CP-violation experiment located at KEK, Japan
CBI: Cosmic Background Imager, a radio telescope located in the Chilean Andes
CDM: Cold Dark Matter
CFHT: Canada-France-Hawaii Telescope
CFHTLS: Canada-France-Hawaii Telescope Legacy Survey
CMB: Cosmic Microwave Background
CMBPOL: CMB POLarision mission
COBE: COsmic Background Explorer
COMBO-17: Classifying Objects by Medium-Band Observations - a spectrophotometric 17-filter survey
COSMOS: Cosmic Evolution Survey
CP: charge-parity conjugation
CTIO: Cerro Tololo Inter-American Observatory
DECam: Camera for Dark Energy Survey
DES: Dark Energy Survey
DEEP2: Deep Extragalactic Evolution Probe, a spectroscopic survey carried out with Keck
DENIS: Deep Near-Infrared Sky Survey
DESTINY: A space-borne near-IR grism survey instrument for probing dark energy with supernovae
DETF: Dark Energy Task Force
DGP: Dvali, Gabadadze & Porrati extra-dimensional cosmological model
DUNE: Dark Universe Explorer
DarkCam: optical camera proposed for the VISTA telescope
Descart: Dark matter from Ellipticity Sources CARTography, ESO/CFHT imaging programme
DoE: Department of Energy
ELT: Extremely Large Telescope
ESA: European Space Agency
ESO: European Southern Observatory
ESSENCE: Equation of State: SupErNovae trace Cosmic Expansion project
FIRST: Faint Images of the Radio Sky at Twenty-centimetres survey
FLAMES: Fibre Large Array Multi Element Spectrograph at the VLT

FMOS: Fiber Multi-Object Spectrograph. An instrument at Subaru
GAIA: Galactic Astrophysics through Imaging and Astrometry. An ESA mission
GALEX : GALaxy Evolution EXplorer
GEMS: Galaxy Evolution From Morphology And SEDs survey
GOODS: The Great Observatories Origins Deep Survey
GUT: Grand Unified Theory
GaBoDS: The Garching-Bonn Deep Survey
Gadget-II: hydrodynamical N-body code
HETDEX: Hobby-Eberly Telescope Dark Energy Experiment
HFI: High-Frequency Instrument for Planck
HIRES: High Resolution Echelle Spectrometer on Keck
HST: Hubble Space Telescope
HyperCam: Camera on Subaru
HyperSuprimeCam: Camera on Subaru
IGM: Intergalactic Medium
ILC: International Linear Collider
IR: Infra Red
ISO: Infrared Space Observatory
JDEM: Joint Dark Energy Mission
JEDI: Joint Efficient Dark-energy Investigation
JHK: 1–2 micron filter bands
JWST: James Webb Space Telescope
KIDS: 1400-square degree gravitational shear survey with OmegaCAM
LHC: Large Hadron Collider
LIGO: Laser Interferometry Gravitational-Wave Observatory
LISA: Laser Interferometry Satellite Antenna gravitational-wave observatory
LOTOSS: Lick Observatory and Tenagra Observatory Supernova Search
LSS: Large Scale Structure
LSST: Large Synoptic Survey Telescope
MDS: Medium Deep Survey with HST
MM: Many-Multiplet method
MMT: Multiple Miror Telescope
MOND: Modified Newtonian Dynamics
NASA: National Aeronautics and Space Administration
NEAT: Near Earth Asteroid Tracking program
NSF: National Science Foundation
PAENS/SHOES: HST supernova survey
POSS: Palomar Observatory Sky Survey
PSF: Point Spread Function
PanSTARRS: Panoramic Survey Telescope & Rapid Response System
QCD: Quantum ChromoDynamics
QSO: Quasi-Stellar Object

QUIET: Q/U Imaging ExperimenT for CMB polarization
RCS: Red-sequence Cluster Survey
ROSAT: Röntgen SATellite
ROSITA: Röntgen Survey with an Imaging Telescope Array
SDSS: Sloan Digital Sky Survey
SED: Spectral Energy Distribution
SKA: Square Kilometre Array
SMBH: SuperMassive Black Hole
SN: SuperNova
SNAP: Supernova Acceleration Probe
SNIFS: Supernova Integral Field Spectrograph
SNIa: SuperNova type Ia
SNLS: SuperNova Legacy Survey
SPIDER: CalTech balloon-borne experiment to search for cosmic gravitational wave background
SPT: South Pole Telescope
STEP: Shear TEsting Program
SUPRIME-33: Suprime-Cam weak lensing cluster survey
SZ: Sunyaev-Zeldovich effect
SuprimeCam: Subaru Prime Focus Camera
TeVeS: tensor, vector and scalar field theory of modified gravity, due to Bekenstein
UKIDSS: UKIRT Infrared Deep Sky Survey
UKIRT: United Kingdom Infra-Red Telescope
UKST: United Kingdom Schmidt Telescope
UV: Ultraviolet
UVES: Ultraviolet and Visual Echelle Spectrograph
VIKING: VISTA Kilo-degree Infrared Galaxy survey
VIMOS: VIsible MultiObject Spectrograph
VISTA: Visible and Infrared Survey Telescope
VLT: The Very Large Telescope
VST: VLT Survey Telescope
VVDS: VIRMOS-VLT Deep Survey
VIRMOS: VLT Visible and InfraRed Multi-Object Spectrograph
WDM: Warm Dark Matter
WFCam: Wide Field Infrared Camera For UKIRT
WFMOS: Wide-Field Multi-Object Spectrograph
WFPC2: Wide Field and Planetary Camera 2
WG: Working Group
WHT: William Herschel Telescope
WIMP: Weakly Interacting Massive Particle
WIRCam: Wide Field IR Camera - wide-field imaging facility at CFHT
WMAP: Wilkinson Microwave Anisotropy Probe

WMAP1: WMAP first year survey
WMAP3: WMAP three year survey
XEUS: X-ray Evolving Universe Spectroscopy mission
XMM: X-ray Spectroscopy Multi-Mirror Mission